ISSN 1000-9620

Marine Science Bulletin

海洋通报

Volume 12 • Number 2 2010

ISSN 1000-9620
02>
9 771000 962001

NATIONAL MARINE DATA AND
INFORMATION SERVICE OF CHINA

MARINE SCIENCE BULLETIN

Vol. 12 No. 2 Oct. 2010

CONTENTS

Wave spectrum characteristics under typhoon wind forcing in coastal waters of the Beibu Bay through numerical simulation by SWAN ····· ZHOU Liang-ming et al. (01)

Impacts of global warming on marine zooplankton ····· ZHANG Da-juan et al. (15)

Research process of the calcium signaling in cyanobacteria····· LU Yong-zhong (26)

Elementary study of differential expression of total soluble proteins in different life phases of *Porphyra yezoensis*····· MENG Chun-xiao et al. (32)

Distribution and composition of tintinnids ciliates in the northern South China Sea during summer ····· LIU Hua-xue et al. (38)

RAPD analysis between color-different crab individuals of *Portunus trituberculatus* ····· CHI Da-li et al. (47)

Correlation and path coefficient analysis for phenotypic traits of noble scallop *Chlamys nobilis* ·····LI Jun-hui et al. (55)

Effects of salinity fluctuation and dietary protein/carbohydrate ratio on the survival and growth of Juvenile *Litopenaeus vannamei* ····· WANG Xing-qiang et al. (61)

Value evaluation of ecological risk of marine chemical spills ····· ZHANG Ji-wei et al. (74)

Research of data architecture in digital ocean ····· ZHANG Feng et al. (85)

LIBRARY
LIBRARY
Pacific Islands Fisheries Science Center
NOAA Fisheries
Honolulu, Hawai'i
Atmospheric Administration
U.S. Dept. of Commerce

Wave spectrum characteristics under typhoon wind forcing in coastal waters of the Beibu Bay through numerical simulation by SWAN

ZHOU Liang-ming[1], WANG Ai-fang[2], WANG Zhi-feng[3], GUO Pei-fang[1], GAO Jing-song[3]

1. *Physical Oceanography Laboratory, Ocean University of China, Qingdao* 266100, *Shandong Province, China;*

2. *Engineering Reconnaissance & Design Institute, Ocean University of China, Qingdao* 266071, *Shandong Province, China;*

3. *College of Physical and Environmental Oceanography, Ocean University of China, Qingdao* 266071, *Shandong Province, China*

Abstract: Wave fields in Beibu Bay during Typhoon Damrey (2005) were simulated by SWAN wave model through inputting high resolution reanalysis wind fields data, current and water level data. Comparisons for wind input and wave hindcast between observation and simulation show good consistency. Distributions of wave parameters such as wave height, wave period, wave length and wave direction under typhoon wind forcing were given. Also, the directional spectra related to the different position from the typhoon center were discussed. And at last, the variation and characteristics of observed frequency spectrum during the passage of Damrey were presented.

Keyword: wave spectrum, typhoon, SWAN, Beibu Bay, wave field

The third generation wave action model–SWAN (Simulationg Waves Nearshore, Booij et al. [1], 1999) was typically designed for wave simulations in the near-shore regions. It takes use of the most advaced wave reaserch achievements and has been applied to several theoretical and field conditions successfully (Rogers et al., 2002[2], 2003[3], 2007[4]; Holthuijsen et al.[5], 2003; Zijlema et al.[6], 2005). Typhoon-generated wave fields are of interest both scientifically for understanding wind-wave interaction physics and operationally for predicting potential hazard. A typhoon with intense and fast-varying winds forms a complex ocean waves field which can propagate thousands of kilometers away from the storm center, resulting in dramatic variation of the wave field in space and time. Waves under typhoon wind were simulated sucessfully by SWAN wave model (Ou et al.[7], 2002). For directional wave spectra under high wind conditions, considerable efforts have been made. Wyatt [8] (1995) described meausrements of the directional spectra of storm wave using high-frequency radar to explain the effect of fetch on the directional spectrum of Celtic Sea storm waves. Wright et al.[9] (2001) and Walsh et al.[10] (2002) studied the spatial variation of hurricane directional wave spectra for both open ocean and landfall cases using NASA Scanning Radar Altimeter for the first time. Holt et al. [11] (1998) examined the capability of synthetic

Received on April 24, 2009

Corresponding author: zhou5299@ouc.edu.cn

aperture radar imagery from ERS-1 satellite to track the wave fields from an intense storm. As a very important way, ocean wave modeling is a very useful and convenient way to obtain the spatial and temporal distribution of directional spectra without the limitations associated with measurements. Moon et al.[12] (2003) and Moon et al.[13] (2004b) investigated the directional wave spectra in deep water under hurricane conditions by WAVEWATCH III wave model.

Directional wave spectra in shallow water under high wind conditions are attracting for scientific reasearch and coastal engineering and different from those in deep water (Wu et al. [14], 1987). In this paper, SWAN was implemented in the Beibu Bay to investigate the directional wave spectrum in shallow water under typhoon wind forcing. During the typhoon passage, available buoy data including wind and wave are used to compare. Brief descriptions of the Beibu Bay, typhoon Damrey, wind fields, current and water elevation, buoy observed data and SWAN wave model are given in section I. Comparisons of the simulated typhoon-generated wave characteristics with observations are also given in this section. The characteristics of wave field, frequency spectra and directional spectra under typhoon wind forcing were discussed in section II. And section III gives the summary and conclusions.

1 Numerical simulation

1.1 Beibu Bay

Beibu Bay is situated at the continental shelf of China to the north, Vietnam to the west, Hainan Island to the east, and the open sea of the South China Sea to the south. Most area of the Beibu Bay is shallow and the depth on the continental shelf is less than 50 m, except the southeast sea area, which abuts to the open sea of the South China Sea (Fig. 1). In South China Sea, about 10 passages of tropical cyclones occur every year, which mainly occur in July and October, and the main propagation direction of TCs is west-forward. So the Beibu Bay is often subject to severe sea states generated by typhoons during the summer. For example, in 1989, six typhoons occured in South China Sea, and the propagation directions are all north-west forward (Fig. 1), where Typhoon Brenda and Gordon landed from Guangdong province, Typhoon Cecil landed in the south of Vietnam, and other three typhoons passed over the Beibu Bay and landed north of Vietnam. In general, typhoons act much more severely on the east coast of Hainan Island than on the west coast, since most of typhoons with the west-forward propagation direction approach Hainan Island from offshore of the east coast. And the intensities of the typhoons used to continue to degrade after landing on the coast.

1.2 Typhoon Damrey

Damrey (2005) formed as a tropical storm east of Philippine on 21 September and turned to northwest until 23 September. During the turn to west the storm was developed into a severe tropical storm at 20:00 on 23. It further intensified with the direction of southwest, and became a typhoon at 00:00 on 25 with the maximum wind speed (10-min averaged) of 42 m/s. It propagated to west with the translation speed of 10 - 15 km/h and striked Hailan Island on 26. Typhoon Damrey made a landfall on the

northern part of Vietnam at around 14:00 on 27 September and weakened into a severe tropical storm. Fig. 2 gives the track of Typhoon Damrey, and Fig. 3 gives a satellite image of Typhoon Damrey at 14:44 on 25 September 2005.

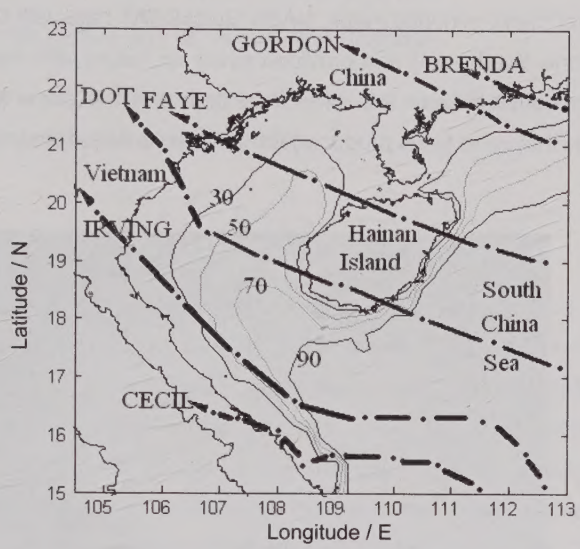

Fig. 1 Topography and typhoon paths (1989) of study area

(contours represent the water depth / m, and dot-line represent the paths of typhoon)

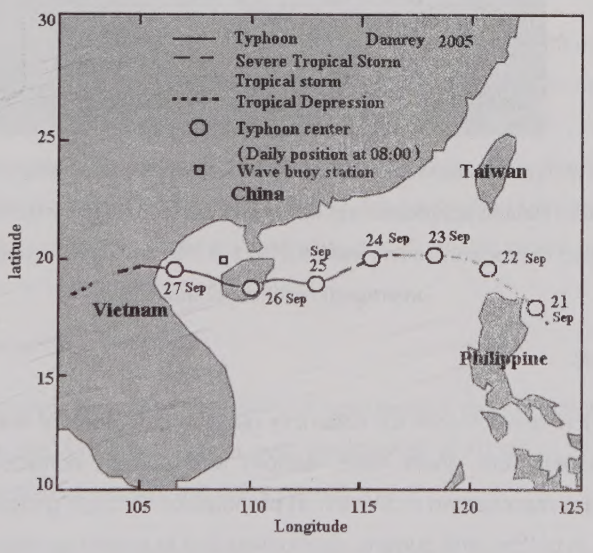

Fig. 2 Track of typhoon Damrey

(circles represent the position of typhoon center at 08:00 daily. The rectangle represents the location of buoy measuring wave and wind.)

1.3 Wind fields

Directional spectra associated with a typhoon are very complicated and have quickly varying

characteristics in time and space. Therefore, numerical modeling of sea surface directional wave spectra requires input wind data of high resolution. The surface wind fields for Typhoon Damrey used as input data to the wave model are objective reanalysis wind fields dataset, which are assimilated by many sources (including historical weather chart, synoptic maps, NASA QuickSCAT data with 0.25° resolution, Typhoon Annual and Tropical Cyclone Yearbooks) and provided every six hours with the resolution of 0.2°×0.2°. Comparisons were carried out between this wind field data and the observations (given in section 2.5), and the results show that wind fields produced from the assimilation method are in good agreement with the actual wind fields.

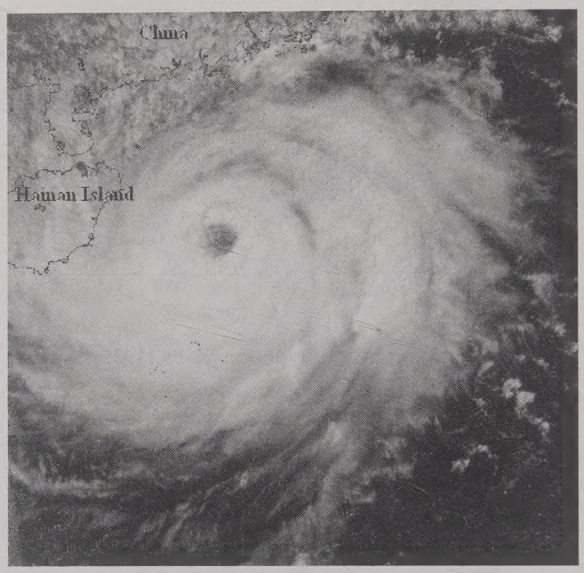

Fig. 3 Satellite image of Typhoon Damrey at 14:44 on 25 September 2005 when the typhoon center was located about 180 km east of Hainan Island and tracked westward (provided by Hainan province Observatory). At this time, the position of typhoon center was 19.0°N, 112.3°E, and the maximum wind speed (10-min averaged) reached 42 m/s.

1.4 Wave model SWAN

SWAN is a numerical wave model for obtaining realistic estimates of wave parameters in coastal areas, lakes and estuaries from given wind, bottom and current conditions. The following wave propagation processes are represented in SWAN: a) propagation through geographic space, b) refraction due to spatial variations in bottom and current, c) shoaling due to spatial variations in bottom and current, d) blocking and reflections by opposing currents, and e) transmission through, blockage by or reflection against obstacles.

The model is based on the wave action balance equation with sources and sinks, and the waves are described with the two-dimensional wave action density spectrum, even when nonlinear phenomena dominate in the surf zone. The spectrum is the action density spectrum $N(\sigma,\theta)$ rather than the energy density spectrum $E(\sigma,\theta)$, since in the presence of currents, action density is conserved whereas energy

density is not (Whitham[15], 1974). The action density is equal to the energy density divided by relative frequency

$$N(\sigma,\theta) = E(\sigma,\theta)/\sigma \tag{1}$$

Where σ is the relative frequency and θ is the wave direction.

The evolution of the wave spectrum is described by the spectral action balance equation which for Catesian coordinates is (Hasselmann et al. [16], 1973)

$$\frac{\partial N}{\partial t}+\frac{\partial}{\partial x}c_x N+\frac{\partial}{\partial y}c_y N+\frac{\partial}{\partial \sigma}c_\sigma N+\frac{\partial}{\partial \theta}c_\theta N=\frac{S}{\sigma} \tag{2}$$

The first term to the left-hand side of this equation represents the local rate of change of action density in time, while the second and third term represent propagation of action in geographical space with propagation velocities c_x and c_y in x and y space, respectively. The fourth term represents shifting of the relative frequency due to variations in depths and currents with propagation velocitiy c_σ. The fifth term represents depth-induced and current-induced refraction with propagation velocity c_θ. The expressions for these propagation speeds are taken from linear wave theory (Mei[17], 1983; Dingemans[18], 1997). S is the source term representing the effects of wind generation, dissipation and nonlinear wave-wave interactions, where dissipation mainly includes whitecapping, bottom friction and depth-induced wave breaking.

The grid in this study is regularly spaced by longitude-latitude grid, extending from 15° to 23° N, 105° to 113° E, and the spatial grid is 1/18° ×1/18°. The wave model used in this study use time step of 600s, wind input interval of 1h. The model input mainly includes wind, current and water level (described in section 1.6). Pierson-Moskowitz spectrum is suitable for sea waves fully developed, while JONSWAP spectrum is suitable for sea waves limited by fetch, that is, for developing process. Considering the water depth of the Beibu Bay that is shallow in generally, the boundary spectra shape in this study is adopted as JONSWAP with the power of high frequency tail of 4.

1.5 Buoy data and validation

During Typhoon Damrey, a buoy named SZF2-1 was located in the northwest sea area of Hainan Island (Fig. 2) to measure the winds and waves, with the location of 19°46′48.00″N, 109°07′24.00″E, and water depth of 19.5 m (here after, we call this point as 'C').

The observed data included wave height, wind speed and wind direction at 10 m height above the sea surface, which were used to compare model input and results. Fig. 4a compares the input wind speed with the observed data at point C from 26 September to 28 September. The root mean square (rms) errors between input and observed winds for this point are 3.8 m/s in speed and 28° in direction. Generally, the wind data for input are in good agreement with observation. Fig. 4b and Fig. 4c compare significant wave heights and mean wave periods between observations and model simulation at point C. The maximums of significant wave height and mean wave period reach 5.5 m and 8.4 s at 6:00 on 26 September

respectively, while the simulation data are smaller than observations. However the model and the observation are very similar. The estimated rms errors for significant wave height and mean wave period are 0.9 m and 1.2 s respectively. Fig. 4d compares measured and hindcasted one-dimensional frequency spectra at 06:00 on Sep 26, 2005. The spectral shape and peak frequency agrees well in general. However, for simulant 1-D spectrum, there is no second peak as observation in higher frequency.

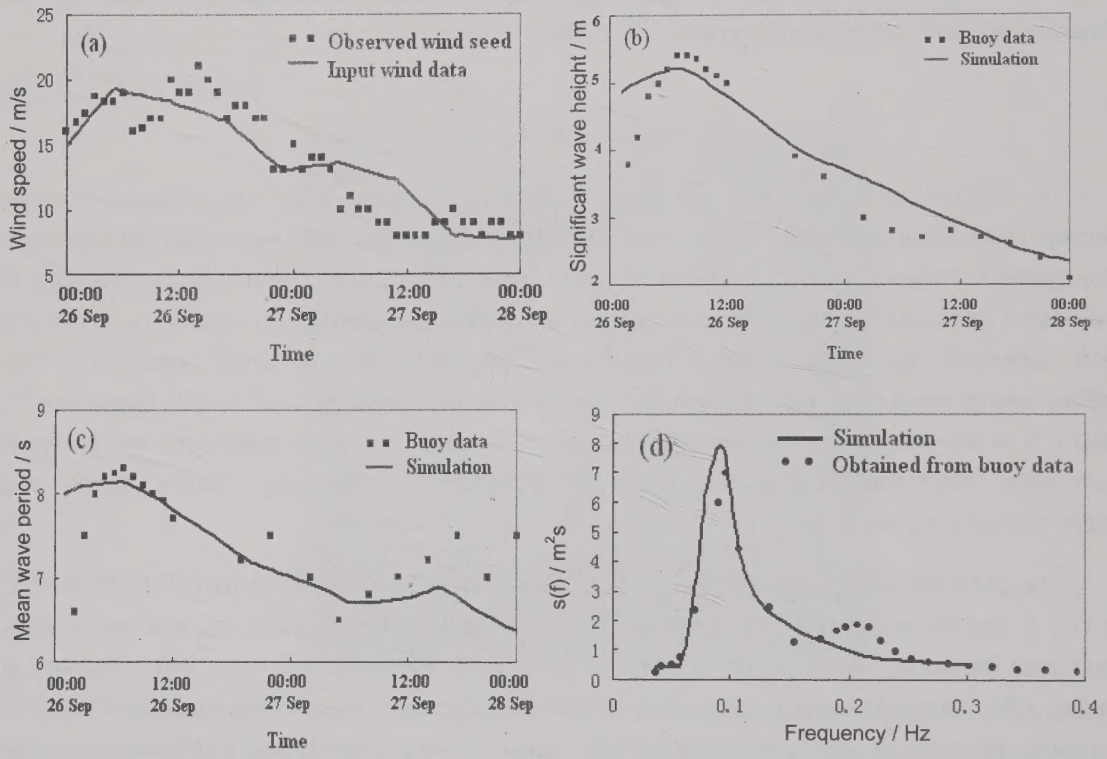

Fig. 4 Comparisons of a) wind speed for model input, b) significant wave height, c) mean wave period and d) wave frequency spectrum (06:00 on 26 Sep, 2005) of simulation results during Typhoon Damrey.

1.6 Current and water elevation

The current and water elevation used as input in this study are simulated by POM model, with the same spatial grid and interval as wind fields data. Also, many comparisons were carried out between observation and simulation of currents and tide elevation, and results indicate that the simulation data can describe the current and tide characteristics of the Beibu Bay well during the passage of typhoon Damrey.

2 Results and discussion

2.1 Wave field characteristics

Distributions of wave parameters such as significant wave height, mean wave period, mean wavelength and mean wave direction under typhoon wind forcing were discussed in this section. Fig. 5

shows distributions of significant wave height (Fig. 5a, contours), mean wave period (Fig. 5b, contours), mean wave length (Fig. 5c, contours) and mean wave direction (Fig. 5d, thick arrows) at 18:00 on 26 September 2005 simulated by SWAN model.

Typhoon winds are typically asymmetric due to the typhoon's movement. Winds are generally higher (lower) to the right (left) of the typhoon because the forward velocity of the storm adds to the wind velocity around the eye. In addition, the effective fetch and duration of the wave growth process are affected by the motion of the storm. The curvature of the wind field limits the fetch, but waves propagating in the direction of the storm motion remain under the influence of aligned wind for longer time and distance. Typhoon waves develop in the open sea and become much more threatening in the coastal waters where shoaling effects are dominating.

From Fig. 5, we find that all wave parameters are not symmetric about the center of the votex. Waves to the right and front of the hurricane track become trapped and waves are exposed to prolong forcing from the wind. As a result, higher and longer waves are formed to the right and front of the track with the same direction as the propagation of typhoon, while lower and shorter waves to the rear and left (Fig. 5a and b). In the rear half of the typhoon center, the dominant wavelength is considerably shorter related to the long wavelength located in the front half (Fig. 5c). The dominant waves propagate at significant angles in the left quadrants. It is noteworth that, being consistent with the significant wave height and the mean wave period, the mean wave length reaches a maximum near the eyewall structure coincident with the highest wind speeds and a little less within the eye.

2.2 Spatial variation of directional wave spectra

Typhoon produces complex and quickly varying wave spectra in space and time. In this section, wave spectra of eight points at 18:00 on Sep. 26, 2005 when typhoon Damrey arrived at 107.8°E, 19.4°N were given for discussion. These points were located in different quadrant with different distances from the typhoon eye (Fig. 6 and Tab. 1).

Tab.1 Locations and distances from typhoon eye for eight points

Point	Longitude / °	Latitude / °	Quadrant	Distance from eye
P11	108.3	20.0	I	R
P12	108.9	20.6	I	2R
P21	108.3	18.8	II	R
P22	108.9	18.2	II	2R
P31	107.3	18.8	III	R
P32	106.7	18.2	III	2R
P41	107.3	20.0	IV	R
P42	106.3	20.6	IV	2R

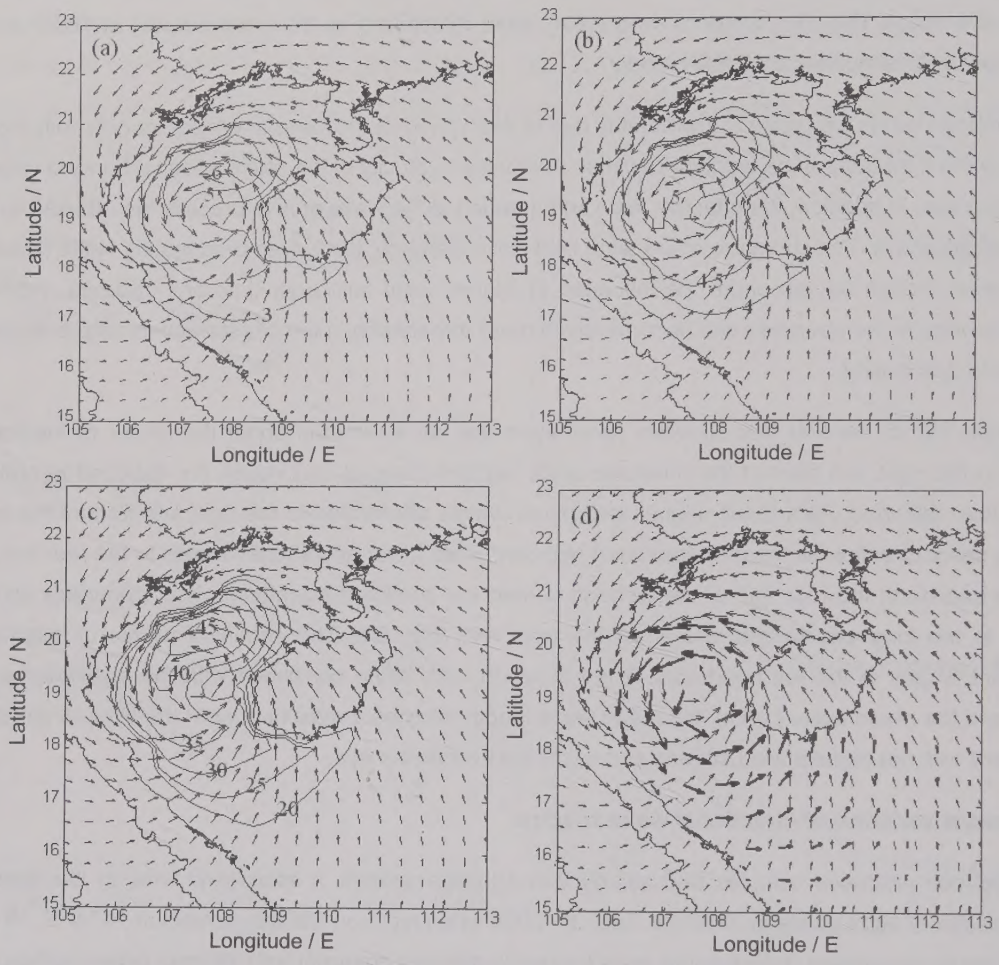

Fig. 5 The wind fields (vector) and spatial distributions of a) significant wave height (contours, m), b) mean wave period (contours, s), c) mean wave length (contours, m), and d) mean wave direction (thick arrows) at 18:00 on Sep. 26, 2005 when Typhoon Damrey center located at 107.8°E, 19.4°N. The direction of arrow represents the wind direction, and the arrow length is proportional to the wind speed.

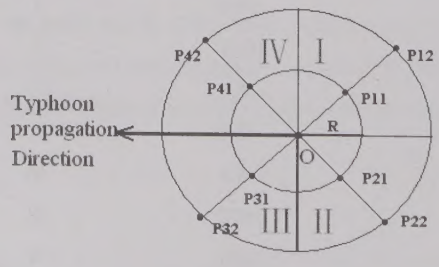

Fig. 6 Locations of eight points related to typhoon center. R is the maximum wind speed radii. The arrow represents the direction of typhoon translation (westward).

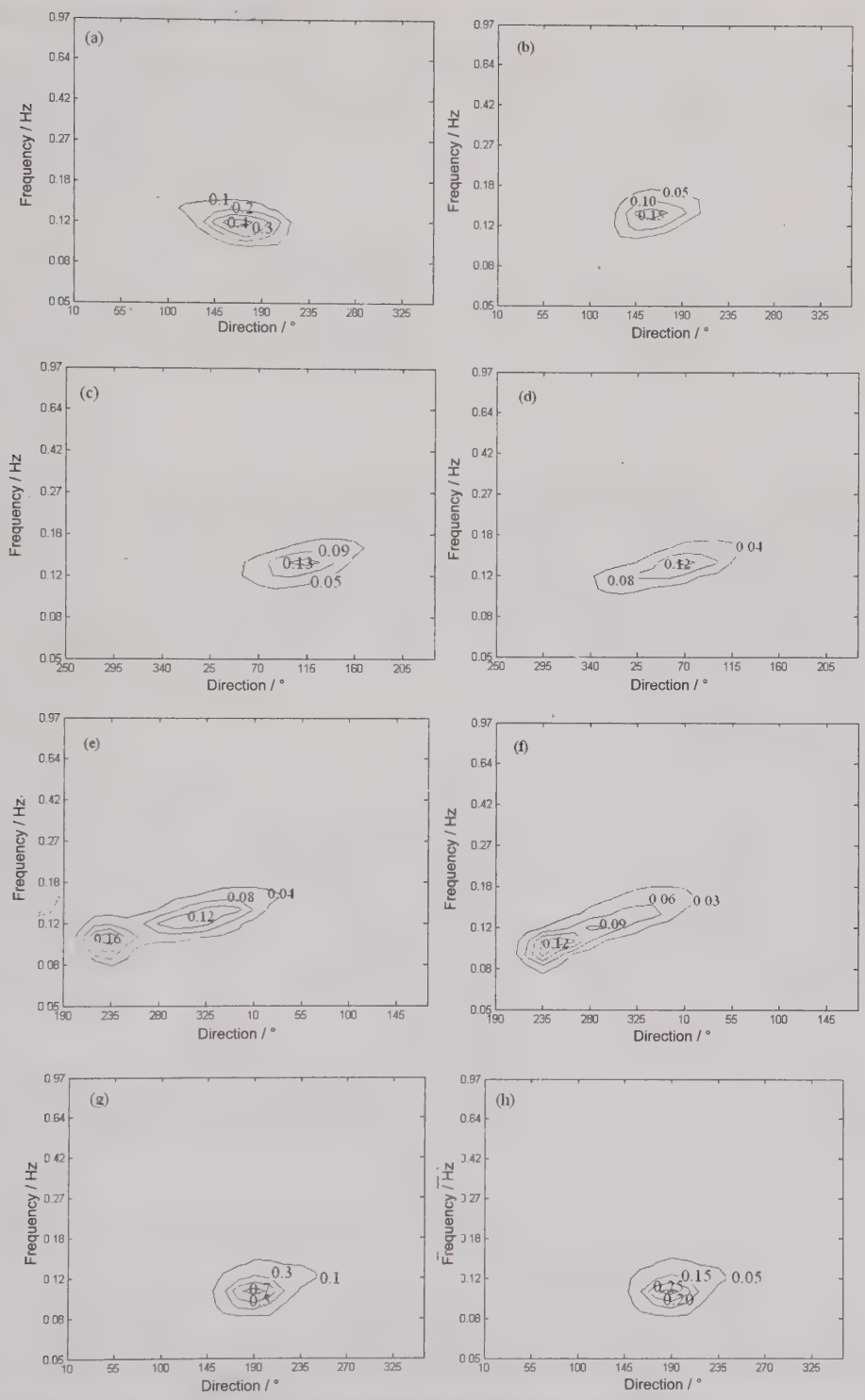

Fig. 7 Directional wave spectra $S(f,\theta)$ ($s^2Hz^{-1}degre^{-1}$) for point P11 to P42 (Fig. 7a to h) at 18:00 on Sep. 26, 2005 when typhoon Damrey arrived at 107.8°E, 19.4°N.

Fig. 7 gives the directional wave spectra for point P11 to P42 at 18:00 on Sep. 26, 2005. In all quadrants, the wave energy in quadrant Ⅳ is the most, then in quadrant Ⅰ and quadrant Ⅲ, where the value of wave energy in quadrant Ⅱ is the least. It is noticeable that in quadrant I and Ⅳ, wave energy at 2R locations is significantly greater than that of at R distance, while in quadrant Ⅱ and Ⅲ, the difference is small.

The peak wave direction in four quadrants are about 170°, 80°, 240° and 190° respectively (in this study, the wave direction is defined as waves going to and measured non-clockwise from positive-x as 0°), which shows that there exists a westward propagating swell in quadrant Ⅰ and Ⅳ. In quadrant Ⅱ, spectra for point 21 and point 22 contain a similar signature with northeast direction. In the southwest quadrant at location point 31 and point 32, the simulated spectra indicate a double peaks wave field with a southward propagating wave.

From the figure we may find such characteristics as following: firstly, wider directional spread is to the left of the typhoon (in quadrant II and III, Fig. 7c, d, e and f) and narrower spread is to the right of the typhoon (in quadrant I and Ⅳ, Fig. 7a, b, g and h); secondly, the wave spectra to the right of the typhoon show a unimodal swell system propagating in the direction of the typhoon translation, whereas the spectra in the rear and left of the typhoon display a more complex structure with two wave peaks, especially for point 31 and point 32 (in quadrant III).

2.4 Frequency spectrum characteristics at point C

Wind wave spectrum are related to the fetch, wind duration (wind direction), wind speed and water depth. Wave fields generated by typhoon are fetched limited out of question. In this section, the spectrum shape parameters such as spectrum width (defined as formula (3)), peak frequency, power of high frequency tail and double peaks et al. of observed data at point C are discussed. Here, the spectrum width *v* is expressed as

$$v = \sqrt{\frac{m_0 m_2}{m_1^2} - 1} \tag{3}$$

where m_0, m_1 and m_2 are the zeroth, 1th and 2th order moments of the spectrum respectively, and the *n*th order is

$$m_n = \int_0^\infty \omega^n s(\omega) d\omega \tag{4}$$

Fig. 8 gives the variations of peak frequency, peak frequency spectrum, high frequency power and spectrum width at obervation station from Sep. 26 to Sep. 28, 2005. From Fig. 8a and Fig. 8b, we find that before the coming of Damrey (from 00:00 to 12:00 on Sep. 26), the peak frequencies are low, while peak spectrum values are high. It indicates that the waves at point C dominated by swell. With Damrey's translation to north-west, the values of peak spectrum decrease, while at about 14:00 on Sep. 26, the peak frequency approaches to 0.26 Hz when Damrey is to the left of point C, and the waves is dominated

by wind-generated waves at this time.

For the well-known spectrum such as Pierson-Moskowitz spectrum and JONSWAP spectrum, the power of high frequency is -5. Kitaigorodskii et al. [19] (1975) pointed out that in the coastal water, the power of high frequency tail is about -3. From Fig. 8c, we may find that the power of high frequency at point C during Typhoon Damrey varies from -3 to -5, with the average value of about -4.2. Typhoon-generated waves are complicated and the spectrum width varies between 0.6 and 0.9 (Fig. 8d), which is wider than those of Pierson-Moskowitz spectrum and JONSWAP spectrum (0.425 and 0.389 respectively. Glazman [20], 1986).

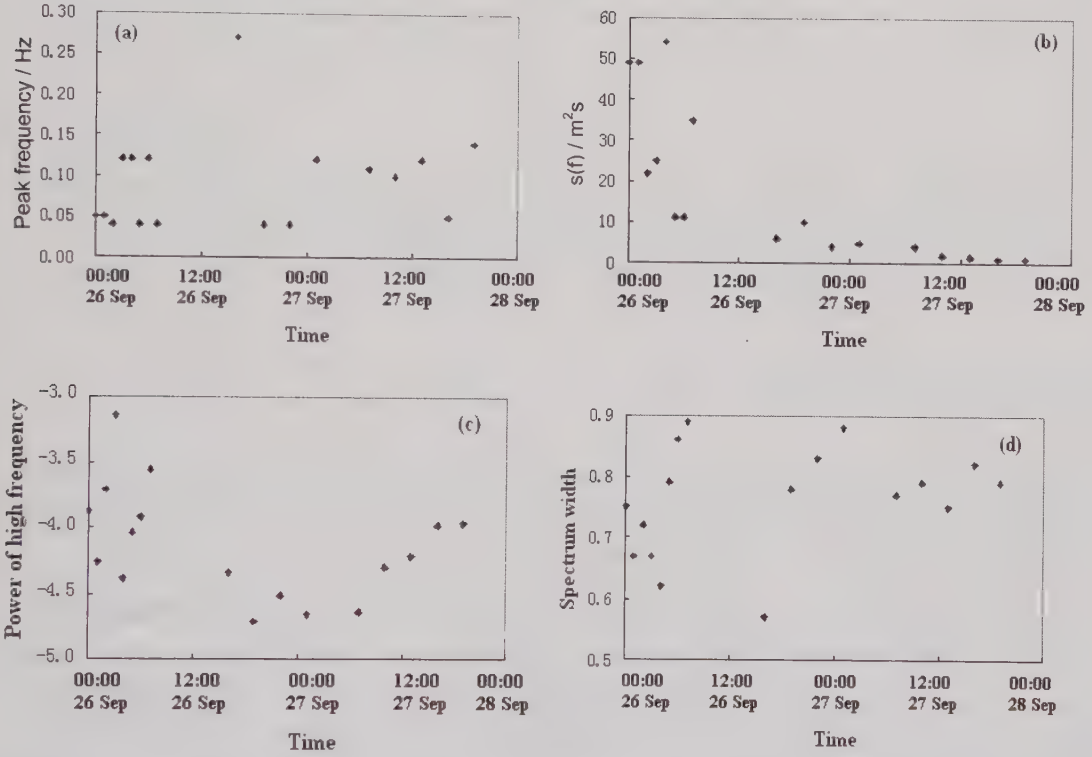

Fig. 8 Variations of a) peak frequency, b) peak frequency spectrum, c) high frequency power and d) spectrum width at obervation station from Sep. 26 to Sep. 28, 2005. Typhoon Damrey landed on the Hainan Island on Sep. 26 and on Vietnam on Sep. 28, 2005.

Both P-M spectrum and JONSWAP spectrum are single-peak wave spectra. However, wave spectra with double peaks often occur when wind waves and swell exist simultaneously, or wind direction change suddenly. Many studies were carried out to express the double-peaked wave spectrum (Strekalov et al. [21], 1972; Ochi and Hubble [22], 1976; Soares [23], 1984). Fig. 9 gives the wave spectrum of observation at point C corresponding to three different times. During the passage of Damrey, the wind-generated waves and swell exist simultaneously at this time, and three kinds of shapes of double-peaked spectra occur. At 04:00 when Damrey landed on Hainan Island, sea waves from south-east direction propagate from Qiongzhou Strait and south open mouth of the Beibu Bay to this station, then the waves dominated by swells with high

energy and most of the energy is concentrated on the low frequency peaks (Fig. 9a). At 14:00 on Sep. 26, the waves were dominated by both swell and wind wave, so the intensity of swell was equivalent to that of wind waves (Fig. 9b). When typhoon passed, the waves were dominated mainly by wind-wave and wave energy becomes very small (Fig. 9c).

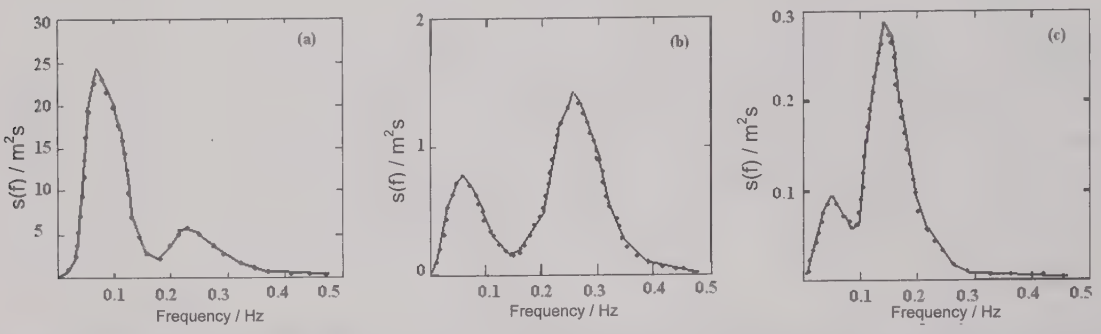

Fig. 9 Wave spectra of observation at a) 04:00 on Sep. 26, b) 14:00 on Sep. 26 and c) 08:00 on Sep. 27, 2005. Piont C is located to the right and front of typhoon center at 04:00 on Sep. 26 with the propagation of typhoon to north-west, and it is located in the right of typhoon center at 14:00 on Sep. 26, and to the right and hind of typhoon center at 08:00 on Sep. 27.

3 Summary and conclusions

The SWAN wave model was implemented to evaluate typhoon waves in the Beibu Bay during the passage of Typhoon Damrey, and objective reanalysis wind field dataset was adopted to derive the input cyclostrophic and gradient wind velocities for the wave model.

From the simulation results, distributions of wave parameters have such main characteristics as following: a) higher and longer waves are formed to the right and front of the typhoon track, while lower and shorter waves to the rear and left; b) in the left quadrants, the dominant waves propagate at significant angles with wind direction; c) consistent with the significant wave height and the mean wave period, the mean wave length reaches maximum near the eyewall structure coincident with the highest wind speeds and a little less within the eye.

From the Fig. 7 we may find such characteristics as follwing: firstly, wider directional spread is to the left of the typhoon (in quadrant II and III, Fig. 7c, d, e and f) and narrower spread is to the right of the typhoon (in quadrant I and Ⅳ, Fig. 7a, b, g and h); secondly, the wave spectra to the right of the typhoon show a unimodal swell system propagating in the direction of the typhoon translation, whereas the spectra in the rear and left of the typhoon display a more complex structure with two wave peaks, especially for point 31 and point 32 (in quadrant III).

For directional spectra, wider directional spread is to the left of the typhoon and narrower spread is to the right of the typhoon. The wave spectra to the right of the typhoon show a unimodal swell system propagating in the direction of the typhoon translation, whereas the spectra in the rear and left of the

typhoon display a more complex structure with both swell and wind wave peaks.

Because the wind-generated waves and swell exist simultaneously during the passages of typhoon, three kinds of double-peaked wave spectra occur, and wave spectra show wider spectrum width. In addition, power of high frequency varies between -3 and -5.

Comparisons of simulated waves and periods with measured data on the west coastal waters of Hainan Island have demonstrated agreement in general, which shows that using realistic wind forcing and a high-resolution wave model may give successful simulations of surface wave fields in coastal waters under high wind conditions. And this allows more complete analysis of the typhoon-generated wave field than do observations at limited time and space.

Acknoledgements

The authors thank to South China Sea Institute of Oceanology, Chinese Academy of Sciences for providing the wind fields, current and water elevation data during the passage of Typhoon Damrey.

References

[1] Booij R C, Ris L H, Holthuijsen. A third-generation wave model for coastal regions: 1, Model description and validation [J]. J. Geophys. Res., 1999, 104: 7 649 - 7 666.

[2] Rogers W E, Kaihatu J M, Petit H A H, et al. Diffusion reduction in an aritrary scale third generation wind wave model [J]. Ocean Eng., 2002, 29: 1 357 - 1 390.

[3] Rogers W E, Hwang P A, Wang D W. Investigation of wave growth and decay in the SWAN model: three regional-scale applications [J]. J. Phys. Oceanogr., 2003, 33: 366 - 389.

[4] Rogers W E, James M K, Larry H, et al. Forcasting and hindcasting waves with the SWAN model in the Southern California Bight [J]. Coastal Engineering, 2007, 54(1): 1 - 15.

[5] Holthuijsen L H, Booij N, Ris R, et al. SWAN cycle-III version 40.20 User manual, 2003, 124pp.

[6] Zijlema M, Westhuysen A J V. On convergence behaviour and numerical accuracy in stationary SWAN simulations of nearshore wind wave spectra [J]. Coast. Eng., 2005, 52: 237 - 256.

[7] Ou Shan-Hwei, Liau Jian-Ming, Hsu Tai-Wen, et al. Simulating typhoon waves by SWAN wave model in coastal waters of Taiwan [J]. Ocean engineering, 2002, 29(8): 947 - 971.

[8] Wyatt L R. The effect of fetch on the directional spectrum of Celtic Sea storm waves [J]. J. Phys. Oceanogr., 1995, 25:1 550 -1 559.

[9] Wright C W, Walsh E J, Vandemark D, et al. Hurricane directional wave spectrum spatial variation in the open ocean [J]. J. Phys. Oceanogr., 2001, 31: 2 472 - 2 488.

[10] Walsh E J, Wright C W, Vandermark D, et al. Hurricane directional wave spetrum spatial variation at landfall. J. Phys. Oceanogr., 2002, 32:1 667 - 1 684.

[11] Holt B, Liu A K, Wang D W, et al. Tracking storm-generated waves in the northeast Pacific Ocean with ERS-1 synthetic aperture radar imagery and buoys [J]. J. Geophys. Res., 1998,103 (C4): 7 917 - 7 929.

[12] Moon I J, Ginis I, Hara T, et al. Numerical simulation of sea-suface directional wave spectra under hurricane wind forcing [J] J. Phys. Oceanogr., 2003, 33: 1 680 - 1 706.

[13] Moon I J, Ginis I, Hara T. Effect of surface waves on air-sea momentum exchange. Part II: behavior of drag coefficient under tropical cyclones [J] J. Atmos. Sci., 2004b, 61:2 334 - 2 348.

[14] Wu Yongcheng, Wang Yimou, Li Lei. The spectrum characteristics of Bohai Bay wind waves under the influence of cold waves [J]. Chin. J. Oceanol. Limnol., 1987, 5(4): 370 - 378.

[15] Whitham G B. Linear and nonlinear waves [M]. Wiley, New York, 636p, 1974.

[16] Hasselmann K, Barnett T P, Bouws E, et al. Measurements of wind-wave growth and swell decay during the Joint North Sea Wave Project (JONSWAP) [J]. Dtsch. Hydrogr. Z. Suppl., 1973, 12, A8

[17] Mei C C. The applied dynamics of ocean surface waves [M]. Wiley, New York, 740 p. 1983.

[18] Dingemans M W. Water wave propagation over uneven bottoms [M]. Part I –linear wave propagation, *Advanced Series on Ocean Engineering*, 13, World Scientific, 471 p. 1997.

[19] Kitaigorodskii S A, Krasitskii V P, Zaslavskii M M. On Phillips' theory of equilibrium range in the spectra of wind-generated waves [J]. J. Phys. Ocearogr., 1975, 5(5): 410 - 420.

[20] Glazman R E. Statistical characterization of sea surface geometry for a wave shope field discontinuous in the mean square [J]. J. Geophys. Res., 1986, 91 (C5): 6 629 - 6 641.

[21] Strekalov S S, Tsyploukhin V P, Massel S T. Structure of sea wave frequency spectrum. Proceedings of 13th Coastal Engineering Conference, 1972, (1): 307 - 314.

[22] Ochi M M, Hubble E N. Six-parameters wave spectra. Proceedings of 15th Coastal Engineering Conference. 1976, (1): 301 - 328.

[23] Soares C G. Representation of double-peaked sea wave spectra [J]. Ocean Engineering. 1984, (11):185 - 207.

利用 SWAN 波浪模式研究北部湾海域台风浪场的波浪方向谱特征

周良明[1]，王爱方[2]，王智峰[3]，郭佩芳[1]，高劲松[3]

（1. 中国海洋大学 物理海洋实验室，山东 青岛，266100；2. 中国海洋大学 工程勘察设计开发院，山东 青岛，266071；
3. 中国海洋大学 海洋环境学院，山东 青岛，266100）

摘 要：以高精度再分析风场为驱动，利用 SWAN 模式模拟了台风“达维” Damrey (2005) 经过北部湾海域时的波浪场。通过与实测的风和波浪实测对比发现，波浪后报结果与实测结果符合较好。文章给出了台风浪期间波高、周期、波长和波向等要素的分布特征，讨论了以台风眼为中心不同海域的波浪方向谱特征。本文最后分析了台风期间实测波浪能谱的变化特征。

关键词：能谱、方向谱、台风、SWAN 模式、北部湾

Impacts of global warming on marine zooplankton

ZHANG Da-juan, LI Shao-jing*, GUO Dong-hui

College of Oceanography and Environmental Science, Xiamen University, Xiamen 361005, *Fujian Province, China*

Abstract: Global warming has been being a serious issue since 1980, and it impacts environment and biosphere. Here, we reviewed the physiological and ecological responses of marine zooplankton which is an important component of biosphere to the global warming. Much research on physiological changes in response to different temperature is given to discuss this issue. Furthermore, we focused on ecological changes of zooplankton to global warming and several indices such as abundance, biomass, biodiversity and biogeographic boundary are enumerated. Phenological changes of zooplankton were presented, followed by the prospects of this subject, viz. observing more functional groups, more concerning on zooplankton in tropical region and investigation on a species-level zooplankton system.

Keyword: global warming, zooplankton, physiological activities, abundance, biodiversity, phenology

1 Introduction

In this review, we examined the studies which concern on the responses of zooplankton to global warming. It is not exhaustive but to emphasize the studies in which global warming has had obvious impacts on zooplankton. All the references we cited tell us that the studies about global warming impacts on zooplankton are just beginning. Previous works mainly focused on copepods response to global warming [1-5], and we put some other marine functional groups under consideration in this review, including cladoceran, euphausiid, foraminifera and jellyfish to illuminate this question.

There is superfluous CO_2 discharged every year because of burning fossil fuel and forest coverage rate decreased, which lead to global warming. At present, the average atmosphere temperature is 0.4 - 0.8 °C higher than that in the 19th century and it will increase 1.4 °C - 5.8 °C by the end of this century [6, 7]. It not only aggravates the physical factors such as sea-level [8 - 10], sea surface temperature (SST), desalination [11] and stratification of seawater [12, 13], but also directly or indirectly influences on the physiological and ecological processes of marine organisms. Recently, much research focuses on zooplankton in response to global warming for several reseaons: 1) zooplankton has short life cycles, widespread and drifting in water under the actions of water movement, in that case, zooplankton can be tight coupled with climate and marine environmental changes, especially temperature and currents; 2) unlike fishes and intertidal organisms, few zooplankton (except *Acetes* and some jellyfishes) are commercially exploited, so their abundance are unaffected by fishing effort. Long time series of trends in

Received on March 23, 2010

Corresponding author: zhangdj@xmu.edu.cn

response to environmental changes of zooplankton are generally not confounded with the trends in exploitation [5, 14, 15].

2 The impacts of global warming on zooplankton physiological processes

Most marine organisms prefer to live in the region where the temperature closes to the tolerance upper limit, and the rising SST would impact zooplankton obviously. On the one hand, increased temperature would impact the biological functions by destroying biological proteins and membrane fluidity, on the other hand, it represents on the changes of respiration rate, metabolic rate, growth rate and development rate, all of these changes varied in different species and different life stages.

Studies on the impacts of increasing SST on physiological processes of marine organisms focus on corals [16 - 20], benthic bivalvia[21] and several commercial fishes[22, 23]. However, few previous investigations focus on zooplankton. The growth rate of zooplankton individuals is affected by temperature and their body size [24 -26]. Huntley proves that: if sufficient food was provided, the temperature could explain more than 90% of the variance of the growth rate. In California, the body size of zooplankton in the warmer regions is smaller than in the normal temperature regions. Because increased SST makes individuals grow faster, and the time develops to sexual maturity shorter [27].We speculate that zooplankton may incline to miniaturization accompanied with the increased SST. Frost points out that the effect of development time of *Calanus pacificus* to sexual maturity on population size is more important than that on brood size, the population structure will be changed with the increasing SST [28]. During 1979 - 1997, the biomass of jellyfish, especially Scyphozoa and Hydromedusae in Bering Sea, gradually increased with the reduction of ice covered area and duration. It is clear that jellyfishes, owing to their rapid growth rate and short generation time, could easily become a dominant component of pelagic ecosystems. The environmental conditions, especially the temperature impacts the growth rate of organisms, but the mechanism is ambiguous [29]. Besides the growth rate, increased SST also impacts spawning rate. Purcell points out that the spawning rate of *Chrysaora quinquecirrha* in warmer water (20 °C, 25 °C and 30 °C) is higher than that in 15 °C water [30].

Global warming not only impacts on physiological processes of marine zooplankton but also on its abundance, biomass, community structure and other ecological processes. Because zooplankton composition in the tropic regions is richer and steadier than that in the temperate regions, it is not easily disturbed by the change of marine environmental conditions. The ecological impacts of global warming on zooplankton are more obvious, hence, we are concerned with zooplankton which live in high latitude regions [5].

3 The impacts of global warming on zooplankton abundance and biomass

With global warming aggravating, some zooplankton assemblages increased abnormally but other species decreased or even disappeared. In Antarctic Peninsula, the abundance of *Salpa thompsoni* has

negative correlation with the extension of ice covered area. With global warming aggravating, its abundance increased obviously. Because of food competition between *S. thompsoni* and *Euphausia superba*, the recruitment of latter species had decreased [31, 32]. After analyzing 15 jellyfishes and ctenophora, Purcell et al. point out that the abundance of 11 species has increased with the increasing temperature but not the other 4 species, and most of these increased species are temperate species [30]. The reason is that the damage of increasing temperature on tropic species is more serious than that on temperate species. Generally speaking, the dominant species in cold and temperate regions are macrozooplankton and microzooplankton, respectively. If the community structure changed, the food web would be changed as well. *Alle alle* is a macrozooplanktonivorous seabird in Antarctic sea, while the presence of small zooplankton redirects the food chain to plankton – eating fish, up through to fish - eating birds *Uria* sp., which changed the nutrition transportation and impacted the higher trophic levels [33].

The compositions of copepod [34, 35], pteropod [36], heteropod [37], krill [38, 39] and ostracod [40] in the East China Sea changes too. The abundance of warm-temperate species of each group has increased. It occurred associated with decreased abundance of other eurythermic and colder species. In El Niño year (1982), the spring abundance of zooplankton in Taiwan strait was higher than in 1984 (not El Niño year), because the intensities of longshore currents, kuroshio, Taiwan warm current were stronger in El Niño year [41]. Furthermore, Huang et al. point out that the summer abundance of copepods of Taiwan straits in 1997(El Niño year) is one times higher than that in 1994 (not El Niño year) [42]. The same result is proved in Bering Sea too. The average abundance of Calanoida in the southeast of Bering Sea is higher in the El Niño year (1997) than in1998 and in 1999. The abundance of Calanoida in 1999 is only 8% - 52% of 1998 and 1997. All of these results suggest that high abundance is with high water temperature [43]. El Niño-Southern Oscillation (ENSO) is complex, and the difference of zooplankton abundances between El Niño year and not El Niño year depends on several factors, such as the intensities of upwelling, current and runoff.

Most researches confirm that the responses of zooplankton to environmental factors in the middle and the high latitude region are much obvious after regime shift. Regime shift has been used to describe the large, decadal-scale switches in the abundance and composition of plankton and fish. At present, it can be defined as an abrupt change in a marine ecosystem and abiotic environmental factors from one stationary state to another, or from one stable equilibrium system changes to another one[44]. Several studies suggest that there was an ecosystem regime shift in the North Sea during 1982 - 1988[45, 46].The evidences are observed from the key ecosystem parameters, individuals to species composition. For example, the warm-temperate species of zooplankton increased associating with the decreased of the colder-water species after regime shift happened. That is because the ecosystem has changed to a warmer equilibrium which is more suitable for the growth of warm-temperate species.

Abundance is the numbers of zooplankton individuals, but biomass is the weight reflection of them. Except anthropogenic contamination, hydro-meteorological factors and ocean currents also impact the abundance and biomass of zooplankton. These two explanations are approved in different regions. During

1993~2003, the zooplankton biomass significantly decreased with the increased temperature in Cudillero, where is the shelf-break station of the Biscay bay in Spain without upwelling, but in Coruna(exist upwelling), zooplankton biomass had no significant changes. The stratification can prevent the supplement and circulation of nutrition into the upper surface. If this oligotraphic state persisted for a long time, the microbial loop would be reinforced and the food web would be changed. *Temora stylifera* is a representative species of the "summer-autumn group" in the Biscay bay, its abundance increased in Cantabrian region but not in Galicia where the upwelling is stronger. In the upwelling region of Guinea, the average zooplankton biomass negatively correlated with SST, and it can explained 82.2% of varieties of zooplankton biomass [47]. *Calanoides carinatus* is an important part of zooplankton biomass in Guinea upwelling region. Global warming can impact its biomass through the tropic Atlantic pressure fields, and then impacts fishery resource further through bottom-up process [48]. Dippner analyses the biomass of *Acartia* spp.、*Centropages hamatus*、*Temora longicornis*、*Evadne nordmanni*、*Podon elongatus*、*Bosmina longispina* and *Syncheata* spp. in the centre of Baltic sea, then points out that the biomass spring of *Acartia* spp.、*E. nordmanni*、*Podon* spp.、*Syncheata* spp. and *T. longicornis* had correlated with SST, but not in summer and winter, high spring biomass with high SST [49].

4 The impacts of global warming on zooplankton biodiversity and community structure

The response of zooplankton on increased SST depends on the place where they live, environmental conditions and their physio-ecological characteristics. Only Piontkovski & Landy have worked on the changes of zooplankton biodiversity in the tropic Atlantic [4]. They point out that during 1963~1989 the biodiversity of zooplankton had no statistical variation but linear relationship with SST. The increased SST impacts the South Atlantic High, the Azores High and the El Niño-Southern Oscillation, and these 3 parameters could explain 87% of zooplankton species diversity fluctuations. The maximal value of copepod species diversity index is mostly associated with maximal positive SST.

The biodiversity of Calanoida in the Northeast North Sea increased, and it has positively correlated with NAO and the Northern Hemisphere Temperature (NHT). After analyzing the relationship between hydrological climatic factors and copepods (e.g. *Calanus fimarchicus* and *C. heleolandicus*) in the Northeast Atlantic, Beaugrand & Ibañez find out that the long term series of zooplankton diversity have changed because the increasing SST of western European basin [2]. The diversities of colder-water, subarctic and arctic species(*Aetideus armatus*, *Heterorhabdus norvegicus* and *Calanus hyperboreus*) decreased during 1960 - 1999, but the diversity of warm-temperate species like *Euchaeta gracilis*、*Euchaeta acuta* and *Undeuchaeta plumosa* increased and had high positive correlation with NHT, and the copepods community reorganized.

The species number of copepods in the Sevastopol Coast (Black Sea) decreased from 13 in 1976 to 7 in 1990, and the community structure has changed as well[1]. Rutherford et al analyze the distribution of planktonic foraminifera around the world, and their results show that its diversity does not strictly adhere to the model of gradually decreasing from equator to polar. Instead, its diversity peak is in the middle

latitudes in all oceans. The distribution model depends on the surface seawater physical structure. Its biodiversity has a greatly positive correlation with the temperature at depths of 0, 50, 100 and 150 m. The SST could explain nearly 90% of the geographic variation of planktonic foraminifera diversity throughout the Atlantic ocean. The distribution model of planktonic foraminifera will be changed with the increased SST [50].

5 The impacts of global warming on the biogeographic boundaries of zooplankton

Another important representation of regime shift in marine ecosystem is the biogeographic boundary shifts of some zooplankton assemblages. After regime shift in the North Sea, the biogeographic shift of the warm-water species have occurred with a northward extension of more than 10° along European continental shelf latitude associated with a decrease in the number of colder-water species[3,46]. Meanwhile, the warm-water species, *C. helgolandicus* replace *C. finmarchicus* became the dominant species. *Centropages chierchiae* and *Temora stylifera* mainly distributed in the Iberian peninsula of the northeast Atlantic in the 1970s and 1980s, and after 1990s, they changed to English channel, and the distribution boundary extended to northward about 6° latitudes, and it moved 200 km every decade[51].

There are three copepod assemblages in the northeast Pacific, "south" copepods(*Paracalanus parvus, Mesocalanus tenuicornis,Clausocalanus* spp. and *Ctenocalanus vanus*),"boreal shelf" copepods(*Calanus marshallae, Pseudocalanus mimus* and *Acartia longiremis*) and "subarctic"copepods(*Neocalanus cristatus, Neocalanus plumchrus, Eucalanus bungii* and *Metridia pacifica*).The composition of zooplankton around the Vancouver island in 1970s mainly included boreal shelf species and south species. Till early 1990s, owing to SST rising, the distribution range of boreal species retracted polarward, while the south species have extended polarward. During 1999 - 2002, the La Niña event occurred, and SST declined sharply and the zooplankton community of southern Vancouver Island reverted to a species assemblage similar to the late 1970s. Since 2003, there was a return to 1990s, the distribution region of the boreal species shrunk [11]. Recent references prove that there is another regime shift in the northeast Pacific during 1998 to 1999. However, before the regime shift occurred, there was a SST rising phenomenon in 1997. The results of CPR (Continuous Plankton Recorder) from the bay of Alaska to California suggest that, the geographic boundaries of temperate species have extended northward, and the boreal species retracted [14]. During the past 50 years, the temperature of the Narragansett Bay has increased about 1.2 °C, and *Mnemiopsis leidyi*, which originally distributed in the south warmer region of this bay, had expanded its distribution range [52]. The competition between invasive and native species may cause multiple effects which involve overall ecosystem functioning such as material flow between trophic levels, primary production relative extent of organic material decomposition, extent of benthic-pelagic coupling [53].

6 The impacts of global warming on zooplankton phonologies

Phenology is used to describe the life cycle of organisms such as migration and breeding times, which is more sensitive to the climatic change [54, 55]. Root et al. find out that the phenology of invertebrates, amphibians, birds and trees has changed 3 - 6 d during the last 100 years, but the average change of zooplankton was 7.6 d per decade, and the changing range is sharply higher than terrestrial organisms[56].

At present, the main monitor indicators of phenology are abundance peak and breeding time [11]. Edwards & Richardson analyze the phenologies of five planktonic functional groups including 66 species plankton in the North Sea, They point out that the summer abundance peak of meroplankton, dinoflagellates, copepods and non-copepod holozooplankton during 1958 - 2002 have moved forward by 27d, 23d, 10dand 10d respectively[55]. The phenologies of diatoms, copepods and non-copepod holozooplankton have positive correlations with SST, but not other functional groups. The correlation coefficients are 0.31, 0.55 and 0.34, respectively. In this region, the response of different groups on global warming is different, which cause the trophic levels mismatch. This phenomenon had also been observed in the upwelling region of Guinea Sea [48].

List Tidal Basin is a semi-closed bay in the Wadden Sea of southeastern North Sea. The water temperature of this bay has increased 0.04 °C per year during 1984 to 2005. The increased temperature not only advanced the development time of zooplankton but also extended the time for development [57]. *Neocalanus plumchrus* is an important species of mesozooplankton in the subarctic region of Pacific ocean, and its abundance peak is significantly correlated with SST, and the peak in the warmer and colder year commonly appear in the May and July, respectively [58], and the peak time is correlated with the temperature of that year [11].The response of biological phenology to the climatic changes depends on different species and different stages. In the Narragansett bay, *Acartia tonsa* and *Acartia hudsonica* are the dominant species of summer and winter, respectively. During the past 50 years, *A. tonsa* had no response to the increased SST, still maintained the origin succession type, but the abundance peak of *A. hudsonica* advanced from April to March, and the disappear time advanced from the middle of July or August to June or the beginning of July. This is because *A. tonsa* lays diapause eggs in deep sea and in winter, but *A. hudsonica* lays diapause eggs when the temperature higher than 15 °C, and the impact of global warming on the latter species is stronger. *M. leidyi* which preys on *A. tonsa*, is another important species in this region, and it appears that time in spring advanced 51 d, then there is mismatch between the prey and predator [52] (Tab.1).

The response of phenology on global warming depends on two factors: one is the species characteristics, e.g. merozooplankton is more sensitive than holozooplankton [15, 55]; the other one is the specificities, if the increased temperature coincided with the important life stages of species (such as breed or development of larva), the impacts would be more serious, vice versa.

7 Prospects

Global warming causes changes not only on marine environmental conditions but also on the physiological and ecological adaptabilities of marine zooplankton. Zooplankton can respond to global warming quickly owing to its physiological and ecological specificities. Zooplankton researchers want to answer basic questions associated with global warming, such as whether jellyfishes or ctenophores will become dominant species; whether large crustaceans will be replaced by smaller ones; whether the number of meroplankton of benthic species will change. Only investigating one or two functional groups are not sufficient. Many other important zooplankton groups, such as jellyfishes, salps should be taken more attentions. On the other hand, Global warming is associated with some other environmental factors, such as seawater acidification and desalination. The interaction effects should be considered seriously. We need to build appropriate models to illuminate this complex question. Meanwhile, we should cooperate with ecosystem modelers, and they will not only help answer our questions concerning the impacts of global warming, but they will also provide a better understanding of the feedback mechanism between marine ecosystem and climate [5].

Tab. 1 The impacts of global warming on phonologies of zooplankton

Research groups	Region	Period	Observation	References
Meroplankton (seven taxa)	the North sea	1958 - 2002	Peak 27 days earlier in summer	[55]
Copepods (twelve taxa)	the North sea	1958 - 2002	Peak 10 days earlier in summer	[55]
Holoplankton exclude copepods	the North sea	1958 - 2002	Peak 10 days earlier in summer	[55]
Copepods	List Tidal Basin	1984 - 2005	Appear 15 days earlier in spring	[57]
Mneiopsis leidyi	Narragansett bay	1951 - 2003	Appear 51 days earlier in spring	[52]
Acartia hudsonica	Narragansett bay	1951 - 2003	Appear time advanced from April to March	[52]
Acartia tonsa	Narragansett bay	1951 - 2003	No changes	[52]
Neocalanus plumchrus	Subarctic of Pacifica	1956 - 1997	Abundance peak 60 days earlier	[52]
Evadne spp.	Helgoland	1975 - 1999	Abundance peak 36.8 days earlier	[59]

As mentioned above, most researches are concerning with the temperate regions or high latitude regions. The studies about zooplankton in the tropical regions are rare, and most of them are from upwelling areas. Although observed and projected warming is greatest towards the poles [60], there is substantial warming in equatorial regions[5]. The tropical region, which dominates much of the world's ocean, is very important in the system of response to global warming. The research on the different functional groups in these regions is necessary.

Although functional groups are important, a species-level zooplankton observing system is necessary. Firstly, there are several papers on physiological changes of zooplankton, but most of them are mainly focus on the ecological changes. The physiological response needs more attentions, especially the physiological mechanisms. Secondly, the phenology is an important index of the response system. The response of phenology of different species to global warming is nonsynchronous, hence, how long the species can adapt to global warming or recover to the synchronous development stage needs more studies in the near future. Thirdly, the generation time of zooplankton is short, whether microevolution occurs during the period of adapt to new conditions or doesn't need more investigations.

Acknowledgements

We are grateful to Prof. Jiaqi HUANG of Xiamen University for valuable suggestions and constructive criticisms. We also thank Zhihuan XU and Xueli ZHANG for perfecting this manuscript.

References

[1] Gubanova A D, Prusova I Y, Shadrin N V, et al. Dramatic change in the Copepod community in Sevastopol Bay (Black Sea) during two Decades (1976 - 1996). Senckenb. Marit., 2001, 31: 17 - 27.

[2] Beaugrand G, Ibañez F. Spatial dependence of calanoid copepod diversity in the North Atlantic Ocean [J]. Mar. Ecol. Prog., Ser. 2002, 232: 197 - 211.

[3] Beaugrand G, Reid P C, Ibañez F, et al. Reorganization of North Atlantic marine copepod biodiversity and climate [J]. Science, 2002, 296: 1 692 - 1 694.

[4] Pionkovski S A, Landry M R. Copepod species diversity and climate variability in the tropical Atlantic Ocean [J]. Fish. Oceanogr. 2003, 12(4/5): 352 - 359.

[5] Richardson A J. In hot water: zooplankton and climate change [J]. ICES J. Mar. Sci., 2008, 65: 1 - 17.

[6] IPCC. A Contribution of Working Groups I, II, and III to the Third Assessment Report of the Intergovernmental Panel on Climate Change [M]. UK: Cambridge University Press, 2001.

[7] Levitus S, Antonov J I, Wang J, et al. Anthropogenic warming of earth's climate system [J]. Science, 2001, 292: 267 - 270.

[8] Cabanes C, Cazenave A, Provost C L. Sea Level Rise during past 40 years determined from satellite and in situ observations [J]. Science, 2001, 294: 840 - 842.

[9] Boyd P W, Doney S C. Modelling regional responses by marine pelagic ecosystems to global climate change [J]. Geophys. Res. Let. 2002, 29(16): 53-1 - 53-4.

[10] Meehl G A, Washington W M, Collins W D, et al. How much more global warming and sea level rise [J]. Science, 2005, 307: 1 769 - 1 772.

[11] Mackas D L, Batten S, Trudel M. Effects on zooplankton of a warmer ocean: Recent evidence from the Northeast Pacific [J]. Prog. Oceanogr., 2007, 75: 223 - 252.

[12] Quéré C L, Aumont O, Monfray P, et al. Propagation of climatic events on ocean stratification marine biology and CO_2 case studies over [J]. Geophys. Res., 2003, 108: 5-1 - 5-17.

[13] Hashioka T, Yamanaka Y. Ecosystem change in the western North Pacific associated with global warming using 3D-NEMURO [J]. Ecol. Model., 2007, 202: 95 - 104.

[14] Batten S D, Welch D W. Change in oceanic zooplankton populations in the north-east Pacific associated with the possible climatic regime shift of 1998/1999 [J]. Deep-Sea Res. II , 2004, 51: 863 - 873.

[15] Hays G C, Richardson A J, Robinson C. Climate change and marine plankton [J]. Trends Ecol. Evol., 2005, 20(6): 337 - 344.

[16] Hoegh-Guldberg O. Climate change, coral bleaching and the future of the world's coral reefs [J]. Mar. Fre. Res., 1999, 50: 839 - 866.

[17] Rosenberg E, Ben-Halm Y. Microbial diseases of corals and global warming. Env. Microbiol., 2002, 4(6): 318 - 326.

[18] Hughes T P, Baird A H, Bellwood D R, et al. Climate change, human impacts, and the resilience of coral reefs. Science, 2003, 301: 929 - 933.

[19] Ayre D J, Hughes P. Climate change, genotypic diversity and gene flow in reef-building corals [J]. Ecol. Let., 2004, 7: 273 - 278.

[20] Obura D O. Resilience and climate change: lessons from coral reefs and bleaching in the Western Indian Ocean. Estuar [J]. Coast. Shelf Sci., 2005, 63: 353 - 372.

[21] Roy K, Jablonski D, Valentine J W. Climate change species range limits and body size in marine bivalves [J]. Ecol. Let., 2001, 4: 366 - 370.

[22] McDonald M E, Hershey A E, Miller M C. Global warming impacts on lake trout in arctic lakes [J]. Limnol. Oceanogr., 1996, 41(5): 1 102 - 1 108.

[23 Mooij W M, De Senerpont Domis L N, Hülsmann S. The impact of climate warming on water temperature, timing of hatching and young-of-the-year growth of fish in shallow lakes in the Netherlands [J]. J. Sea Res., 2008, 615: 1 - 12.

[24] Huntley M E, Lopez M D G. Temperature-dependent production of marine copepods: a global synthesis [J]. Amer. Natur, 1992, 140(2): 201 - 242.

[25] Hirst A G, Sheader M. Are *in situ* weight-specific growth rates body-size independent in marine planktonic copepods? A re-analysis of the global syntheses and a new empirical model [J]. Mar. Ecol. Prog. Ser., 1997, 154: 155 - 165.

[26] Kleppel G S, Davis C S, Carter K. Temperature and copepod growth in the sea: a comment on the temperature-dependent model of Huntley and Lopez [J]. Amer. Natur., 1996, 148(2): 397 - 406.

[27] Rebstock G A. Climate regime shifts and decadal scale variability in calanoid copepod populations off southern California [J]. Glob. Chan. Biol., 2002, 8: 71 - 89.

[28] Frost B W. Variability and possible adaptive significance of diel vertical migration in *Calanus pacificus*, a planktonic marine copepod [J]. Bul. Mar. Sci., 1988, 43(3): 675 - 694.

[29] Brodeur R D, Mills C E, Overland J E, et al. Evidence for a substantial increase in gelatinous zooplankton in the Bering Sea, with possible links to climate change [J]. Fish. Oceanogr., 1999, 8(4): 296 - 306.

[30] Purcell J E. Climate effects on formation of jellyfish and ctenophore blooms: a review [J]. J. Mar. Biol .Ass. U.K., 2005, 85: 461 - 476.

[31] Loeb V, Siegel V, Holm-Hansen O, et al. Effects of sea-ice extent and krill or salp dominance on the Antarctic

food web [J]. Nature, 1997, 387: 897 - 900.

[32] Pakhomov E A, Froneman P W, Perissinotto R. Salp/krill interactions in the Southern Ocean: spatial segregation and implications for the carbon flux [J]. Deep-Sea Res. II, 2002, 49: 1 881 - 1 907.

[33] Stempniewicz L, Błachoqiak-Samołłyk K, Węsławski J M. Impact of climate change on zooplankton communities, seabird populations and arctic terrestrial ecosystem: A scenario [J]. Deep- Sea Res. II, 2007, 54: 2 934 - 2 945.

[34] Xu Z L, Jiang M, Chao M, et al.Quantitative distribution of pelagic copepods in the East China Sea [J]. J. Fish.China., 2003, 27(3): 258 - 264.

[35] Xu Z L. Relationships between population characters of *Undinula vulgaris*(Copepoda) and environment in the East China Sea [J]. Chin. J. Appl. Ecol., 2006, 17(1): 107 - 112.

[36] Xu Z L. Studies on distribution of Pteropods abundance in the East China Sea [J]. Acta Oceanol. Sin., 2005, 27(4): 148 - 154.

[37] Xu Z L, Li C J. Horizontal distribution and dominant species of heteropods in the East China Sea [J]. J. Plankton Res., 2005, 27: 373—382.

[38] Xu ZL, Li C J. Abundance distribution of Euphausiids in the East China Sea [J]. J. Fish.China. 2005, 29(3): 373 - 378.

[39] Xu Z L, Li C J. Species composition and diversity of pelagic euphausiids in the East China Sea [J]. Acta. Oceanol. Sin., 2005, 24(5): 98 - 106.

[40] Xu Z L. Characteristics for distribution of pelagic Ostracods in the East China Sea [J]. Acta Oceanol. Sin., 2006, 28(2): 101 - 108.

[41] Hong H S, He F X, Chen G. Relationship between ENSO events and plankton abundance in western Taiwan strait [J]. T. Oceanol. Limnol., 1998, 4: 1 - 9.

[42] Huang J Q, Zhu C S, Li S J. Effects of ENSO events on pelagical copepoda in southern Taiwan strait in summer [J]. Mar. Sci., 2000, 24(4): 1 - 4.

[43] Coyle K O, Pinchuk A I. Climate-related differences in zooplankton density and growth on the inner shelf of the southeastern Bering Sea [J]. Prog. Oceanogr., 2002, 55: 177 - 194.

[44] Scheffer M, Carpenter S, Foley J A, et al. Catastrophic shifts in ecosystems [J]. Nature, 2001, 413: 591 - 596.

[45] Reid P C, Borges M F, Svendsen E. A regime shift in the North Sea circa 1988 linked to changes in the North Sea horse mackerel fishery [J]. Fish. Res., 2001, 50: 163 - 171.

[46] Beaugrand G. The North Sea regime shift: evidence causes mechanisms and consequences [J]. Prog. Oceanogr., 2004, 60: 245 - 262.

[47] Valdés L, López-Urrutia A, Cabal J, et al. A decade of sampling in the bay of Biscay:what are the zooplankton time series telling us? [J]. Progr. Oceanogr., 2007, 74: 98 - 114.

[48] Wiafe G, Yaqub H B, Mensah M A, et al. Impact of climate change on long-term zooplankton biomass in the upwelling region of the gulf of Guinea [J]. ICES J. Mar. Sci. Adv. Access., 2008, 1 - 7.

[49] Dippner J W, Kornilovs G., Sidrevics L. Long-term variability of mesozooplankton in the Central Baltic Sea [J]. J. Mar. Syst., 2000, 25: 23 - 31.

[50] Rutherford S, Hondt S D, Prell W. Environmental controls on the geographic distribution of zooplankton diversity [J]. Nautre, 1999, 400: 749 - 753.

[51] Lindley J A, Daykin S. Variations in the distributions of *Centropages chierchiae* and *Temora stylifera* (Copepoda: Calanoida) in the north-eastern Atlantic Ocean and western European shelf waters [J]. ICES J. Mar. Sci., 2005, 62: 869 - 877.

[52] Sullivan B K, Costello J O, Keuren D V. Seasonality of the copepods *Acartia hudsonica* and *Acartia tonsa* in Narragansett Bay, RI, USA during a period of climate change [J]. Estuar. Coast. Shelf Sci., 2007, 73: 259 - 267.

[53] Occhipinti-Ambrogi A. Global change and marine communities: Alien species and climate change [J]. Mar. Pollut. Bul., 2007, 55: 342 - 352.

[54] Hughes L. Biological consequences of Global Warming: is the signal already [J]. Tree, 2000, 15(2): 56 - 61.

[55] Edwards M, Richardson A J. Impact of climate change on marine pelagic phenology and trophic mismatch [J]. Nature, 2004, 430: 881 - 884.

[56] Root T L, Price J T, Hall K R, et al. Fingerprints of global warming on wild animals and plants [J]. Nature, 2003, 421: 57 - 60.

[57] Martens P, Beusekom JEE. Zooplankton response to a warmer northern wadden sea. Helgol. Mar. Res., 2008, 62: 67 - 75.

[58] Mackas D L, Goldblatt R, Lewis A G. Interdecadal variation in developmental timing of *Neocalanus plumchrus* populations at Ocean Station P in the subarctic North Pacific [J]. Can. J. Fish.Aquat. Sci., 1998, 55: 1 878 - 1 893.

[59] Greve W, Hoffmann S. Helgoland Roads meso- and macrozooplankton time-series 1974 to 2004: lessons froms 30 years of single spot, high frequency sampling at the only foo-shore island of the north sea [J]. Helgol. Mar. Res., 2004, 58: 274 - 288.

[60] IPCC. Summary for policymakers. In Climate Change 2007: The Physical Science Basis. Contribution of Working Group I to the Fourth Assessment Report of the Intergovernmental Panel on Climate Change. Ed. by S. Solomon, D. Qin, M. Manning, Z.Chen, M. Marquis, K. B. Averyt, M. Tignor et al. Cambridge University Press, Cambridge, 2007.

全球变暖对海洋浮游动物的影响

张达娟，李少菁，郭东晖

(厦门大学 海洋与环境学院，福建 厦门 361005)

摘 要：全球变暖作为一个重要的环境问题，自上世纪 80 年代初就已引起学者的广泛关注。它不仅对海洋生态环境及生物圈已产生了一定的影响。本文主要从浮游动物角度出发综述了全球变暖对其生理活动、生态分布及生物气候学的影响。运用不同温度条件下浮游动物生理学上的变化来说明全球变暖对浮游动物的生理影响；通过分析浮游动物生物多样性、生物量，丰度和生物地理分布等指标来阐述其对全球变暖的生态响应；通过讨论浮游动物的最高丰度时间和繁殖时间这 2 个重要物候学指标来说明其对全球变暖的响应。最后，提出了今后的研究方向，即调查更广泛的生物功能群、关注处于热带海洋中的浮游动物以及在浮游动物个体水平上开展研究工作。

关键词：全球变暖；浮游动物；生理活性；丰度；生物多样性；生物气候学

Research process of the calcium signal ing in cyanobacteria

LU Yong-zhong

Biology Department, Qingdao Uinversity of Science and Technology, Qingdao 266042, Shandong Province, China

Abstract: The potential involvement of calcium in signalling in cyanobacteria has been investigated in recent years. Enough evidences showed that the cyanobacteria were capable of sensing and distinguishing different environmental stimuli, and making responses in ways of Ca^{2+} transients, which were the results of influx or efflux of Ca^{2+} aroused by different environmental stimuli. The calcium signal elicited by nitrogen starvation was crucial to heterocyst differentiation in filamentous cyanobacteria *Anabaena* species. Identification of a calcium-binding protein（CcbP） from *Anabaena* sp. PCC 7120 provided further evidence, and the degradation and down-regulation of CcbP accounted for the generation of calcium signal when nitrogen starvation exits. However, the encoding and decoding mechanisms of the calcium signals in cyanobacteria still remain unclear. In order to reveal the exact role of it, a detailed, systematic investigation will be needed, especially for the calcium dynamics at the single cell level.

Keywords: calcium signal, cyanobacteria, prokaryote

1 Introduction

The Ca^{2+} ion has been firmly established as a ubiquitous signalling molecule in eukaryotes, participating in a plethora of cellular processes from acclimative stress responses to the survival and programmed cell death [1]; also it has been well understood that the generation of specificity in Ca^{2+} signals is dependent on influx and efflux from the extracellular milieu, cytosol and intracellular organelles [2]. Different input signals create their characteristic Ca^{2+} fingerprints, and these fingerprints are distinguished by frequency, amplitude, duration, and number of Ca^{2+} oscillations [3]. Ca^{2+}-binding proteins (CaBPs) and protein kinases decode these complex Ca^{2+} fingerprints through conformational coupling and covalent modifications of proteins. This decoding of signals can lead to a physiological response with or without changes in gene expression [4, 5].

Compared to the eukaryotes, the role for this divalent cation in prokaryotes is still elusive, though evidences for calcium as a regulator in bacteria are increasing [6]. For example, the bacterial intracellular free Ca^{2+} concentration was very similar to that of the eukaryotes(100 - 300 nM); the bacterial cells also had ion channels, primary and secondary transporters, and CaBPs, which might be involved in Ca^{2+} homeostasis, and had striking structure similarities with their eukaryotic counterparts; a number of

Received on June 13, 2010

Corresponding author: luyongzhong888@sina.com

bacterial processes such as maintenance of cell structure, motility, cell division, gene expression and cell differentiation processes such as sporulation, heterocyst formation and fruiting body development were related to the free calcium. So it is reasonable to speculate that the intracellular free calcium could be available as a signalling molecule in bacteria, but whether messages are carried by Ca^{2+} in the same way as those in the eukaryotes isn't clear, since they have different cellular structure.

2 Evidences for calcium signal in cyanobacteria

As a large group of photosynthetic, oxygenevolving prokaryotes, cyanobacteria are equipped with complex signal transduction systems to recognize and respond to a variety of environmental stimuli. Evidences of Ca^{2+}-signal transduction were presented in both the filamentous and the unicellular cyanobacteria. In the filamentous blue green alga *Anabena* sp PCC7120, calcium transients in response to the environmental stimuli were studied using aequorin. Results from these studies suggested that the cyanobacteria were capable of sensing and distinguishing different environmental stimuli as evidenced by the responses shown in terms of the Ca^{2+} transients [7-10]. Heat shock treatment of cells in a water bath (44 °C) resulted in a threefold increase in cytosolic free-Ca^{2+} (1.14 ± 0.17 μM after 2 mins to 3.10 ± 0.25 μM after 20 mins) gradually returning to basal levels whereas cold shock treatment under the same conditions evoked a smaller Ca^{2+} transient of shorter duration (1.04 ± 0.23 μM after 10 mins). The magnitude of the intracellular free-Ca^{2+} increase evoked by NaCl was dependent upon NaCl concentration: a small but significant elevation was elicited by 50mM NaCl, lasting about 2 mins, with the peak height of 0.72 ± 0.17 μM; with 100 mM NaCl, the magnitude of the peak was 1.86 ± 0.45 μM; with 200 mM NaCl, the magnitude was much higher, with a value of 5.18±0.43μM. The transients induced by 100 and 200 mM NaCl were much slower, and with 200 mM, the basal levels were not completely reached after 20 min. Sucrose was shown to induce significant Ca^{2+} transients at concentrations of 100 mM and above. With 100 mM sucrose, the amplitude of the peak induced was 0.89 ± 016 μM, and the transient lasted around 3 mins. A Ca^{2+}elevation that reached 1.63 ± 0.23 μM and lasted around 20 mins was provoked by 150 mM sucrose. The peak height of the elevation evoked by 200 mM sucrose was 2.30 ± 0.36 μM. The magnitude of the calcium transient triggered by light-to-dark transitions depended on the fluence rate previously irradiated and could reach a peak height over 2 μM free calcium when the fluence rate of light was around 400 μmol photons $s^{-1}m^{-2}$.

The sources of the Ca^{2+} transients under different stimuli were also determined using Ca^{2+} channel blockers, such as verapamil, the Ca^{2+}-chelator EGTA and the calmodulin-inhibitor trifluoperazine[7-10]. Results suggested that the increased calcium associated with heat shock derived from both extracellular and intracellular spaces while that with cold shock arose from extracellular space, and the main source of the Ca^{2+} transients both in response to salt and osmoticum was the extracellular space. The transients responded to light-to-dark transitions was also from extracellular space and probably modulated by calcium-binding proteins.

The mechanisms for mobilization of calcium in these processes were also investigated. Studies in *Nostoc MAC* showed that the cellular Ca^{2+} uptake was light and ATP dependent, and the addition of

3(3,4-dichlorophenyl)-1,1-dimethyl urea (DCMU) or exogenous ATP proved the vital role of PS II-generated energy, moreover proton gradient across the cell membrane and ATP hydrolysis were involved in the transmembrane movement of Ca^{2+} [11]; in *Nostoc calcicola* Breb, Ca^{2+} efflux also depended on the photosynthetic energy generation, membrane potential and ATP hydrolysis [12].

Ca^{2+} channels play roles in Ca^{2+} transmembrone movement. Cells of the cyanobacterium *Synechocystis* sp. PCC 6803 were found to be equipped with a mechanosensitive ion channel MscL, which might operate as a verapamil/amiloride-sensitive outward Ca^{2+} channel that was involved in the plasma-membrane depolarization-induced Ca^{2+} release from the cells under temperature stress conditions[13]. A Ca^{2+} /H^{+} antiporter in their plasma membranes might exist in *Synechocystis* sp. PCC 6803, *Anabaena* sp. PCC 7120, and *Thermosynechococcus* elongatus BP-1 [14].

3 Calcium signal in cyanobacterial heterocyst formation

A calcium signal was also trigered when it was deprived of combined nitrogen. A rapid increase of calcium level could be detected 4 hrs after the removal of combined nitrogen, and a Ca^{2+}-binding protein, CcbP, was proved to account for it [15]. In the absence of combined nitrogen, inactivation of CcbP resulted in multiple contiguous heterocysts, whereas overexpression of *ccbP* suppressed heterocyst formation.

It was reported recently that nitrogen starvation also trigered a Ca^{2+} transient in the unicellular cyanobacterium *Synechococcus* elongatus PCC 7942 [16]. The addition of 2-oxoglutarate(2-OG), or its analogues 2,2-difluoropentanedioic acid (DFPA) and 2-methylenepentanedioic acid (2-MPA), to cells growing with combined nitrogen elicted the same result, suggesting that an increase in intracellular 2-OG levels preceded the Ca^{2+} transient. The signalling protein P(II) and the transcriptional regulator NtcA appeared to be needed to trigger the signal. Heterocyst differentiation in filamentous cyanobacteria provides an excellent prokaryotic model for studying multicellular behaviour and pattern formation. Multiple signals have recently been identified as necessary for the initiation of heterocyst differentiation, the formation of the heterocyst pattern and pattern maintenance [17]. The calcium signal was proved to be crucial to the heterocyst differentiation.

When filaments were starved of combined nitrogen, 2-OG accumulated and enhanced the DNA-binding activity of global nitrogen regulator NtcA, which in turn led to the expression of *hetR*. NtcA and HetR together constituted the main regulatory loop controlling the initiation of heterocyst development, and an increased level of calcium in developing cells was just the result of their combined action. Degradation of CcbP by HetR released bound Ca^{2+} that contributed significantly to the increase of intracellular calcium concentration during the process of heterocyst differentiation in *Anabaena* sp. strain PCC 7120[18]. The down-regulation of *ccbP* in differentiating cells and mature heterocysts, which also was critical to the regulation of calcium concentration, depended on NtcA (as shown in Fig. 1). The Ca^{2+} level was found to be about 10-fold higher in heterocysts than in vegetative cells, which correlated with the levels of CcbP (which were high in vegetative cells and undetectable in heterocysts). The mechanism for

HetR and NtcA to selectively regulate the free calcium levels in vegetative and differentiating cells needs further investigation.

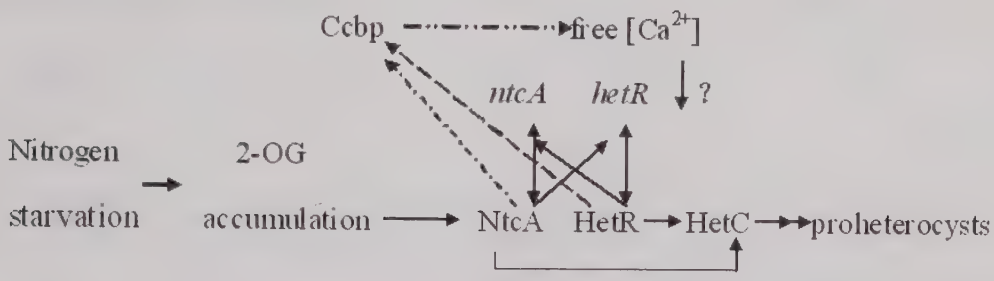

Fig. 1 Regulatory circuit possibly involved in the early stages of heterocyst development.Arrows with real lines indicate promoting processes for heterocyst differentiation, those with dotted lines represent suppressing processes.

4 Discussion

It is clear that evidences in support of the role of Ca^{2+} as a regulator in cyanobacteria are accumulating. However, the extent and importance remains unclear. Till now, only several kinds of cyanobacteria have been studied, and how to work for this kind of ion in cyanobacteria still remains a question.

This could possibly result from the difficulties encountered in Ca^{2+} research, such as the lack of reliable methods to measure calcium just as in other bacteria. The issue of whether the divalent cation encodes specificity has been controversial, whereas in eukaryotic cells it is well documented that Ca^{2+} signalling patterns encode specific cellular responses [19]. The cyanobacterial calcium transients presented now only could be interpreted in terms of the mean intracellular calcium concentration of the whole population of filaments or cells in the cell suspension, and maybe the calcium dynamics at the single cell level can tell the truth.

Another issue is that if the calcium signal indeed exists, how is it decoded? In the eukaryotes, Ca^{2+}-binding proteins and protein kinases do that [20]. Recently, some candidate CaBPs were identified in the database of *Anabaena* sp. PCC 7120 genomes [21]. Could such proteins function as sensors or storage proteins? or is it possible that some of these proteins may be associated with Ca^{2+} channels/ Ca^{2+} pumps regulating Ca^{2+} fluxes?

Above all, a full assessment of the processes involving calcium awaits further analysis, and only a detailed, systematic investigation will reveal the molecular basis of the role of calcium in cyanobacteria.

Acknowledgements

This work was supported by the Start-up Foundation for Introduced Talents in Qingdao University of Science and Technology.

References

[1] Dodd A N, Kudla J, Sanders D. The language of calcium signaling [J]. Annu Rev Plant Biol., 2010, 61: 593 - 620.

[2] Saris N E, Carafoli E. A historical review of cellular calcium handling, with emphasis on mitochondria [J]. Biochemistry, 2005, 70(2): 187 - 194.

[3] Berridge M J. The AM and FM of calcium signaling [J]. Nature, 1997, 386(6627): 759 - 760.

[4] Sathyanarayanan P V, Poovaiah B W. Decoding Ca^{2+} signals in plants [J]. CRC Crit Rev Plant Sci., 2004, 23(1): 1 - 11.

[5] Winslow M M, Crabtree G R. Decoding Calcium Signaling [J]. Science, 2005, 307(5706): 56 - 57.

[6] Dominguez D C. Calcium signalling in bacteria [J]. Mol Microbiol, 2004, 54(2): 291 - 297.

[7] Torrecilla I, Leganes F, Bonilla I, et al. Use ofrecombinant aequorin to study calcium homeostasis and monitor calcium transients in response to heat and cold shock in cyanobacteria [J]. Plant Physiol, 2000, 123:161 - 176.

[8] Torrecilla I, Leganes F, Bonilla I, et al. Calcium transients in response to salinity and osmotic stress in the nitrogen-fixing cyanobacterium *Anabaena* sp. PCC7120, expressing cytosolic apoaequorin [J]. Plant Cell Environ, 2001, 24(6): 641 - 648.

[9] Torrecilla I, Leganes F, Bonilla I, et al. Light-to-dark transitions trigger a transient increase in intracellular Ca^{2+}modulated by the redox state of the photosynthetic electron transport chain in the cyanobacterium *Anabaena* sp. PCC7120 [J]. Plant Cell Environ, 2004, 278: 10 - 19.

[10] Torrecilla I, Leganes F, Bonilla I, et al. A calcium signal is involved in heterocyst differentiation in the cyanobacterium *Anabaena* sp. PCC7120 [J]. Microbiol, 2004, 150: 3 731 - 3 739.

[11] Pandey P K, Singh B B, Mishra R, et al. Ca^{2+} Uptake and Its Regulation in the Cyanobacterium *Nostoc* MAC [J]. Curr Microbiol.,1996, 32(6):332 - 335.

[12] Pandey PK, Gour RK, Bisen PS.Energy-dependent Ca(2+) efflux from the cells of nostoc calcicola Breb: role of modifying factors[J]. Curr Microbiol., 1999,39(5):254-258.

[13] Nazarenko L V, Andreev I M, Lyukevich A A, et al. Calcium release from *Synechocystis* cells induced by depolarization of the plasma membrane: MscL as an outward Ca^{2+} channel [J]. Microbiol, 2003, 149: 1 147 - 1 153.

[14] Waditee R, Hossain G S, Tanaka Y, et al. Isolation and functional characterization of $Ca^{2+/H+}$ antiporters from cyanobacteria [J]. J Biol Chem., 2004, 279(6):4 330 - 4 338.

[15] Zhao Y, Shi Y, Zhao W, et al. CcbP, a calcium-binding protein from *Anabaena* sp. PCC 7120, provides evidence that calcium ions regulate heterocyst differentiation [J]. Proc Natl Acad Sci U S A., 2005, 102(16): 5 744 - 5 748.

[16] Leganes F, Forchhammer K, Fernandez-Pinas F. Role of calcium in acclimation of the cyanobacterium *Synechococcus* elongatus PCC 7942 to nitrogen starvation [J]. Microbiol, 2009, 155(Pt 1): 25 - 34.

[17] Zhang C C, Laurent S, Sakr S, et al. Heterocyst differentiation and pattern formation in cyanobacteria: a

chorus of signals [J]. Mol Microbiol, 2006, 59(2): 367 - 375.

[18] Shi Y, Zhao W, Zhang W, et al. Regulation of intracellular free calcium concentration during heterocyst differentiation by HetR and NtcA in *Anabaena* sp. PCC 7120 [J]. Proc Natl Acad Sci U S A., 2006, 103(30): 11 334 - 11 339.

[19] McAinsh M R, Pittman J K. Shaping the calcium signature [J]. New Phytol., 181(2):275 - 294.

[20] DeFalco T A, Bender K W, Snedden W A. Breaking the code: Ca^{2+} sensors in plant signaling [J]. Biochem J. 2009, 425(1):27 - 40.

[21] Zhou Y, Yang W, Kirberger M, et al. Prediction of EF-hand calcium-binding proteins and analysis of bacterial EF-hand proteins [J]. Proteins, 2006, 65(3): 643 - 655.

蓝藻钙信号的研究进展

卢永忠

（青岛科技大学生物系，山东 青岛 266042）

摘 要：近年来对钙离子在蓝藻信号传导中的潜在作用进行了研究。大量证据表明，蓝藻能够“感知”与“区分”不同的环境刺激，并以钙瞬变的形式产生反应。这是不同的环境刺激所引起的钙离子的内流或外流的结果。由氮缺乏所引起的钙信号对丝状蓝藻鱼腥藻异型胞的分化非常关键。鱼腥藻 PCC 7120 中钙结合蛋白（CcbP）的发现为钙信号在蓝藻中的作用提供了进一步的证据，CcbP 的降解或表达下调是氮缺乏时钙信号产生的主要原因。但是与真核生物相比，蓝藻钙信号的编码与解码机制还不清楚。因此，为了解钙信号如何在蓝藻中发挥作用，还要进行系统的、深入的研究，特别是从细胞水平了解钙信号的动力学特征。

关键词：蓝藻；钙信号；原核生物

Elementary study of differential expression of total soluble proteins in different life phases of *Porphyra yezoensis*

MENG Chun-xiao [1], GAO Zheng-quan [1], WANG Yi-tao[1], LUO Tao[1], Ye Nai-hao [2*]

1 School of Life Sciences, Shandong University of Technology, Zibo 255049, Shandong Province, China;

2 Yellow Sea Fisheries Research Institute, Chinese Academy of Fishery Sciences, Qingdao 266071, Shandong Province, China

Abstract: Total soluble proteins of different life stages, filamentous sporophytes cultivated in high temperatures, and blade gametophytes harvested in different seasons, were identified by SDS-PAGE. The types and amounts of expressed proteins also varied amongst the samples. The fewest soluble proteins were present in filamentous sporophytes. There were more types and amounts of soluble protein in conchospores than in filamentous sporophytes, but fewer than in bulgy sporophytes. More types of protein were detected in filamentous sporophytes cultivated in high temperatures than in those growing in normal situations. The most types and amounts of protein were found in blade gametophytes in all samples. Blade gametophytes harvested last year and stored at -20 ˚C showed only minor differences in expression of proteins when compared with those harvested in different seasons.

Keywords: *Porphyra yezoensis*, total soluble proteins, differential expression

Introduction

Porphyra yezoensis is the cultivar of choice for farming and forms one of the largest aquaculture industries in China and Japan [1-4]. It is regarded as a macroalgal candidate for genomics [5]. As there are obvious morphological differences between the life phases of *P. yezoensis*, differential expression of total soluble proteins in each phase may be anticipated. However, there had not been any research on the differential expression of proteins present in different life stages of *P. yezoensis*. There has been little research on differential expression of total soluble proteins present at different life stages of algae and higher plants. Homark [6] and Hushovd et al. [7] studied the differential expression of total soluble proteins in haploid and diploid stages of the filamentous marine green alga *Ulva mutabilis* Føyn. Both studies found some proteins which were likely to be related to metagenesis. Zhang and Tang reported differential expression of proteins during the development of rice [8]. Hising et al. investigated expression of proteins in root tissues of varying maturity [9]. In the present paper, total soluble proteins of the above life stages, filamentous sporophytes cultivated in high temperatures, and blade gametophytes harvested in different seasons, were identified by SDS-PAGE, which is helpful for the research of gene expression profile of different life stages in *P. yezoensis*.

Received on October 20, 2009

*Corresponding author: zq7723@126.com

1 Materials and methods

1.1 Acquirement of samples

Research subjects were: blade gametophytes, filamentous sporophytes, bulgy sporophytes, conchospores and filamentous sporophytes cultivated in high temperatures with either high or low illumination levels. Blade gametophytes were sourced from Hongdao aquatic factory in Jiaozhou Bay, Shandong province, China. In mid-April, healthy, mature and large gametophytes were randomly selected. They were cleaned and put in shady and breezy places to volatilize the water. Three to five days later, the desiccated gametophytes were cultivated in a bacteria-free medium which had been kept in the dark for a week. The medium was continuously stirred. Using microscopy, the density of carpospores was monitored. When the density reached 10,000/ml, the medium was filtered. The filtrate was inoculated in conical flasks and kept at 17 ˚C, with air exchange, illumination of 1800 lx, and a light regime of 12 h light/dark. The culture medium was replaced every week. Villiform filamentous sporophytes (conchocelis) were observed approximately one month later. The conchocelis were cut into several segments and cultivated again in bacteria-free medium to enlarge biomass. Sufficient sample numbers were cultivated in three to four months. Bulgy sporophytes were induced in sea water medium which contained high levels of phosphor for a month from sporophyte. Bulgy sporophytes changed into *Conchocelis rosea* when cultivated in high temperatures with low illumination for one month, and conchospores were released. Harvested conchospores were stored at -70 ˚C. Filamentous sporophytes cultivated in high temperatures (26 ˚C) were subjected to either high illumination (3 000 lx) or low illumination (1 000 lx). They were cultivated in sea water medium with a light regime of 12 h light/dark.

1.2 Extraction of the total soluble proteins from samples

Extraction buffer (0.1 M Tris, 1 mM EDTA, 0.05 M Vc, 8 M Urea, 1 mM PMSF, 1 % β-mercaptoethanol, 1 % Triton X-100, pH 7.8) was added into each sample (5 ml/g sample). Samples were ground for 20 mins in an ice bath and centrifuged at 13,000 × *g* for 10 mins at 4 ˚C (Eppendorf centrifuge 5804R) .The types and amounts of total soluble protein in the supernatants were determined according to Bradford [10].

1.3 SDS-PAGE

SDS-PAGE was used to examine composition of total polypeptides according to Laemmli [11]. Samples were first precipitated in cold acetone of 9 volumes, mixed with loading buffer (0.25 M Tris, 5 % glycerol, 1 % SDS, 0.025 % beta-mercaptoethanol) and applied to gel which had been heated in boiling water for 5 mins. Separating and stacking gels were 12 % (pH 8.8), and 5 % (pH 6.8), respectively. Following electrophoresis, the gel was stained with Coomassie brilliant blue CBB G250 (4.75 % ethanol, 8.5 % H_3PO_4, 0.000 1 % CBB G250) for 6 h and destained with water.

2 Results

SDS-PAGE results showed differential expression of total soluble proteins during different life stages of *P. yezoensis* (Fig. 1). There were the fewest soluble proteins in filamentous sporophytes, in which 18 kD phycoerythrin was predominant, although 32 kD and 34 kD proteins were also present. Types and amounts of protein found in conchospores were more than those in filamentous sporophytes, but fewer than those in bulgy sporophytes. The molecular weights of proteins found in bulgy sporophytes were between 14 kD and 110 kD, with the majority of proteins between 28 kD and 64 kD. The most types and amounts of protein were found in blade gametophytes in the four samples.

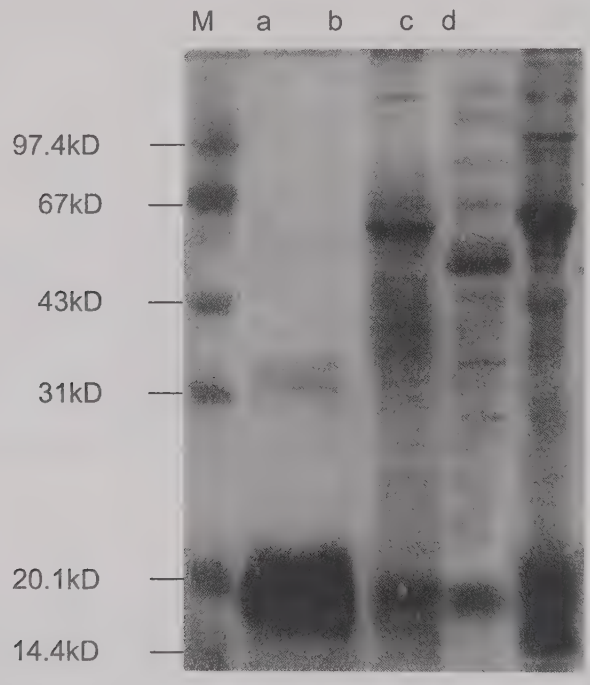

Fig. 1 SDS-PAGE of soluble protein differential expression of different phases.

(M: marke, a, b, c and d represented filamentous sporophyte, bulgy sporophyte, conchospores blade gametophyte. Lane a 40μg/lane, b, c, d lane 20μg/lane)

Protein s cultivated in different environments and blade gametophytes harvested in different seasons. Only three kinds of soluble proteins: 18 kD phycoerythrin, 32 kD and 34 kD proteins (arrows 1 and 2), were detected in filamentous sporophytes cultivated in normal conditions. Much more types of protein were detected in filamentous sporophytes cultivated in high temperatures. However, sporophytes cultivated in high illumination expressed more types of proteins than at low illumination, even though both groups were cultivated in high temperatures. They included 38 kD, 28 kD, 16 kD, and 7 kD proteins (arrows 3, 4, 5 and 6). Blade gametophytes harvested last year and harvested in different seasons had almost the same SDS-PAGE profiles except little difference. 139 kD protein was only found in blade

gametophytes harvested last year (arrow 7). 121 kD protein was only expressed in blade gametophytes harvested in March (arrow 8). 145 kD and 7 kD proteins were only detected in blade gametophytes harvested in May (arrows 9 and 12). 145 kD and 7 kD proteins were only detected in blade gametophytes harvested in this year (arrows 10 and 11).

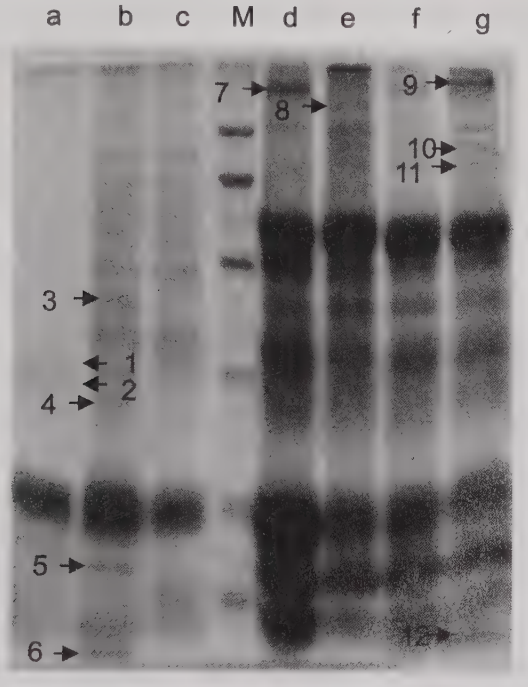

Fig. 2 SDS-PAGE of soluble protein differential expression of filamentous sporophyte samples cultivated in different situations and blade gametophytes harvested in different seasons.

(M:marker, a: filamentous sporophyte, b: filamentous sporophyte cultivated at high temperature and high illumination, c: filamentous cultivated at high temperature and low illumination, d: harvested in last year stored at -20 °C, e: blade gametophytes harvested in this March, f: blade gametophytes harvested in this April; g: blade gametophytes harvested in this May. A, b, c lane 20μg/lane, d, e, f, g lane 40μg/lane)

3 Discussion

In this study, 18 kD phycoerythrin was expressed most (more than 70% of total soluble proteins) in diploid filamentous sporophytes. It contrasted with higher plants. The content of phycoerythrin in blade gametophytes was the highest in four samples. We presumed that filamentous sporophytes be a diploid phase of *P. yezoensis*, they might only play a role in continuing strip without vast metabolism. Several essential types of soluble proteins expressed to meet basic needs, e.g. phycoerythrin. Bulgy sporophytes was the prelude which was brief but crucial in the life history of *P. yezoensis*. Therefore, it needed to express many essential proteins in order to continue to strip successfully. After meiosis, diploid bulgy sporophytes changed into *Conchocelis rosea* releasing haploid conchospores which developed into

haploid blade gametophytes, which was the most important stage, the largest in size and occupied the longest time in the life history of *P. yezoensis*. This phase undergone the most complicated physiological changes and had high metabolic requirement. Due to all these factors, blade gametophytes required the most types and amounts of proteins compared with the other life stages of *P. yezoensis*.More types of protein were detected in filamentous sporophytes cultivated in a high temperature environment than those in normal conditions. This may be due to high temperatures inducing filamentous sporophytes to develop into bulgy sporophytes.

Results from blade gametophytes stored at -20 ˚C and harvested in different seasons were very similar. Since gametophytes were alive, cold related proteins related to withstanding low temperatures were expressed, e.g. 139 kD protein (arrow 7 in Fig.1). As blade gametophytes were at different mature and decrepit states in March, April and May, proteins were expressed according to the harvest time.

P. yezoensis has a unique metagenesis and an interesting life history. The present study showed clearly soluble proteins were differentially expressed using SDS-PAGE studies. Evidently, further research, such as research of gene expression profile of different life stages was required.

Acknowledgments

This work was supported by the National Natural Science Foundation of China (No. 40706050, 40706048 and 30700619), the National Science & Technology Pillar Program (No. 2006BAD01A13 and 2008BAC49B04), National special fund for transgenic project (No. 2009ZX08009-019B), Natural Science Foundation of Shandong Province (No. 2009ZRA02075), and Qingdao Municipal Science and Technology plan project (No. 09-2-5-8-hy).

References

[1] Gao Z Q, Meng C X, Wang G C, et al. Isolation and characterization of photosystem II from the filamentous sporophyte of *Porphyra yezoensis* [J]. Indian Journal of Biochem & Biophy, 2008, 45: 244 - 249.

[2] Wang S J. Biotechnology of seaweed [M]. Shanghai :Shanghai scientific technical press, 1994, pp.19.

[3] Liu H Q, Yu W G , Dai J X, et al. Cryopreservation of protoplasts of the alga *Porphyra yezoensis* by vitification [J]. Plant Sci., 2004, 166: 97 - 102.

[4] Fei X G, Lu S, Bao Y, et al. Seaweed cultivation in China [J]. World Aquac, 1998, 29:22 - 24.

[5] Waaland J R, Stiller J W, Cheney P. Macroalgal candidates for genomics [J]. J Phycol, 2004, 40: 26 - 33.

[6] Hoxmark R C. Protein composition of different stages in the life cycle of *Ulva mutabilis* Føyn [J]. Planta(Berl), 1976, 130: 327 - 332.

[7] Hushovd O T, Gulliksen O M, Nordby Ø. Absence of major differences between soluble proteins from hploid gametophytes and diploid sporophytes in the green alga *Ulva mutabilis* Føyn [J]. Planta, 1982, 156: 89 - 92.

[8] Zhang B, Tang X H. Studies on rice embryo proteins with development stage specificity [J]. Acta Phytophysiologica Sinica, 1992, 18: 85 - 92

[9] Hsing Y C, Tsou C H, Hsu T F, et al. Tissue-and stage-specific expression of a soybean (Glycine max L.)seed-maturation,biotinylated protein [J]. Plant molecu biol, 1998, 38: 481 - 49.

[10] Bradford M M. A rapid and sensitive method for the quantitation of microgram quantities of protein utilizing of protein dye binding [J]. Anal biochem, 1976, 72: 248 - 254

[11] Laemmli U K. Cleavage of structural proteins during the assembly head of bacteriophage T_4 [J]. Nature, 1970, 227: 680 - 685

不同时期和生长状态条斑紫菜总可溶性蛋白差异表达初探

孟春晓[1]，高政权[1]，王依涛[1]，罗韬[1]，叶乃好[2]

（1. 山东理工大学生命科学学院，山东 淄博，255049；2. 中国水产科学院黄海水产研究所，山东 青岛，266071）

摘 要：用 SDS-PAGE 技术研究了不同时期条斑紫菜样品、高温下培养的丝状体以及不同季节收获的叶状体的总可溶性蛋白。结果表明，这些样品总可溶性蛋白的表达数量和种类相差很大。壳孢子中总可溶性蛋白的表达数量和种类明显比丝状体中多，但比膨大丝状体中少；高温条件下培养的丝状体比正常条件下培养的丝状体表达更多数量和种类的可溶性蛋白；所有样品中，以叶状体表达的溶性蛋白的表达数量和种类最多；上年收获的与本年度不同季节收获的叶状体在蛋白质表达图谱上差别很小。

关键词：条斑紫菜，总可溶性蛋白，差异表达

Distribution and composition of tintinnids ciliates in the northern South China Sea during summer

LIU Hua-xue [1, 3], HUANG Liang-min [1], TAN Ye-hui [1], SONG Xing-yu [1*], HUANG Jian-rong [2], Li Tao[1]

1. *South China Sea Institute of Oceanography ,China Academy of Science, Guangzhou* 510301, *Guangdong Province, China;*

2. *School of Life Sciences, Sun Yat-Sen University, Guangzhou* 510275, *Guangdong Province, China;*

3. *Graduate University of China Academy of Science, Beijing* 100049, *China*

Abstract: Tintinnids were enumerated and identified in samples collected from 36 stations between 18°-22°N, 107°-122 °E in the northern South China Sea (NSCS). 44 species belonging to 24 genera of tintinnids were recorded. The dominant species were *Helicostomella longa* and *Tintinnopsis radix*. Tintinnids abundance ranged from 0 to 2 200 cell/L, and mean abundance was 221cell/L in the surface water. Tintinnids abundance and species numbers decreased from coast to offshore. Upwelling and Pearl River discharge influenced the distribution of tintinnids by regulating nutrients supply. Maximum abundance (2 200 cell/L) was found in the surface water of A1. Tintinnids abundance showed positive relationship with chlorophyll a (Chl a) concentration, and no significant relationship was found between tintinnids abundance and temperature.

Keywords: tintinnids; composition; distribution; northern South China Sea

Tintinnids ciliates are primarily feeders upon nano-plankton, mainly bacteria, minute algae, and small flagellates (Kofoid,et al., 1932). Due to their ubiquitous distribution, small size, and rapid metabolic and growth rates (Verity, 1985; 1987), they are undoubtedly considered to play an important role in transferring the production of Pico and nano-plankton to meso- and macrocarnivores (Stoecker and Govoni, 1984; Giffort, 1991).Investigations of feeding revealed that tintinnids ciliates ingest a large variety of pico- and nano-sized prey, ranging in size from about 2 μm to particles about half the diameter of their lorica oral openings (Rassoulzadegan et al., 1988). Tintinnids are the link between the microbial and metazoan food webs, providing a pathway between bacterial and nanoplanktonic production and zooplankton and fish biomass (Pierce and turner, 1994).

The South China Sea (SCS) is one of the world's largest marginal seas, with a surface area of about 3.5×10^6 km^2, extending from the equator to 22°N (Fang et al., 1998). A deep basin with a surface area of about 1.5×10^6 km^2 and a maximum depth of 5 000 m is located to the east of the broad shelf (Shaw and Chao, 1994). Northeastern monsoon prevails in winter and spring, whereas the southwestern monsoon prevails in summer and autumn (Chen et al., 2004). SCS receives large amount of nutrients from Pearl

Received on April 2, 2010

*Corresponding author: hxliu@scsio.ac.cn

River discharge to support productivity, and about 80% of its discharge occurs when the southwestern monsoon prevails from April to September, and the remaining 20% occur from October to March (Zhao, 1990).

What role did tintinnids play in NSCS was still unknown, particularly on its distribution and composition. In this study, we aimed to determine the community structure and distribution of tintinnids, to gain insight into the character of tintinnids in NSCS during southwest monsoon period.

1 Material and methods

1.1 Field sampling

The cruise was conducted in the NSCS in August 10th - 30th, 2007(Fig. 1).Three kinds of areas were grouped based on the water depth. Stations with bottom depths＜50 m, 50 - 200 m and ＞200 m were designed as coast, shelf, offshore. Discrete samples were collected at various depths with a Rosette sampler fitted with 2.5-L Niskin Bottles and mounted on the CTD (Seabird, USA) for the determination of salinity and temperature.

Tintinnids samples were collected from the surface and bottom layer in the coast and shelf area (depth＜200 m), and seawater from surface and 200 m depth were collected in the offshore (depth＞200 m). Samples were preserved by adding the acid lugol's solution (final concentration 2%), and then stored at 4 °C in the dark before tintinnids identification.

Seawater samples for the analysis of chlorophyll a were immediately filtered through GF/F filters (Whatman, 25 mm), which were stored at -20 °C. The phytoplankton pigments retained on GF/F filters were extracted in 90% acetone. The Chl a concentration in the extract was measured before and after acidification with a fluorometer (Turner 10-AU-005).

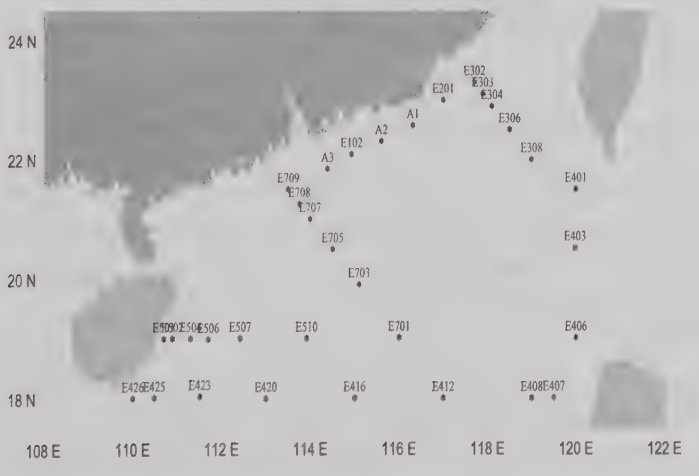

Fig. 1 Sampling station in northern South China Sea

1.2 Laboratory analysis

For enumeration, tintinnids samples were settled down for 24 hours in their bottles in the dark at 4 °C, the upper 900 ml of the sample was slowly siphoned off. The bottom 100 ml of the sample was transferred into settling chambers to settle for 24 h before examined (Safi et al., 2007). Tintinnids were identified using lorica morphology and the species descriptions according to literatures of Kahl (1935), Kofoid and Campbell (1929, 1939), Carey (1992) and Xu (2002).

Pearson correlation analysis and multivariate regression were applied to find the potential relationship between the distribution of tintinnids and abiotic variable by SPSS 12.0.

2 Result and discussion

2.1 Environmental variables

Surface seawater temperature varied from 20.7 °C to 29.6 °C, and low temperature area was found in the Guangdong coast, which was influenced by Pearl River discharge and upwelling. Surface seawater salinities in the coast (32.63) and in the shelf (33.59) were lower than in the offshore (33.65). Fresh water from Pearl River diluted the upper seawater in the coast and shelf. Bottom seawater intruded the coast at 25m depth, where salinity was higher than in the shelf and offshore at the same depth.

Mean Chl a concentration decreased from coast to offshore, and surface Chl a in coast (1.52 mg/m^3) was higher than that in the shelf (0.36 mg/m^3) and offshore(0.12 mg/m^3). Elevated chlorophyll concentrations also appeared along the coast, maximum surface Chl a occured in E709 (3.729 mg/m^3), and the relatively high Chl a concentrations may be attributed to nutrient input from river discharge.

The character of mean water column integrated chlorophyll a (IB) was similar to the surface Chl a distribution. Mean IB decreased along the salinity gradient, so Mean IB in the coast was higher than that in the shelf and the offshore.

2.2 Tintinnids composition and distribution in the NSCS

44 species tintinnids belonging to 24 genera were identified, of which, *Tintinnopsis* was the most abundant genus in terms of species (8). Tintinnids species number ranged between 0 and 11, and mean number of species in surface water (3.4) was higher than that in the bottom water (1.4). Mean abundance in surface water (221 cells/L) was higher than that in - bottom water (66.4 cells/L)

In surface water, tintinnids abundance varied between 0 and 2200 cells/L. No tintinnids were identified in E408, E412 and E416. Mean abundance of tintinnids was 221 cell/L, and maximum abundance occurred in surface water of A1 (2200 cell/L), followed E709 (1325 cell/L). Dominant tintinnids species was *Helicostomella longa* (18.5%), *followed Tintinnopsis urula* (8.22%), *Tintinnopsis radix* (7.88%), *Tintinnopsis minuta* (6.5%). 10 species of tintinnids were identified in A1, which was the richest in

this study; followed E709 (9) and E708 (9). These stations all located in coast area, which was rich in nutrients and phytoplankton.

In bottom water, tintinnids abundance varied between 0 and 550 cells/L. Mean abundance of tintinnids was 66.4cell/L, maximum abundance occurred in E201 (550 cell/L), followed E303 (400 cell/L). 5 species of tintinnids were identified in E201, E303 and E304, followed E302 (4). Dominant tintinnids species was *Leprotintinnus simple* (22.1%), followed *Tintinnopsis oriental* (12.8%), Tintinnopsis *beroidea*(10.5%), *Codonellopsis morchella*(9.3%).

Tab. 1 Tintinnids species identified in the northern South China Sea during summer

Amphorella	***Marshallia***
Amphorella qudrilineata	*Marshallia aperta*
*Amphorella qudrilineata**	***Parundella***
Amphorellopsis	*Parundella aculeata*
*Amphorellopsis acuta**	***Proplectella***
Climatocylis	*Proplectella claparedei**
Climatocylis scalaroides	***Protorhabdonella***
Craterella	*Protorhabdonella curta**
*Craterella retusa**	*Protorhabdonella simplex**
Codonellopsis	***Rhabdonella***
*Codonellopsis morchella**	*Rhabdonella omor*
Codonellopsis ostenfeldi	*Rhabdonella conica*
Codonellopsis borealis	*Rhabdonella poculum*
Coxliella	*Rhabdonella sanyahensis**
Coxliella longa	***Salpingella***
Dadyiella	*Salpingella minutissma*
Dadyiella acutiformis	***Stenosemella***
*Dadyiella ganymedes**	*Stenosemella pacifica**
Dictyocysta	***Steenstrupella***
Dictyocysta reticulata	*Steenstrupella gracilis**
Epiplocylis	*Steenstrupella steenstrupella **
Epiplocylis lato	***Tintinnopsis***
Epiplocyloides	*Tintinnopsis bütschlii*
Epiplocyloides reticulata	*Tintinnopsis minuta**
Eutinnus	*Tintinnopsis oriental**
*Eutintinnus fraknoii**	*Tintinnopsis radix**
*Eutinnus fraknoii**	*Tintinnopsis schotti*
Favella	*Tintinnopsis tubulosa**
Favella campanula	*Tintinnopsis tocantinencis*
Helicostomella	*Tintinnopsis urula*
*Helicostomella longa**	***Undella***
Leprotintinnus	*Undella ostenfedi*
*Leprotintinnus simple**	*Undella turgida**

*** represent >1% (the species abundance to total abundance)**

Low Chl a concentration and tintinnids abundance indicated that oligotrophic conditions prevailed in most area of the NSCS. To better understand the distribution pattern of tintinnids in NSCS, we chose 13

stations to two transect according to the longitude and latitude gradient (Fig. 2). Each transect includes 7 stations, transect 1 ranged from 113°E to 118°E, including E302, E201, A1, A2, E102, A3 and E709; transect 2 ranged from 18°N to 21.5°N, including E709, E708, E707, E705, E703, E701, and E412.

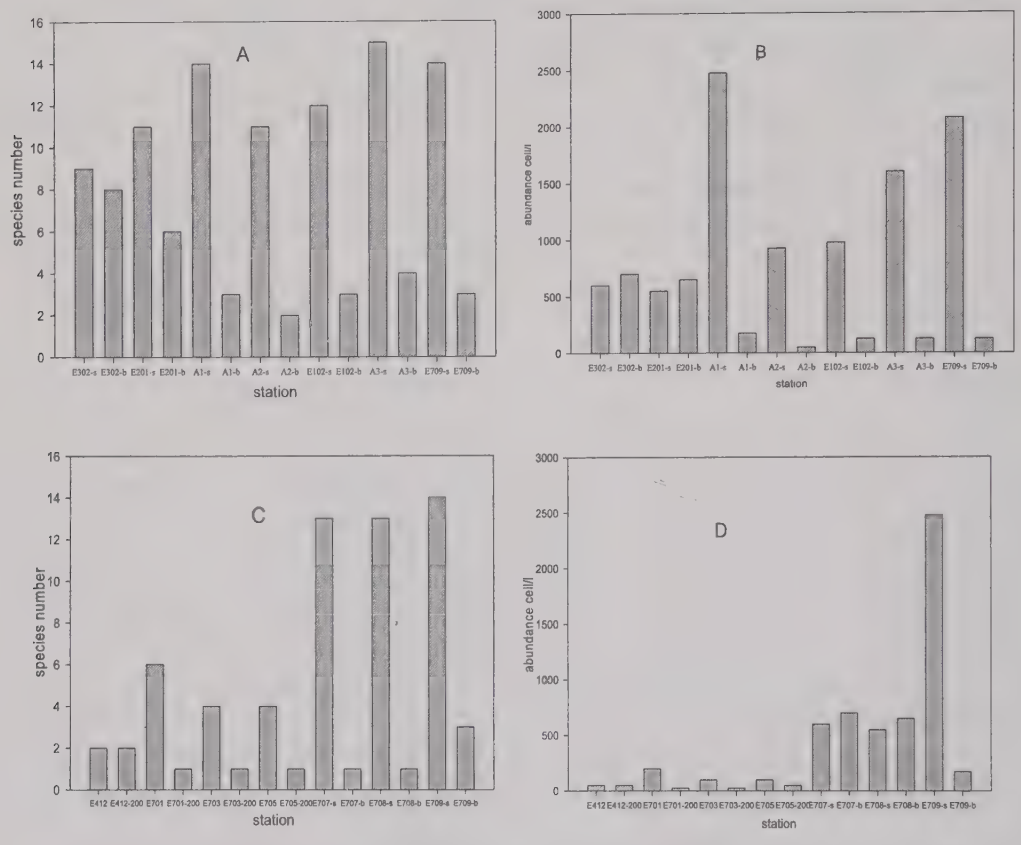
A
B
C
D
species number
abundance cell/l
station
E302-s E302-b E201-s E201-b A1-s A1-b A2-s A2-b E102-s E102-b A3-s A3-b E709-s E709-b
E412 E412-200 E701 E701-200 E703 E703-200 E705 E705-200 E707-s E707-b E708-s E708-b E709-s E709-b

Fig. 2 Tintinnids species number and abundance in surface and bottom water in the NSCS

A) tintinnids species number of transect 1; B) tintinnids abundance of transect 1;

C) tintinnids species number of transect 2; D) tintinnids abundance of transect 2

Mean tintinnids species number and abundance in transect 1 were higher than those in transect 2. Transect 1 located in the coast of NSCS, where received a large number of nutrients through runoff. High diversified tintinnids assemblage and abundance occurred in the coast were common phenomena in the world.

Chl a and nutrient decreased along the transect 2. Fig.3 showed low temperature and low salinity in surface water at E709 station Pearl River discharges sustain the high Chl a and tintinnids assemblage, so tintinnids species number and abundance decreased along the latitude gradient (Fig. 2).

In both transects, surface species number and abundance were higher than in bottom water (Fig. 2), which was consistent with the result of the whole NSCS.

Helicostomella longa was the dominant tintinnids, and differs from the other species of

Helicostomella in smaller size and stouter form; this species was characterized by the presence of a small clean lorica, and the aboral end of which is more acute. *Helicostomella longa*, *Tintinnopsis urula*, *Tintinnopsis radix*, *Tintinnopsis minuta*, these 4 species hold 41.1% of tintinnids abundance in the NSCS.

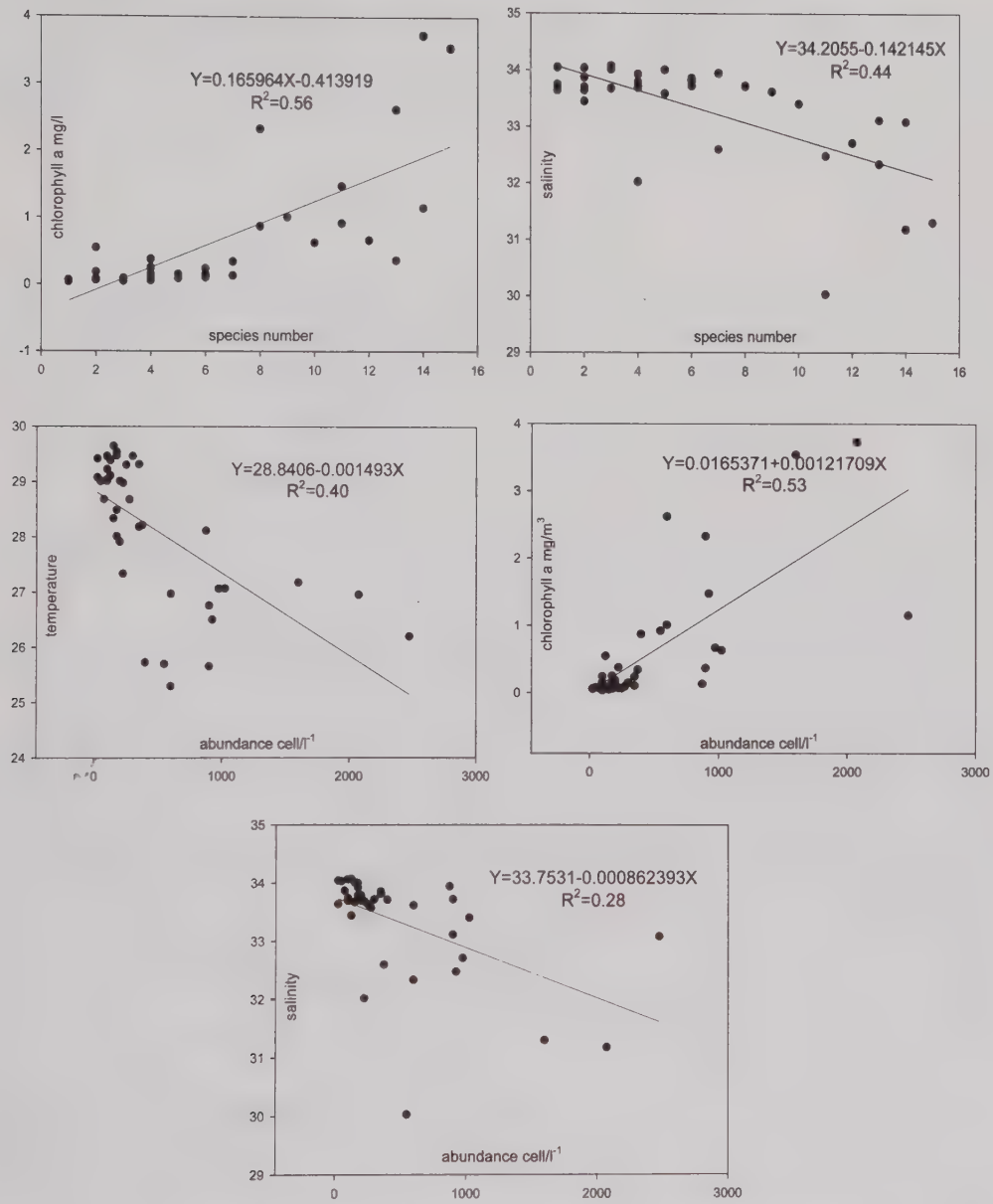

Fig. 4 Relationship between tintinnids and environmental parameters

2.3 Relationships with environment variables

Mean Chl a concentration decreased from coast to offshore during summer, which was similar to the trend of tintinnids abundance. Correlation analysis was carried to understand the relationship between

abiotic and biotic variables.

No significant relationship was found between tintinnids abundance and temperature or salinity (Fig. 4). Pearl River discharge, upwelling, surface circulation and kuroshio all have impact on the biogeochemistry and distribution of tintinnids in NSCS. The relationship between tintinnids and hydrographic condition need further study. Chl a concentration showed a positive relationship with tintinnids abundance ($P < 0.01$), and species number ($P < 0.05$), as tintinnids ciliates were primarily feeders upon phytoplankton, high Chl a stimulated the growth of tintinnids.

Acknowledgements

We grateful acknowledge the captain and crew of the RV "shiyan3" for ship operations. Financial support for this study was provided by the National Science Committee through Grants NSC 40531006, U0633007, 40576052.

Reference

[1] Cariou J B, Dolan J R, Dallot S. A preliminary study of tintinnid diversity in the NW Mediterranean Sea [J]. J Plankton Res., 1999, 21:1 065 - 1 075.

[2] Carey P G. Marine Interstitial Ciliates [M]. London: Chapman & Hall pp 314 - 324, 1992.

[3] Chen Y L, Chen H Y, Karl D M, et al. () Nitrogen modulates phytoplankton growth in spring in the South China Sea [J]. Continental Shelf Research, 2004, 24: 527 - 541.

[4] Dolan J R, Vidussi F, Claustre H. Planktonic ciliates in the Mediterranean Sea: longitudinal trends [J]. Deep-Sea Research, 1999, 46: 2 025 - 2 039.

[5] Dolan J R, Claustre H, Carlotti F, et al. Microzooplankton diversity: relationships of tintinnid ciliates with resources, competitors and predators from the Atlantic Coast of Morocco to the Eastern Mediterranean [J]. Deep-Sea Research 2002, I (49): 1 217 - 1 232.

[6] Dolan J R, Jacquet S, Torre´ton J P. Comparing taxonomic and morphological biodiversity of tintinnids (planktonic ciliates) of New Caledonia [J]. Limnol. Oceanogr., 2006, 51(2): 950 - 958.

[7] Fang G, Fang W, Fang Y, et al. A survey of studies on the South China Sea upper ocean circulation [J]. Acta Oceanographica Taiwanica 1998, 37: 1 - 16.

[8] Kofoid C A. Campbell A S. A conspectus of the marine and freshwater ciliata belonging to the suborder Tintinoinea, with descriptions of new species principally from the agassiz expedition to the eastern tropical pacific [J]. Univ. Calif. Pub. Zool., 1929, pp 1 - 403.

[9] Kofoid C A, Campbell A S. The ciliata: the Tintinnoinea [J]. Bull. Mus. Comp. Zool., 1939, pp 1 - 473.

[10] Modigh M, Castaldo S. Variability and persistence in tintinnid assemblages at a Mediterranean coastal site [J]. Aquat Microb Ecol., 2002, 28: 299 - 311.

[11] Modigh M, Castaldo S. Saggiomo M, et al. Distribution of tintinnid species from 42°N to 43°S through the Indian Ocean [J]. Hydrobiologia, 2003, 503: 251 - 262.

[12] Perez M T, Dolan J R, Fukai E. Planktonic oligotrich ciliates in the NW Mediterranean: growth rates and consumption by copepods [J]. Mar. Ecol. Prog. Ser., 1997, 155: 89 - 101.

[13] Perez M T, Dolan J R, Vidussi F, et al. Diel vertical distribution of planktonic ciliates within the surface layer of the NW Mediterranean (May 1995) [J]. Deep-Sea Res., 2000, 47: 479 - 503.

[14] Pierce R W, Turner J T. Ecology of planktonic ciliates in marine food webs. Rev. Aquat. Sci., 1992, 6:139 - 181.

[15] Pierce R W, Turner J T. Global biogeography of marine tintinnids [J]. Mar. Ecol. Prog. Ser., 1993, 94:11 - 26.

[16] Pierce R W, Turner J T. Plankton studies in Buzzards Bay, Massachusetts, USA. IV. Tintinnids, 1987 to 1988 [J]. Mar. Ecol. Prog. Ser., 1994, 112: 235 - 240.

[17] Pitta P, Giannakourou A. Planktonic ciliates in the oligotrophic Eastern Mediterranean: vertical, spatial distribution and mixotrophy [J]. Mar. Ecol. Prog. Ser., 2000, 194: 269 - 282.

[18] Rassoulzadegan F, Laval P M, Sheldon R W. Partitioning of the food ration of marine ciliates between picoand nanoplankton. Hydrobiologia 1988, 159:75 - 88.

[19] Pierce R W, Turner J T. Global biogeography of marine tintinnids [J]. Mar. Eco. Prog. Ser.,1993, 94: 11 - 26.

[20] Shaw P, Chao S. Surface circulation in the South China Sea [J]. Deep-Sea Research I, 1994, 41: 1 663 - 1 683.

[21] Stoecker D K, Michaels A E. Respiration, photosynthesis and carbon metabolism in planktonic ciliates [J]. Mar. Biol., 1991, 108:441 - 447.

[22] Safi K A, Griffiths F B, Hall J A. Microzooplankton composition, biomass and grazing rates along the WOCE SR3 line between Tasmania and Antarctia [J]. Deep-Sea Research I, 2007, 54: 1 025 - 1 041.

[23] Thompson G A. Tintinnid diversity trends in the southwestern Atlantic Ocean (29-60°S) [J]. Aquat. Microb. Ecol., 2004, 35: 93 - 103.

[24] Verity.PG. Grazing, respiration, excretion, and growth rates of tintinnids Limnol [J]. Oceanogr., 1985, 30 (6): 1 268 - 1 282.

[25] Verity PG. Abundance, community composition, size distribution, and production rates of tintinnids in Narragansett Bay, Rhode Island [J]. Estuarine Coastal and Shelf Science, 1987, 24: 671 - 690.

[26] Xu K D, Hon H S, Song W B, et al. Study on tintinnine ciliates in the Tai wan strait (Cilipohora: Tintinnina) [J]. Acta Zootaxonomica Sinica, 2001, 26(4): 454 - 466.

[27] Zhao H. Evolution of the Pearl River Estuary [M]. Beijing: Ocean Press, 1990.

夏季南海北部沙壳纤毛虫种类组成及空间分布

刘华雪[1,3]，黄良民[1]，谭烨辉[1]，宋星宇[1]，黄建荣[2]，李 涛[1]

（1. 中国科学院南海海洋所 海洋生物资源可持续利用重点实验室，广东 广州 510301；2. 中山大学 生命科学学院，广东 广州 510275；3. 中国科学院研究生院，北京 100049）

摘 要：2007 年 8 月夏季中国科学院南海海洋研究所南海北部开放航次期间，在北纬 18° - 22°，东经 107° - 122 ° 范围内使用“实验三号”科考船进行了水体中沙壳纤毛虫的采样研究，探讨了沙壳纤毛虫的空间分布和种类组成。在 36 个站位中共鉴定出 24 属 44 种沙壳纤毛虫，其中优势种为长形旋口虫 *Helicostomella longa* 和根突拟铃虫 *Tintinnopsis radix*，沙壳纤毛虫丰度变化范围为 0 – 2 200 cell/L，平均丰度为 221 cell/L，从沿岸向外海方向，沙壳纤毛虫种类和丰度逐渐减少，其中 A1 站丰度最高（2 200 cell/L），种类数最多（10）。夏季南海北部沙壳纤毛虫丰度与叶绿素 a 呈显著正相关，而与温度相关性不明显。夏季南海北部的上升流和珠江冲淡水携带的营养盐刺激了浮游植物的生长，影响着南海北部沙壳纤毛虫的种类组成和空间分布。

关键词：沙壳纤毛虫；种类组成；空间分布；南海北部

RAPD analysis between color-different crab individuals of *Portunus trituberculatus*

CHI Da-li [1, 2], YAN Bin-lun [1*], SHEN Song-dong [2], GAO Huan [1]

1. *Jiangsu Key Laboratory of Marine Biotechnology, Huaihai Institute of Technology, Lianyungang* 222005, *Jiangsu Province, China;*

2. *School of Life Sciences, Suzhou University, Suzhou* 215123, *Jiangsu Province, China*

Abstract: The blue swimming crabs *Portunus trituberculatus* with tea-green and/or purple carapace color have been discovered on the shore of eastern part of China these days. In this paper, 40 color-different crab individuals were evaluated using 80 RAPD primers. 30 primers were selected using bulk segregation analysis (BSA) and RAPD-PCR analysis. The results showed that the ratio of polymorphic loci was 61.29%, and Nei's gene diversity was 0.375 6, and Shannon's information index was 0.554 5 among purple crab individuals; and the ratio of polymorphic loci was 62.44%, and Nei's gene diversity was 0.3451, and Shannon's information index was 0.5099 among tea-green crab individuals. It was clear that the genetic diversity between purple and tea-green crabs was similar, which indicated close phylogenetic relationships between the purple and tea-green crabs. In addition, two primers (SBS A09 and SBS G16) got specific DNA bands by comparing forty individuals of color-different crab individuals through RAPD-PCR analysis and the following electrophoresis. They indicated close phylogenetic relationships between purple and tea-green crabs.

Keywords: body-color; phylogenetic relationships; *Portunus trituberculatus*; RAPD

1 Introduction

Portunus trituberculatus is an important fishery species belonging to class Malacostraca, order Decapoda, family Portunidae. Given the commercial and ecological importance of the blue swimming crab, it has attracted great interests, and has been artificially propagated and widely stocked as one of the most common edible crabs in the eastern part of China, while there is a surprising scarcity of information concerning the molecular biology of this species. The few studies on molecular biology of *P. trituberculatus* published to date are based on protein polymorphisms (allozyme data)[1, 2, 3], phylogenetic identification[4, 5], and analysis of the complete mitochondrial genome sequence[6, 7] and so on.

The normal carapace (especially for the cephalothorax) color of *P. trituberculatus* is tea-green; while some crab individuals whose carapaces and appendages are purple in natural existence through their whole life span have been discovered in their natural habitats (East China Sea) in recent years. Both

Received on December 16, 2009

*Corresponding author: yanbinlun@ yahoo.com.cn

purple and tea-green crabs have similar, even the same physical characteristics except for the carapace color. The ratio of number of purple crabs to that of all wild captured ones is about 9% according to our preliminary statistical researches.

Generally, color is considered as a morphological character in many species. Within species, color morphs may enhance camouflage, improve communication and/or confer reproductive advantage [8]. As an important character to distinguish species, coloration has proved to be of systematic importance among several species of decapod crustaceans [9].

Random amplified polymorphic DNA (RAPD) has been used for the discrimination of fishery and aquaculture products [10]. This technique was one of the genetic markers that have been initially applied on *P. trituberculatus* to identify the genetic structure, with the results showing conformed to conventional taxonomy [5]. We determined here the phylogenetic relationships and genetic differences between purple and tea-green crab individuals of *P. trituberculatus* by RAPD technique.

2 Materials and methods

2.1 Sample and genomic DNA extraction

The blue swimming crabs with two different colors were collected from a commercial market in Lianyungang, China and kept in water-circulating systems for laboratory breeding experiments in summer and autumn of 2007. The ambulatory muscle tissues from twenty tea-green crabs and twenty purple ones were excised and preserved at -40 °C in a refrigerator.

The genomic DNA was isolated from ambulatory muscle tissues using columns of the "SiMax™ Genome DNA Kit" (Shanghai SBS Genetech Co., Ltd., Shanghai, China). Quality and quantity of DNA preparation were checked with a Gene Quant *Pro* (Amersham Biosciences™, England) spectrophotometer for absorption at 260 nm and samples were diluted to a concentration of 50 ng/μL. Six purple individual DNA samples or six tea-green ones were prepared and contributed to two separate genomic DNA pools: one was purple crab DNA pool and another tea-green crab DNA pool, with the intention of providing a common genetic background for each pool and leaving the color linked materials as the primary difference between the two pools.

2.2 Selection of primers

RAPD primers were purchased from SBS Genetech Co., Ltd. (Shanghai, China) and a total of 80 primers were initially screened against two separate genomic DNA pools for their ability and diversity to amplify DNA fragments. Two replications were made to assess the consistency of the band profiles. The selected primers should produce robust amplification patterns and no band was detected in any negative control amplification.

2.3 PCR amplification

The reproducibility of the RAPD amplifications were assessed using selected primers with individual crab DNA samples with different carapace colors.

RAPD amplifications were carried out in a Multicolor Real-Time PCR Detection System (Gene cycler™, Bio-Rad, USA) with 20 μL reaction volume containing 12.6 μL sterile distilled H_2O, 2 μL 10× PCR buffer (10 mM Tris-HCl, pH 9.0; 50 mM KCl and 0.1% Triton X-100), 1.6 μL dNTPs (10 μM), 1.4 μL 25 mM $MgCl_2$, 0.1 μL *Taq* polymerase (5 U/μL), 1.5 μL of primer (10 μM), and 0.8 μL template DNA (genomic DNA, 300 ng/μL). Samples without genomic DNA were included in each amplification run as controls.

The thermal cycle profile was as follows: 94 °C for 5 min followed by 40 steps of 1 min at 94 °C, 1 min at 36 °C and 1.5 mins at 72 °C with a final extension step of 10 mins at 72 °C.And the PCR products were electrophoresed on a 1.0% agarose (OXOID™, England) gel stained with GoldView (0.005%) and the number of bands was recorded using a gel documentation system (Bio-Rad Laboratories-Segrate (Milan) Italy). The size of the amplification products was estimated from 100 bp DNA ladder (Shanghai SBS Genetech Co., Ltd., Shanghai, China).

2.4 Data analysis

For RAPD profiles, the well-resolved and consistently reproducible fragments ranging from 100~3000 bp were scored as present (1) or absent (0) for each analysis. Bands with the same migration distance were considered homologous. A pair-wise similarity matrix was computed and analysed using POPGENE 1.31 software (Yeh and Boyle, 1999).

3 Results

3.1 Selection of Primers and amplified band diversity

Initially, the primers were selected after a preliminary screening using genomic DNA pools as templates in PCR reactions for their ability to produce clear and reproducible pattern of multiple bands. 30 primers were selected using bulk segregation analysis (BSA) and RAPD-PCR analysis.

For any of the primers used, band scores did not differ between repeat assessments or between gels. Each of the primers produced large numbers of polymorphic bands. The data of the total number of bands (TNB), number of polymorphic bands (NPB), percentage of polymorphic bands (%PB), amplified fragment size (AFS) obtained for each primer are shown in Tab. 1 and Tab. 2.

The 30 selected primers generated totally 227 clear repeatable bands ranging from 100 to 3000 bp in size, averaging 7.57 bands per primer, and 217 and 221 bands for that of purple and tea-green crab individuals respectively, while the number of polymorphic bands generated from purple and tea-green individuals are 133 and 138 respectively, with the genetic diversity 61.29% and 62.44% correspondingly,

which indicated similar genetic diversity between two color-different crab individuals.

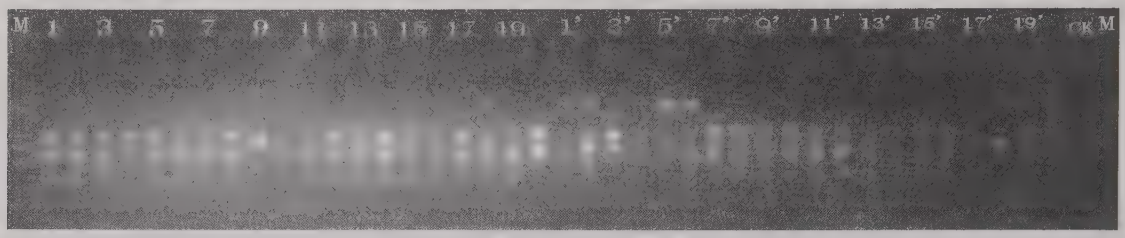

Fig. 1 Agarose gel electrophoresis of RAPD patterns of tea-green and purple crabs amplified with primer SBS A09. Lanes 1 - 20 are PCR products from tea-green crabs; Lanes 1' - 20' are PCR products from purple crabs; CK represents the control without genomic DNA in the PCR reactions; M represents the 2 000 bp DNA ladders.

Tab. 1 List of random 10-bp primers used in RAPD analysis of purple crab individuals of *Portunus trituberculatus*. Total number of bands (TNB), number of polymorphic bands (NPB), percentage of polymorphic bands (%PB) and amplified fragment size (AFS) obtained per RAPD primer.

Sl. No.	Primer	Primer sequence (5'-3')	TNB	NPB	%PB	AFS
1	SBS A02	TGCCGAGCTG	6	4	66.67	250-2000
2	SBS A04	AATCGGGCTG	8	6	75.00	250-2500
3	SBS A05	AGGGGTCTTG	4	3	75.00	250-1500
4	SBS A06	GGTCCCTGAC	6	3	50.00	500-1500
5	SBS A07	GAAACGGGTG	9	7	77.78	250-1500
6	SBS A09	GGGTAACGCC	7	4	57.14	250-2500
7	SBS A13	CAGCACCCAC	7	4	57.14	500-3000
8	SBS A15	TTCCGAACCC	8	7	87.50	600-1000
9	SBS A16	AGCCAGCGAA	8	6	75.00	250-2000
10	SBS A19	CAAACGTCGG	8	4	50.00	100-1500
11	SBS Z03	CAGCACCGCA	7	5	71.43	250-1500
12	SBS Z04	AGGCTGTGCT	9	5	55.56	250-2000
13	SBS Z05	TCCCATGCTG	9	5	55.56	500-2000
14	SBS Z06	GTGCCGTTCA	10	6	60.00	100-2000
15	SBS Z07	CCAGGAGGAC	8	5	62.50	250-2000
16	SBS Z08	GGGTGGGTAA	7	6	85.71	250-1500
17	SBS Z10	CCGACAAACC	10	4	40.00	250-2000
18	SBS Z13	GACTAAGCCC	7	6	85.71	250-3000
19	SBS Z15	CAGGGCTTTC	9	6	66.67	250-2000
20	SBS Z19	GTGCGAGCAA	10	5	50.00	250-2500
21	SBS G10	AGGGCCGTCT	8	5	62.50	250-2500
22	SBS G14	GGATGAGACC	6	3	50.00	250-2000
23	SBS G16	AGCGTCCTCC	9	4	44.44	250-2000
24	SBS G17	ACGACCGACA	5	2	40.00	250-2000
25	SBS L02	TGGGCGTCAA	6	2	33.33	250-2000
26	SBS L03	CCAGCAGCTT	4	3	75.00	250-2000
27	SBS L07	AGGCGGGAAC	7	4	57.14	250-2000
28	SBS L08	AGCAGGTGGA	5	2	40.00	250-2500
29	SBS L13	ACCGCCTGCT	6	3	50.00	750-2000
30	SBS L15	AAGAGAGGGG	4	4	100.00	250-2000
	Total		217	133	61.29	

Different primers revealed different degrees of DNA polymorphisms among these crab individuals; with a primer, the number of amplified loci varied from 5 (SBS A05, SBS G17, SBS L03, SBS L08 and SBS

L15) to 10 (SBS Z05, SBS Z06, SBS Z10 and SBS Z19). The lowest level of polymorphisms among tea-green crab individuals was detected with primers SBS L08 (20%); and the primers SBS L02 (33.33%) for the purple ones.

Two primers (SBS A09 and SBS G16) got specific DNA bands by comparing twenty purple and tea-green individuals through RAPD-PCR analysis and the following electrophoresis. One specific DNA band (750 - 1 000 bp) was discovered using the primer SBS A09 (Fig. 1), with 22.22% and 75.00% polymorphisms within purple and tea-green crab individuals, respectively; and one specific DNA band (1 000 - 2 000 bp) from the primer SBS G16 showed 35.00% and 75.00% polymorphisms within purple and tea-green crab individuals, respectively (Fig. 2).

Tab. 2 List of random 10-bp primers used in RAPD analysis of tea-green crab individuals of *Portunus trituberculatus*. Total number of bands (TNB), number of polymorphic bands (NPB), percentage of polymorphic bands (%PB) and amplified fragment size (AFS) obtained per RAPD primer.

Sl. No.	Primer	Primer sequence (5'-3')	TNB	NPB	%PB	AFS
1	SBS A02	TGCCGAGCTG	6	5	83.33	250-2000
2	SBS A04	AATCGGGCTG	7	4	57.14	250-2500
3	SBS A05	AGGGGTCTTG	6	5	83.33	250-1500
4	SBS A06	GGTCCCTGAC	7	7	100.00	500-1500
5	SBS A07	GAAACGGGTG	8	8	100.00	250-1500
6	SBS A09	GGGTAACGCC	7	4	57.14	250-2500
7	SBS A13	CAGCACCCAC	5	3	60.00	500-3000
8	SBS A15	TTCCGAACCC	8	6	75.00	600-1000
9	SBS A16	AGCCAGCGAA	8	7	87.50	250-2000
10	SBS A19	CAAACGTCGG	8	5	62.50	100-1500
11	SBS Z03	CAGCACCGCA	8	8	100.00	250-1500
12	SBS Z04	AGGCTGTGCT	7	5	71.43	250-2000
13	SBS Z05	TCCCATGCTG	10	6	60.00	500-2000
14	SBS Z06	GTGCCGTTCA	10	5	50.00	100-2000
15	SBS Z07	CCAGGAGGAC	8	4	50.00	250-2000
16	SBS Z08	GGGTGGGTAA	8	5	62.50	250-1500
17	SBS Z10	CCGACAAACC	10	3	30.00	250-2000
18	SBS Z13	GACTAAGCCC	9	7	77.78	250-3000
19	SBS Z15	CAGGGCTTTC	9	5	55.56	250-2000
20	SBS Z19	GTGCGAGCAA	9	6	66.67	250-2500
21	SBS G10	AGGGCCGTCT	8	5	62.50	250-2500
22	SBS G14	GGATGAGACC	6	3	50.00	250-2000
23	SBS G16	AGCGTCCTCC	9	4	44.44	250-2000
24	SBS G17	ACGACCGACA	5	2	40.00	250-2000
25	SBS L02	TGGGCGTCAA	6	2	33.33	250-2000
26	SBS L03	CCAGCAGCTT	5	3	60.00	250-2000
27	SBS L07	AGGCGGGAAC	8	4	50.00	250-2000
28	SBS L08	AGCAGGTGGA	5	1	20.00	250-2500
29	SBS L13	ACCGCCTGCT	6	2	33.33	750-2000
30	SBS L15	AAGAGAGGGG	5	4	80.00	250-2000
	Total		221	138	62.44	

3.2 Genetic diversity

The results showed that the ratio of polymorphic loci was 61.29%, and Nei's gene diversity was

0.375 6, and Shannon's information index was 0.554 5 among purple crab individuals; and the ratio of polymorphic loci was 62.44%, Nei's gene diversity was 0.345 1, Shannon's information index was 0.509 9 among tea-green crab individuals (Tab. 3). The Nei's unbiased measures of genetic identity estimated 0.968 2 for purple and tea-green crabs (Tab. 4).

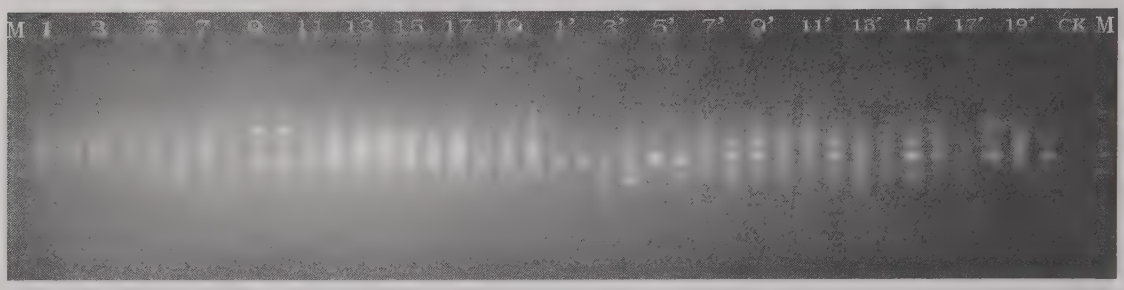

Fig. 2 Agarose gel electrophoresis of RAPD patterns of tea-green and purple crabs amplified with primer SBS G16. Lanes 1-20 are PCR products from tea-green crabs; Lanes 1'-20' are PCR products from purple crabs; CK represents the control without genomic DNA in the PCR reactions; M represents the 2000 bp DNA ladders.

Tab. 3 Genetic diversity of *Portunus trituberculatus*

Population	Number of alleles observed (*Na*)	Effective number of alleles (*Ne*)	Nei's gene diversity (*H*)	Shannon's infor-mation index (*I*)
Tea-green	1.944 4	1.612 0	0.345 1	0.509 9
Purple	2.000 0	1.654 6	0.375 6	0.554 5

Tab. 4 Nei's unbiased measures of genetic identity (above diagonal) and genetic distance (below diagonal) between purple and tea-green crabs of *Portunus trituberculatus*

Pop. ID	Tea-greeen	Purple
Tea-green	-	0.968 2
Purple	0.032 3	-

4 Discussions

RAPD-PCR analysis has been applied in many species (including animals and plants) as an important tool for the phylogenetic classification and identification. In this paper, RAPD marker was applied to characterize and compare genetic diversity between purple and tea-green crabs of *P. trituberculatus*. The ratios of polymorphic loci of purple and tea-green individuals were 61.29% and 62.44%, respectively, and Nei's gene diversities of them were 0.375 6 and 0.345 1, respectively, and Shannon's information indices of them were 0.554 5 and 0.509 9, respectively. The Nei's unbiased measures of genetic identity estimated 0.968 2 for purple and tea-green crabs. While there was no significant genetic divergence between color-different crab individuals through RAPD analysis, it indicated close phylogenetic relationships between purple and tea-green crabs.

Carapace color played an important role in the life circle of a crab. Firstly, carapace color could be correlated with environmental factors and make the crab invisible by means of protective coloring. With purple or tea-green carapace color, the blue swimming crabs can be well camouflaged which can help them survive the danger from predators or capture the prey easily. Secondly, color was often associated with the parts of a crab used in social interactions [11]. Horch et al. [12] showed evidence for a two pigment visual systems in the fiddler crab, *Uca thayeri* and found the crabs may at least be dichromats, with the ability to discriminate colors and thus use them in communication [11]. Thirdly, the carapace color was shown to be associated with some physiological properties in some crab species. The fiddler crab *U. pugilator* was found to change their carapace colors becoming light in the warm treatment and dark in the cold treatment [13]. Reid et al. [14] studied the behavioral and physiological ecology of the shore crab *Carcinus maenas*, and found that male crabs with green carapace color have been shown to be more tolerant of salinity fluctuations and aerial exposure than red male ones. Conversely, red males compete more successfully for mates and food, however, this advantage is gained at the cost of reduced tolerance to the conditions of intertidal life.

The newly discovered purple crabs kept their carapace color permanent through their whole life span. And there is no other carapace color crabs with a large quantitative number discovered in their natural habitats. It is expected that the carapace color may be regulated by multiple genes located on the chromosomes, since there was no specific RAPD primer that could exactly distinguish purple and tea-green crabs from each other specifically. More details about mechanism of color differentiation in the blue swimming crab *P. trituberculatus* are now under investigation.

Acknowledgments

This work was supported by the grant of the Key Project in the National Science & Technology Pillar Program in the Eleventh Five-year Plan Period (No. 2006BAD09A01).

References

[1] GAO B Q, LIU P, LI J.. Isozyme polymorphism in Portunus trituberculatus from wild population [J]. Journal of Fisheries of China, 2007, 31(1): 1 - 6.

[2] SONG W W, WANG C L, MU C K. Pilot study of allozyme in Portunus trituberculatus individual development [J]. Journal of Zhanjiang Ocean University, 2006, 26(1): 74 - 76.

[3] ZHU D F, YU H W, WANG C L. Changes of isozyme patterns during early ontogeny in Portunus trituberculatus [J]. Journal of Fisheries of China, 2005, 29(6): 751 - 756.

[4] GAO B Q, LIU P, LI J. Analysis of morphological variations among four wild populations of Portunus trituberculatus [J]. Journal of Fishery Sciences of China, 2007, 14(2): 223 - 228.

[5] JIN S, ZHAO Q S, WANG C L. RAPD Genetic Markers in Six Species of Marine Crab [J]. Zoological Research, 2004, 25(2): 172 - 176.

[6] GUO T H, KONG X Y, CHEN S Q. A study of the sequence of mitochondrial 16srRNA and COI gene fragments of Portunus trituberculatus [J]. Journal of Ocean University of China, 2004, 34(1): 22-28. (in Chinese)

[7] Yamuchui M M, Miya M U, Nishida M. Complete mitochondrial DNA sequence of the swimming crab, Portunus trituberculatus (Crustacea: Decapoda: Brachyura) [J]. Gene, 2003, 311: 129 - 135.

[8] Korzan W J, Robison R R, ZHAO S. Color change as a potential behavioral strategy [J]. Hormones and Behavior, 2008, 54(3): 463 - 470.

[9] Hiller A, Kraus H, Almon M. The Petrolisthes galathinus complex: Species boundaries based on color pattern, morphology and molecules, and evolutionary interrelationships between this complex and other Porcellanidae (Crustacea: Decapoda: Anomura) [J]. Molecular Phylogenetics and Evolution, 2006, 40(2): 547 - 569.

[10] Asensiio L. PCR-based methods for fish and fishery products authentication [J]. Trends in Food Science & Technology, 2007, 18(11): 558 - 566.

[11] Detto T, Zeil J, Magrath R D. Sex size and colour in a semi-terrestrial crab, Heloecius cordiformis (H. Milne Edwards, 1837) [J]. Journal of Experimental Marine Biology and Ecology, 2004, 302(1): 1-15.

[12] Horch K, Salmon M, Forward R. Evidence for a two pigment visual system in the fiddler crab, Uca thayeri [J]. Journal of Comparative Physiology A, 2002, 188(6): 493– 499.

[13] Silbiger N, Munguia P. Carapace color change in Uca pugilator as a response to temperature [J]. Journal of Experimental Marine Biology and Ecology, 2008, 335(1): 41 - 46.

[14] Reid, D G, Abello P, Kaiser M J. Carapace colour, inter-moult duration and the behavioural and physiological ecology of the shore crab Carcinus maenas [J]. Estuarine. Coastal and Shelf Science, 1997, 44(2): 203 - 211.

用 RAPD 方法对不同色三疣梭子蟹的分析

迟大利[1,2]，阎斌伦[1]，沈颂东[2]，高 焕[1]

（1. 淮海工学院江苏省海洋生物技术重点建设实验室，江苏连云港 222005；2. 苏州大学生命科学学院，江苏 苏州 215123）

摘 要：为寻找三疣梭子蟹体色相关的分子标记，本文用 RAPD 方法对紫色和茶绿色两种三疣梭子蟹基因组 DNA 进行体色相关遗传标记的筛选及其遗传多样性分析。从 80 个随机引物中共筛选了 30 个重复性好多态性高的引物，RAPD 分析结果表明：紫色梭子蟹个体组成的群体多态性位点比例为 61.29%，Nei 氏基因多样性指数为 0.375 6，Shannon 信息指数为 0.554 5；茶绿色梭子蟹个体组成的群体多态性位点比例为 62.44%，Nei 氏基因多样性指数为 0.345 1，Shannon 信息指数为 0.509 9。紫色和茶绿色三疣梭子蟹之间 Nei 氏无偏差遗传相似性指数为 0.968 2，遗传距离为 0.032 3。这些结果表明，紫色和茶绿色三疣梭子蟹群体的遗传多样性程度接近，具有相似的遗传多样性基础。另外，有 2 个随机引物(SBS A09 和 SBS G16)扩增得到群体特异性片段各 1 条。

关键词：体色；亲缘关系；三疣梭子蟹；RAPD

Correlation and path coefficient analysis for phenotypic traits of noble scallop *Chlamys nobilis*

LI Jun-hui, DU Xiao-dong*, DENG Yue-wen, WANG Qing-heng

Fisheries College of *Guangdong Ocean University*, *Zhanjiang* 524025, *Guangdong Province, China*

Abstract: In April of 2006, a base population of the noble scallop *Chlamys nobilis* was established by collecting parental breeders from the stocks in Wushi, Zhanjiang. In December of 2006, 200 individuals were randomly sampled from the base population and subjected for correlation and path coefficient analysis. It was found that there were statistically significant phenotypic correlations among the traits ($P < 0.01$). Total weight was significantly and positively correlated with the shell length (r = 0.934 3), shell height (r = 0.895 9), shell width (r = 0.899 1), muscle weight (r = 0.882 0) and shell weight (r = 0.937 9), respectively. Shell length, shell width, muscle weight, shell height and shell weight had positive and direct effects on the total weight, with values of 0.397 1, 0.321 9, 0.172 1, 0.089 6 and 0.066 9, respectively. Shell length, shell width and muscle weight had higher direct effects on the total weight than shell height and shell weight. A combined evaluation of correlation, direct effects and indirect effects showed that direct selection for shell length, shell width, muscle weight, shell height and shell weight would be effective to improving the total weight. It was concluded that these traits could be regarded as the selection criteria in breeding programs of the species.

Keyword: *Chlamys nobilis*, phenotypic traits, correlation, path coefficient analysis

Introduction

Chlamys nobilis Reeve is the species in tropic seas and mainly distributed along the coasts of China, Japan and Indonesia. Due to its delicious favor and rapid growth, the species is abundantly cultured in the southern coasts of China and the annual commercial landings of the noble scallop were around 20,000 metric tons. However, the noble scallop culture in southern China has recently suffered a lot from slow growth and mass mortalities. Breeding studies have initiated to develop superior lines to improve the growth and the resistance to diseases as well as increasingly deteriorating environments. The current breeding studies on the species have included polyploidy induction [1, 2], hybrid [3, 4] and mass selection [5].

When planning a selection breeding program, it is important for the breeders to know the relationship of the selected traits. Most of the traits of interest to breeders are complex and result from the interaction of the traits. Correlation analysis can provide an understanding of the relationship among the traits. Further understanding will be obtained by the path coefficient analysis, which may partition relationship

Received on March 29, 2010

Corresponding author: duxd@gdou.edu.cn

into direct and indirect effects of some traits on a special trait [6]. The breeders have successfully performed the correlation and path coefficient analysis to assist in identifying some economic traits of several shellfish species, which were involved in *Chlamys farreri*[7], *Pinctada martensii*[8], *Perna viridis* [9], *Patinopecten yessoensis* [10], *Chlamys nobilis* [11], *Saxidomus purpurata* [12] and *Argopecten irradians irradians* [13].

The present study was to evaluate correlation coefficient for phenotypic traits and estimate the relative contribution of some traits to total weight by path coefficient analysis, which can provide some useful information on selection for superior lines in the base population of the species.

1 Materials and methods

1.1 The establishment of the base population

In April of 2006, 120 mature animals were randomly collected from the cultivated stocks in Wushi, Zhanjiang. The breeders were mass spawned in the hatchery. Larvae were reared following the techniques of Du et al (2004) [14]. Fertilized eggs were incubated in 500-l polyethylene tanks until the D-shape larvae occurred at 24 h after fertilization. And then, the larvae were transferred to 1 000-l polyethylene tanks. The density was about 1 individual/ml. Water temperature was at 28 ± 1 °C and salinity was at 30 ± 1ppt. Daily feeding consisted of *Isochrysis galban* from Day 2 to 5, and a mixture of *I. galban* and *I. zhanjianggensis* from Day 6 to 15. Feeding ration was increased with ages. Every other day, 500 l of sea water were replaced in each tanks and water was completely changed on Day 5, 10 and 15. At approximately 15 days, plastic films were provided as substrate for metamorphosis. At approximately 35 days, individuals as large as 2–5 mm were removed from films, transferred to the nets and suspended in floating nets in the sea of Wushi, Zhanjiang. Shells were cleaned and placed in new nets at appropriate intervals.

1.2 Sampling and measurement

In December of 2006, 200 individuals were randomly sampled from the base population, and then subjected to the experiment where phenotypic traits were individually measured. The methods for phenotypic trait measurement were detailed by Liu et al (2002) [7]. The measured traits were the shell length (mm), shell height (mm), shell width (mm), muscle weight (g), shell weight (g) and total weight (g). Shell length, shell height and shell width were measured to the nearest 0.01mm by venier calipers, while shell weight, muscle weight and total weight were measured to the nearest 0.01g by electronic balance.

1.3 Statistical analysis

The simple phenotypic correlation coefficients among the measured traits were first evaluated using software SPSS 11.0 version, and then separated into direct and indirect effects by path coefficient analysis as described by Liu et al (2002) [7]. In the path analysis, total weight was the dependent variable and the other traits were considered as independent variables.

2 Results

The mean values of the measured traits and their coefficients of variation (CVs) are listed in Table 1. The CVs of the measured traits were high, with values ranging from 10.49% for shell height to 24.89% for muscle weight.

Tab. 1 Mean values and coefficient of variation of phenotypic traits of the noble scallop *Chlamys nobilis*

Traits	SL	SH	SW	SHW	MW	TW
Mean / SD	60.17(7.03)	65.28(6.85)	22.51(2.88)	21.52(4.54)	4.17(1.04)	32.98(6.49)
CV%	11.68	10.49	12.83	21.09	24.89	19.68

Note: SL, shell length / mm; SH, shell height / mm; SW, shell width / mm; Shell weight (SHW); MW, muscle weight / g; TW, total weight / g.

Phenotypic correlations among the phenotypic traits are listed in Tab. 2. There were statistically significant correlations among the traits ($P < 0.01$). Total weight exhibited highly significant and positive correlations with the shell length (r = 0.934 3), shell height (r = 0.895 9), shell width (r = 0.899 1), muscle weight (r = 0.882 0) and shell weight (r = 0.937 9) ($P < 0.01$). The results indicated relative utility of the traits for selection with respect to total weight.

Tab. 2 Phenotypic correlations among the traits of the noble scallop *Chlamys nobilis*

Traits	SH	SW	MW	SHW	TW
SL	0.872**	0.791 7**	0.843 4**	0.901 9**	0.934 3**
SH		0.781 5**	0.822 5**	0.930 5**	0.895 9**
SW			0.772 6**	0.863 7**	0.899 1**
MW				0.813 4**	0.882 0**
SHW					0.937 9**

** $P < 0.01$

The path analysis revealed that the indirect effects of other five traits on total weight were larger than direct effects (Tab. 3). Shell length had the highest direct relationship with total weight (0.397 1), followed by shell width (0.321 9), muscle weight (0.172 1), shell height (0.089 6) and shell weight (0.066 9). Shell weight had the highest phenotypic correlation with total weight, but the direct relationship on total weight was lowest. Shell weight exerted its effects on total weight by shell length (0.358 2), followed shell width (0.278 1), muscle weight (0.148 7) and shell height (0.083 4).

Tab. 3 Direct and indirect effects of the other five traits on the total weight of the noble scallop *Chlamys nobilis*

Trait	correlation	Direct effect	Indirect effect				
			SL	SH	SW	MW	SHW
SL	0.934 3	0.397 1	-	0.078 1	0.254 9	0.143 5	0.060 3
SH	0.896 2	0.089 6	0.346 3	-	0.251 7	0.141 6	0.062 2
SW	0.899 1	0.321 9	0.314 5	0.070 1	-	0.133 0	0.057 8
MW	0.882 0	0.172 1	0.331 2	0.073 7	0.248 8	-	0.054 4
SHW	0.937 9	0.066 9	0.358 2	0.083 4	0.278 1	0.148 7	-

3 Discussion

Many studies have been reported that there exists highly additive variance of growth in the stocks of shellfish species, and good results can be obtained when the mass selection for growth is performed. For example, Zheng et al. (2004) reported that 10.2% gain for shell length growth after one-generation mass selection for superior growth in a stock of bay scallop *Argopecten irradians irradians* Lamarck from Laizhou Shandong [15]. Highly genetic gain was also detected by mass selection for the growth in *Ostrea edulis* [16], *Argopecten irradians concentricus* [17] and *Pinctada martensii* [18-20]. In the present study, the base population had high coefficient of variation for growth traits measured, indicating high variation for growth traits. It is expected to obtain improvement in growth by mass selection for fast-growing individuals at an appropriate intensity in the base population.

Highly positive correlation among phenotypic traits was observed in *Ostrea edulis* [21], *Ostrea chilensis* Philippi [22], *Chlamys farreri* [7] and *Pinctada martensii* [8, 23]. Highly significant correlation was observed by regression analysis on 11 quantitative traits, for example, shell thickness, shell weight and condition factors of individuals of the first generation produced by inter- and intra-crosses of geographically different populations of pearl oyster *Pinctada martensii* [23]. Our results also showed that there was significantly positive relationship among the measured growth characters. The results indicated that selection for a trait would result in the improvement in other traits. The explanation for the high relationship among the traits was made by pleiotropy in the determination of these traits [24].

Path coefficient analysis has been successfully used to detect the direct and indirect effects of the phenotypic traits in several shellfish species. By path coefficient analysis on a stock of scallop *Chlamys farreri* collected in Dalian Liaoning, the results showed that shell length, shell height and shell width exerted positively direct effects on total weight [7]. In the present study, shell length, shell height, shell width, shell height and muscle weight had positive and direct effects on total weight. Our results indicated these traits could be considered as the selection indices in the improvement of total weight.

Conclusively, shell length, shell height, shell width, muscle weight and shell weight was positively

and significantly correlated with the total weight. Moreover, shell length, shell height, shell width, shell weight and muscle weight had positive and direct effects on the total weight. The results of correlation and path analysis showed that these traits (shell length, shell height, shell width, muscle weight and shell weight) might be regarded as the indices of direct selection for the improvement of total weight.

References

[1] Lin Y G, He M X, Qing N, et al. Triploid induction in the scallop, *Chlamys nobilis* and growth comparisons [J]. Tropic Oceanology, 1995, 14(4): 84 - 89.

[2] Zeng Z, Chen N M, Lin Q, et al. Induced triploidy in scallop *Chlamys nobilis* [J]. Journal of Oceanography in Taiwan Strait, 1995, 14(2): 155 - 162.

[3] Wan J F, Bao Z M, Liu G X, et al. Segregation of ISSR markers in hybrid larvae of two scallop species [J]. High Technology Letter, 2004, 5: 82 - 87.

[4] Liu G X, Bao Z M, Hu J J, et al. ISSR analysis of two species of scallop (*Chlamys farreri*, *C. nobilis*) and their intra- and inter-species mating descendants [J]. Periodical of Ocean University of China, 2006, 36(1): 71 - 75.

[5] Deng Y W, Wang Q H, Huang R L, et al. Comparison of amylase and cellulase activities of two size groups in a base population of Huagui scallop *Chlamys nobilis* [J]. Journal of Marine Sciences, 2008, 26(2): 37 - 40.

[6] Rodriguez D, Jasso D, Angulo-Sanchez J L, et al. Correlation and path coefficient analyses of the agronomic traits of a native population of guayule plants [J]. Industrial Crops and Products, 2001, 14: 93 - 103.

[7] Liu X L, Chang Y Q, Xiang J H, et al. Analysis of effects of shell size characters on live weight in Chinese scallop *Chlamys farreri* [J]. Oceanologia Et Limnologia Sinica, 2002, 33(6): 673 - 678

[8] Deng Y W, Du X D, Wang Q H, et al. Correlation and path analysis for growth traits in F_1 population of pearl oyster *Pinctada martensii* [J]. Marine Science Bulletin, 2008, 10(2): 68 - 73.

[9] Wang Q H, Deng Y W, Du X D, et al. Effect of morphometric traits on edible part weight of *Perna viridis* [J]. Journal of Guangdong Ocean University, 2009, 29(4): 5 - 8.

[10] Zhang C S, Chang Y Q, Cao X B, et al. Analysis of effect of body shape traits on soft-tissue weight and adductor weight in *Patinopecten yessoensis* Jay [J]. Journal of Fisheries of China, 2009, 33(1):87 - 94.

[11] Zheng H P, Sun Z W, Zhang T, et al. Correlation and path analysis to quantitative traits of noble scallop *Chlamys nobilis* Reeve at one-year old [J]. Chinese Agricultural Science Bulletin, 2009, 25(20):322 - 326.

[12] Li Z X. Mathematical analysis of effects of morphometric attributes on body weight for *Saxidomus purpurata* [J]. Chinese Agricultural Science Bulletin, 2009, 25(5): 279 - 282.

[13] .Li Z X, Wang C D. Comparison of growth and path analyses of inbred and cross-bred populations in the bay scallop *Argopecten irradians irradians* [J]. Chinese Agricultural Science Bulletin, 2009, 25(8): 282 - 285.

[14] Du T, Luo J, Liang F L. Artificial breeding of scallop *Chlamys nobilis* [J]. Journal of Zhanjiang Ocean University, 2004, 24(4): 69 - 71.

[15] Zheng H P, Zhang G F, Liu X, et al. Different responses to selection in two stocks of the bay scallop, *Argopecten irradians irradians* Lamarck (1819) [J]. Journal of Experimental Marine Biology and Ecology, 2004, 313: 213 - 223.

[16] Newkirk G F, Haley L E. Selection for growth rate in the European oyster, *ostrea edulis*: response of second

generation groups [J]. Aquaculture, 1983, 33:149 - 155.

[17] Crenshaw J W, Heffernan P B, Walker R L. Heritability of growth rate in the southern Bay scallop, *Argopecten irradians concentricus* [J]. Journal of Shellfish Research, 1991, 10: 55 - 63.

[18] Wang A M, Shi Y H, Yan B. Effects of selection on larval growths for second generation of different selected pearl oysters, *Pinctada martensii* [J]. High Technology Letters, 2004, 8: 94 - 97.

[19] He M X, Shi J H, Lin Y G. et al. Studies on growth traits of first generation of a selective line of *Pinctada martensii* (Dunker) [J]. Journal of Tropical Oceanography, 2006, 25(1): 19 - 22.

[20] Deng Y W, Fu S, Du X D, et al. Realized heritability and genetic gain estimates of larval shell length in the Chinese pearl oyster *Pinctada martensii*, at three different salinities [J]. North American Journal of Aquaculture, 2009, 71:302 - 306.

[21] Toro J E, Newkirk G F. Divergent selection for growth rate in the European oyster *Ostrea edulis*: response to selection and estimation of genetic parameters [J]. Marine Ecology Progress Series, 1991, 4(2): 101 - 108.

[22] Toro J E, Aguila P, Vergara A M. Spatial variation in response to selection for live weight and shell length from data on individually tagged Chilean native oyster (*Ostrea Chiensis* Philippi, 1845) [J]. Aquaculture, 1996, 146(1-2): 27 - 36.

[23] Wang A M, Shi Y H, Zhou Z G. Morphological trait parameters and their correlations of the first generation from matings and crosses of geographical populations of *Pinctada martensii* (Dunker) [J]. Marine Fisheries Research, 2004, 25(3): 39 - 45.

[24] Falconer D S. Introduction to quantitative genetics [M]. New York : Longman Inc. 1981.

华贵栉孔扇贝表型性状相关和路径分析

李俊辉，杜晓东，邓岳文，王庆恒

（广东海洋大学水产学院，广东 湛江，524025）

摘 要：2006 年 4 月，从广东湛江乌石养殖群体中挑选性腺成熟的个体作为亲本繁殖子一代。2006 年 12 月从子一代群体随机取样 200 个个体，测量壳长、壳高、壳宽、肌肉重、壳重和全湿重共 6 个性状指标，利用测量数据进行表型性状相关和路径分析。结果表明：（1）表型性状间存在显著的相关性（$P < 0.01$）。全湿重与壳长、壳高、壳宽、肌肉重和壳重存在显著的正相关（$P < 0.01$），相关系数分别为 0.934 3、0.895 9、0.899 1、0.882 0 和 0.937 9。（2）壳长、壳宽、肌肉重、壳高和壳重对全湿重具有正直接影响，其值分别为 0.397 1、0.321 9、0.172 1、0.089 6 和 0.066 9。本研究结果说明了对壳长、壳高、壳宽、肌肉重和壳重进行直接选择可以提高全湿重，这些性状可以作为选育的指标。

关键词：华贵栉孔扇贝，表型性状，相关分析，路径分析

Effects of salinity fluctuation and dietary protein/ carbohydrate ratio on the survival and growth of Juvenile *Litopenaeus vannamei*

WANG Xing-qiang, CAO Mei, YAN Bin-lun

Jiangsu Key Laboratory of Marine Biotechnology, Huaihai Institute of Technology, Lianyungang 222005, *Jiangsu Province, China*

Abstract: A factorial study was conducted to determine the effects of salinity (constant (S0) and fluctuating (S10)) and isoenergetic diet of different protein/carbohydrate ratios (P/C: 4.1, 1.9, 1.0 and 0.6) on the survival and growth of juvenile *Litopenaeus vannamei*. The experiment lasted for 35 days. The results showed that I) At S0 and S10, specific growth rate and apparent digestibility coefficient exhibited decreasing trend, while food conversion ratio exhibited increasing trend, with decreasing P/C ratio. At S0, food consumption and specific growth rate of the shrimp fed 4.1 P/C were significantly higher than those fed 1.0 and 0.6 P/C, whereas at S10, no significant differences were detected among different treatments; II) At 4.1 and 1.9 P/C, food consumption and specific growth rate were higher in the shrimp maintained at S0 as compared with those at S10, while at 1.0 and 0.6 P/C, an inverse trend was observed. Among four P/C ratios, food conversion ratio of the shrimp at S0 was the lowest.

Keyword: *Litopenaeus vannamei*; salinity fluctuation; protein/carbohydrate ratio; survival; growth

Introduction

The white shrimp *Litopenaeus vannamei* (Boone, 1931) is the most important shrimp species for cultivation in saltwater or low-salinity ponds along the east coast of China, which accounted for approximately 80% of total shrimp production in China [1]. Diseases in this species had received considerable attention as viruses affected *L. vannamei* farms with losses of hundreds of millions of dollars [2, 3]. To reduce potential infection of commercial shrimp production facilities by catastrophic diseases-related viruses, an appropriate and cost-effective "ecological" strategy towards disease prevention with zero or limited water exchange in shrimp farming is suggested, reducing pumping costs and the volume of discharge to ambient waters [4]. However, the water salinity in zero or very low discharge shrimp production system is influenced heavily by the rainfall [5], monsoon and topography. Salinity of most of the coastal ponds in China can vary widely between 5‰ and 40‰, from the rainy and typhoon season to dry season, significantly impacting the stable shrimp production [2]. Although salinity is one of the major physical factors influencing the survival, growth and metabolism of aquatic animals, most previous studies

Received on April 21, 2009

Corresponding author: xqwangcaomei@yahoo.com.cn

usually were conducted at constant salinity, whereas moderate and extreme fluctuating salinity is more typical for the shrimp ponds [6, 7]. In a laboratory study, Mu et al. (2005) found that a salinity fluctuation from 30‰ to 26‰ or 23‰ resulted in significant increases, whereas to 20‰ resulted in significant decreases in growth and food consumption for *Fenneropenaeus chinensis* juveniles [5].

From a production standpoint, the major costs in any form of intensive shrimp culture are associated with feeding, which represent up to 50% - 60% of the total production costs [8]. As protein constitutes one of the major nutrients and ingredient costs in practical diet formulations for shrimp, it is important from a nutritional, environmental and economical point of view to improve protein utilization for tissue synthesis rather than for energy purposes, and adequate non-protein energy sources must be provided in feeds to meet the energetic requirements of the shrimp [1, 6, 9]. Koshio et al. (1993) found that the minimum dietary protein content for maximum growth could be reduced when dietary energy content was increased for the kuruma prawn *Penaeus japonicus*, indicating that prawns may require less protein when their energy requirement is met by non-protein nutrient sources [10]. Arantakananda and Lawrence (1993) reported that maximum growth for *L. vannamei* could be obtained with a dietary protein level of 15% and an optimal energy to protein ratio of 120 kJ/g proteins [11].

In general, carbohydrate is considered as the most economical source of dietary energy in penaeid shrimp, and studies on a variety of penaeid species had indicated an improved growth on diets with an adequate dietary carbohydrate supply [1, 9]. Hari et al. (2006) reported the possibility of reducing the dietary protein level in favor of addition of carbohydrate to the water column without any significant reduction in shrimp production [12]. Cousin (1995) found satisfactory performances of *L. vannamei* in diets with carbohydrate content up to 50%, showing that carbohydrate can act as a significant energy source [13]. Rosas et al. (2001) reported that dietary carbohydrate contents could be boosted to at least 23% with no negative effect on the growth of *L. vannamei* [14]. This better efficiency of using carbohydrate for routine metabolism, thus liberating protein for tissue aggregation, was also reported in *L. vannamei* [15], *Penaeus monodon* [16], and *P. indicus* [17].

Since the beginning of shrimp culture, it has been hypothesized that nutritional requirements can change according to variations in abiotic factors, such as salinity, temperature, dissolved oxygen, since all parameters alone and/or in conjunction modify the energetic requirements of shrimp [18]. As *L. vannamei*, being a euryhaline shrimp species and having high capacity of osmoregulation, can respond to fluctuating environmental conditions that may occur in ponds due to climate, hydrographic and anthropogenic influences and the response may require a considerable amount of energy, it is possible that protein and carbohydrate metabolism adaptation takes place [1, 9]. To create an adequate condition for optimal production for the species, this study was designed to investigate the long-term (35 days) survival and growth of juvenile *L. vannamei* subjected to salinity fluctuation in a cyclical manner based on the suitable salinity range (from salinity 17‰ to salinity 27‰) and fed with different diet of different protein/carbohydrate ratios.

1 Materials and methods

1.1 Diet preparation

Four approximately isoenergetic diets (F1, F2, F3, F4) were formulated with protein/carbohydrate ratios (P/C) of 4.1, 1.9, 1.0, 0.6, respectively. The diets were prepared by mixing dry ingredients and water (2:1, w/w) in pellet diets produced by meat grinder in 1.6 mm diameter. The diets were then oven-dried (70 °C for 24 h) to 6.1% - 6.4% moisture and stored at 4 °C for use. Ingredient and proximate composition of the diets are shown in Tab. 1. Crude protein, lipid, ash and carbohydrate in diets were determined by the standard methods of AOAC (1995), and gross energy content by 1 281 Oxygen Bomb Calorimeter (Parr Instrument, USA)[19].

Tab. 1 Ingredient and proximate composition of the experimental diets

Formulation / %	F1	F2	F3	F4
Fish meal	52.5	41.5	31.5	24.5
Soybean meal	17.5	12.5	7	0
Peanut meal	17.5	12.5	7	0
Wheat flour	0	21	42	63
Fish oil	2.5	2.5	2.5	2.5
Lecithin	2	2	2	2
Sodium alginate	2	2	2	2
Vitamin mix[1]	2	2	2	2
Mineral mix[2]	4	4	4	4
Proximate analysis / %				
Moisture	6.14	6.22	6.27	6.31
Protein	50.16	41.53	33.03	24.90
Lipid	6.50	6.44	6.33	6.27
Ash	12.63	11.51	10.35	9.05
Carbohydrate	12.11	22.24	32.08	42.00
Gross energy (kJ·/ g)	17.85	17.81	17.79	17.77
Protein/carbohydrate ratio	4.1	1.9	1.0	0.6

Notes: [1]Vitamin mix, each 1000 g of diet contained: thiamin-HCl, 60 mg; riboflavin, 100 mg; folic acid, 10 mg; pyridoxine-HCl, 140 mg; niacin, 400 mg; calcium pantothenate, 140 mg; choline chloride, 4 000 mg; inositol, 4 000 mg; ascorbic acid, 4 000 mg; biotin, 2 mg; ρ-amino benzoic acid, 150 mg; α-tocopherol, 400 mg; menadione, 34 mg; cyanocobalamine, 0.8 mg; retinol acetate, 150 000 IU; cholecalciferol, 60 000 IU

[2]Minieral mix, each 1000 g of diet contained: $Ca(H_2PO_4)_2$, 8.800 g; $CaCO_3$, 8.240 g; K_2HPO_4, 4.000 g; NaH_2PO_4, 11.200 g; $MgSO_4·7H_2O$, 5.095 g; KCl, 1.600 g; $FeSO_4·7H_2O$, 0.400 g; $AlCl·6H_2O$, 0.016 g; $ZnSO_4·7H_2O$, 0.432 g; $MnSO_4·H_2O$, 0.080 g; $CuSO_4·5H_2O$, 0.008 g; $CoCl_2·6H_2O$, 0.112 g; KI, 0.016 g; Na_2SeO_3, 0.001 g

1.2 Source and acclimation of experimental shrimp

The experiment was carried out at Jiangsu Key Laboratory of Marine Biotechnology, Huaihai Institute of Technology, Lianyungang, P. R. China. *L. vannamei* juveniles (average wet weight: 0.052 ± 0.012 g) were obtained from Haiyangyuan Shrimp Breeding Farm, Ganyu, P. R. China. The shrimp were initially held in a fiberglass tank (200×200×200 cm) at salinity 31‰ for 7 days, and were acclimated to 22‰ by lowering the salinity at a rate of 3‰/d with adding tap water (about 0.2‰ salinity).

1.3 Experimental design

A 2×4 factorial experiment was performed. Eight treatment groups with three replications per treatment were used. Two salinity patterns, S0, a control group exposed to a constant flux of seawater [22‰] and S10, a treatment group exposed to a fluctuating salinity varied daily between 17‰ and 27‰ in a cyclical manner at each of the four P/C ratios (4.1, 1.9, 1.0 and 0.6, Fig. 1) were established. The salinity of the treatment S10 was set at the minimum (17‰) on the first day and was increased gradually to the maximum (27‰) the next day, then was decreased to the minimum once again for the following day until the end of the experiment. A system consisting of 4 fiberglass tanks (200×100×60 cm) with aeration was used. In two of the tanks, the salinity was 22‰ throughout the experiment (the treatment S0), while in the other two tanks, the salinity was fluctuating daily (S10). Two pumps (35W) with a preprogrammed salinity controller (on or off power supply), which was specially designed to generate the needed salinity pattern by controlling the seawater (60‰) against the freshwater (about 0.2‰ salinity), were applied to control the increase, decrease and maintenance of the tank salinity at a rate of about 0.5‰·/h (Fig. 1). Six glass aquaria (60×45×40 cm) with each aquarium covered with 1-mm screen to prevent the shrimp from jumping out were immersed in each tank. To make sure the salinity change would be the same for all the aquaria in the same tank, and two quadrate holes (2×2 cm), covered with 0.5-mm screen, were drilled at each of four sides of the aquaria.

After 24 h of feed deprivation, 240 shrimps with wet weight ranging from 0.070 g to 0.080 g were selected from those in the acclimating fiberglass tank and were haphazardly stocked into 12 aquaria for the corresponding salinity treatments, i.e., constant salinity of S0 and fluctuating salinity of S10, with 10 shrimps in each aquarium. Shrimps at both salinity treatments were fed in excess by hand twice daily for four experimental diets (F1, F2, F3, F4) at 06:00 and 18:00, respectively. Each feeding lasted approximately 2.5 h and uneaten food was collected, dried at 70 ˚C. Twice a day, intact feces were collected from each tank, freeze-dried immediately, and then held at 20 ˚C until analysis. The experiment lasted for 35 days. During the experiment, dissolved oxygen was maintained above 6.0 mg/L, pH from 7.7 to 8.2, ammonia < 0.24 mg/L and photoperiod 14 L:10 D with light period from 06:00 to 20:00.

1.4 Data analysis

Specific growth rate (SGR), food conversion ratio (FCR), and apparent digestibility coefficient (ADC) were calculated as follows:

$$SGR = 100 \times (\ln W_2 - \ln W_1)/t$$

$$FCR = 100 \times C/(W_2 - W_1)$$

$$ADC = 100 \times (C - F)/C$$

where W_2 and W_1 are final and initial wet weight of the shrimp (g); C, food consumption in dry weight (g); F, fecal production in dry weight (g); t, duration of the experiment (d).

Data were subject to a two-way ANOVA. When overall differences were significant at <5% level,

Tukey's test was used to compare the mean values between individual treatments. When the values are given in percentages, the data were square-root arc-sine transformed before being analyzed. Statistical analysis was performed using SPSS (Statistic package for social science) 11.0.

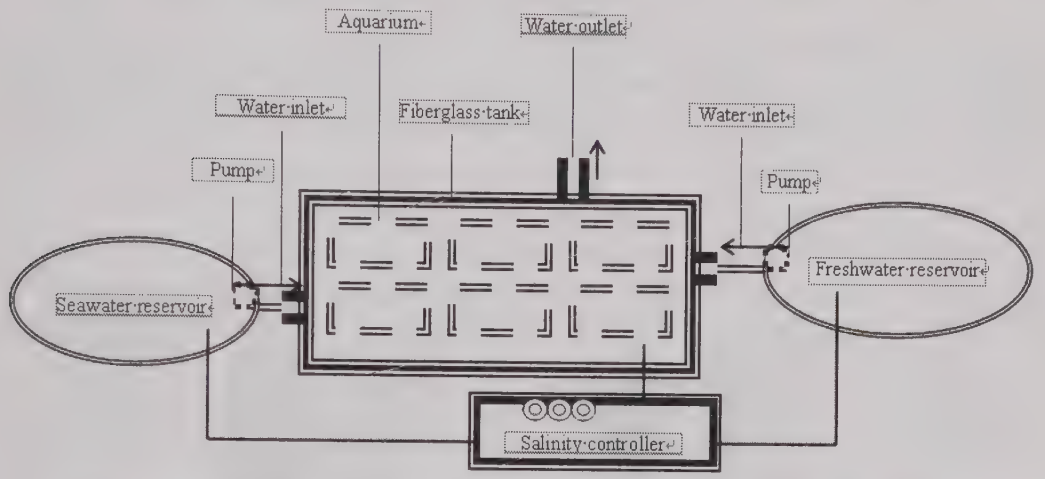

Fig. 1 Diagram of the fluctuating salinity control system. Controlled by the programmed salinity controllers, the fluctuation salinity could attain by pumping the freshwater and seawater alternately. Arrows indicate the directions of water flow.

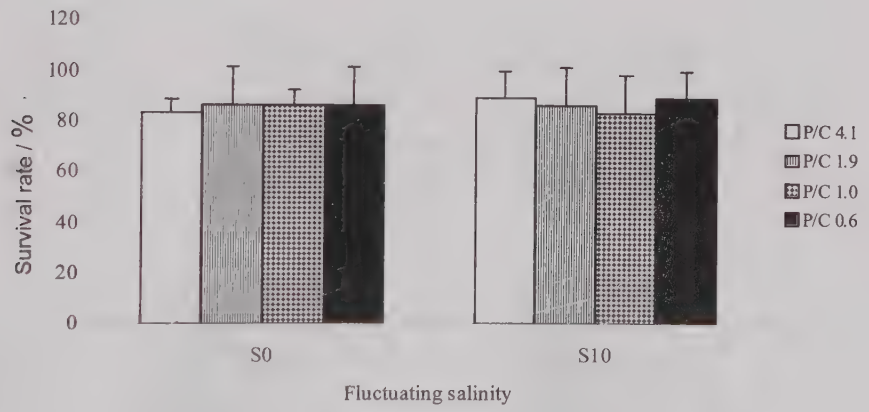

Fig. 2 Effects of fluctuating salinity and different dietary protein/carbohydrate ratio (P/C) on survival rate of *Litopenaeus vannamei* juveniles

(values are means of three replications groups for each treatment of *L. vannamei* juven)

2 Results

The results showed that at S0 and S10, specific growth rate and apparent digestibility coefficient exhibited decreasing trend, while food conversion ratio exhibited increasing trend with decreasing P/C ratio (Fig. 4, 6, 7). At 4.1 and 1.9 P/C, food consumption and specific growth rate were higher in the shrimp

maintained at S0 as compared with those at S10, while at 1.0 and 0.6 P/C, the inverse trend was observed (Fig. 4 and 5). Among four P/C ratios, food conversion ratio of the shrimp at S0 had the lowest value. ANOVA showed that final wet weight, specific growth rate and food consumption were significantly affected by fluctuating salinity, P/C and the interaction between fluctuating salinity and P/C (Fig. 3, 4 and 5). No significant differences were detected in the other treatments (Fig. 2, 6 and 7). At S0, food consumption and specific growth rate of the shrimp fed 4.1 P/C were significantly higher than those fed 1.0 and 0.6 P/C, whereas at S10, no significant differences were detected among the different treatments.

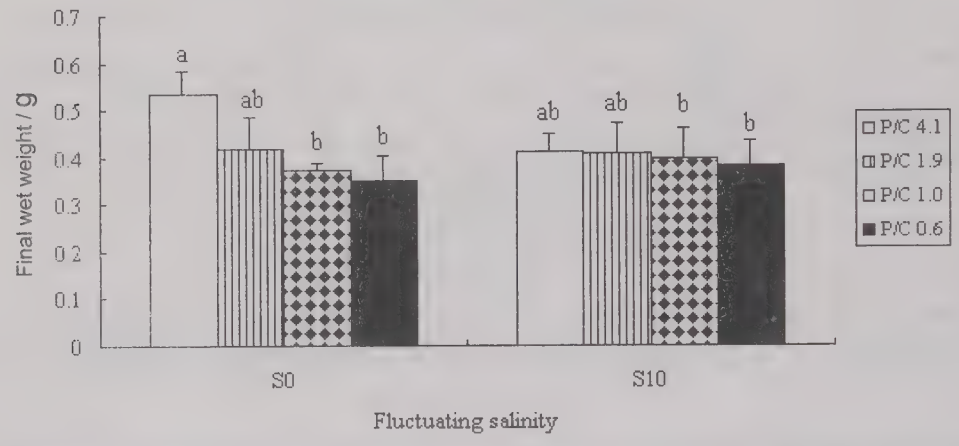

Fig. 3 Effects of fluctuating salinity and different dietary protein/carbohydrate ratio (P/C) on final wet weight of *Litopenaeus vannamei* juveniles

(values are means of three replications groups for each treatment of *L. vannamei* juveniles; means with different letters are significantly different (P<0.05))

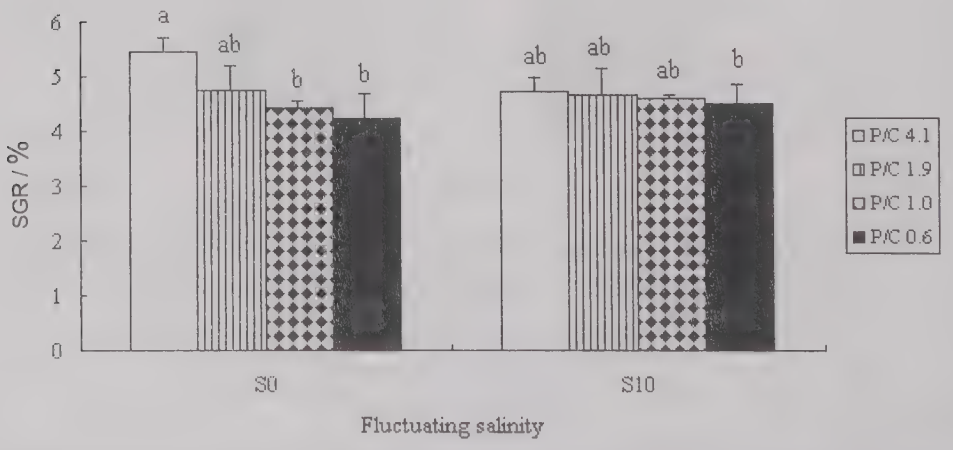

Fig. 4 Effects of fluctuating salinity and different dietary protein/carbohydrate ratio (P/C) on specific growth rate (SGR) of *Litopenaeus vannamei* juveniles

(values are means of three replications groups for each treatment of *L. vannamei* juveniles; means with different letters are significantly different (P<0.05))

3 Discussion

3.1 The effect of salinity fluctuation on the survival of *L. vannamei* juveniles

The survival rate has been used as a useful indicator to evaluate physiological conditions and to detect the effects of lethal stresses for the cultured shrimp [6, 20]. Generally, euryhaline shrimps are exposed to a wide range of salinities and are often subjected to extreme salinity conditions during pond culture. They possess the ability to tolerate low or high salinities by a combination of avoidance behaviors, tolerance of internal change (osmoconformity) and physiological compensation (osmotic, ionic, volume regulation) that enable them to maintain constant cell and body volume [21, 22, 23]. Galli and Stern (1998) reported that the survival of *L. vannamei* was drastically reduced when salinity decreased below 0.18‰, indicating the limited capability for *L. vannamei* juveniles to tolerate very extreme salinities [24]. By contrast, the survival of *L. vannamei* in the current experiment ranged from 83.33 to 90.00% and was not significantly different among the treatments (Fig. 2), indicating that neither fluctuating salinity nor P/C tested influenced survival, although excessive fluctuation in abiotic factors (e.g. oxygen, temperature, salinity) might increase shrimp's stresses and susceptibility to diseases [5].

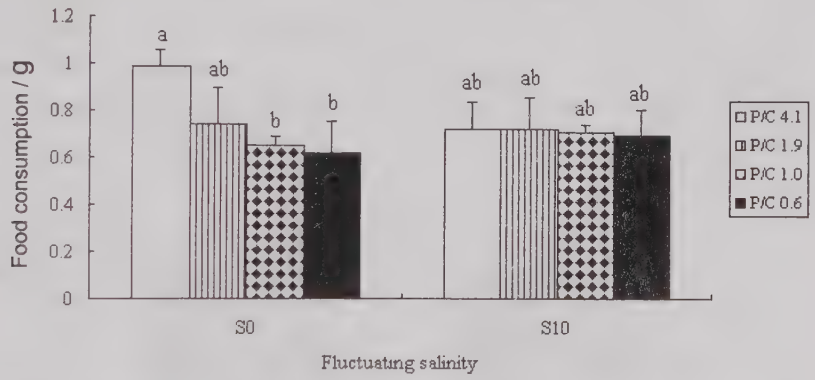

Fig. 5 Effects of fluctuating salinity and different dietary protein/carbohydrate ratio (P/C) on food consumption of *Litopenaeus vannamei* juveniles

(values are means of three replications groups for each treatment of *L. vannamei* juveniles; means with different letters are significantly different (P<0.05))

3.2 The effect of salinity fluctuation on growth of *L. vannamei* juveniles

Growth rate is one of the most important indices determining economic performance in shrimp farming, which may reflect the adaptation to various environmental conditions [9]. Among the ecological factors, salinity is specific to the aquatic environment [1, 6]. The isosmotic point has been associated with optimal conditions for aquatic animals regarding growth and it is generally believed that more energy is expended for osmoregulation by several penaeid shrimp subjected to hypo/hyper-osmotic environments as compared with those maintained under salinities near isosmotic conditions [25]. *L. vannamei* is known to

inhabit wild ranges of salinity, from 1‰ to 40‰, and exhibits hyper-osmotic regulation at low salinity levels and hypo-osmotic regulation at high salinity levels with an isomotic point of 718 mOsm/kg, which is equivalent to 25‰ [26, 27]. Huang (1983) compared the growth of *L. vannamei* in response to salinity (5, 15, 25, 35 and 45‰), and concluded that 25‰ was the best for the maximum growth [28]. Wang et al. (2006) considered salinity of 22.93‰ to be ideal for *L. vannamei* culture [29]. By contrast, Bray et al. (1994) reported that *L. vannamei* juveniles had growth optima between 5‰ and 15‰ [30]. Ponce-Palafox et al. (1997) demonstrated that optimum salinity was around 33‰ - 40‰ for *L. vannamei* [31]. In addition to differences in experimental conditions and shrimp size, the discrepancies among results of previous studies may be that the optimal salinity for growth of *L. vannamei* is not a single point but a range, as *L. vannamei* is adapted to environments with natural fluctuating salinity levels, and generally grows faster in fluctuating salinities within the limit of the ecological norms [5]. In the present study, fluctuating salinity had significant effects on final wet weight, specific growth rate and food consumption of *L. vannamei* juveniles (Fig. 3, 4 and 5), and at 4.1 and 1.9 P/C, food consumption and specific growth rate were higher in the shrimp maintained at S0 as compared with those at S10. The response of food conversion ratio to fluctuating salinity was similar to that of food consumption and specific growth rate (Fig. 6). If the above hypothesis is true, these data suggested that the fluctuating range of S10 deviated from the isosmotic zone so much that *L. vannamei* juveniles suffered from osmotic and ionic imbalances. In order to recover the normal balances, the shrimp may have to expend a considerable amount of energy and, as a result, less energy is available for growth [1]. Consistent with our study, Mu et al. (2005) also observed significantly decreased growth and food consumption for *Fenneropenaeus chinensis* juveniles with a salinity fluctuation from 30‰ to 20‰ [5].

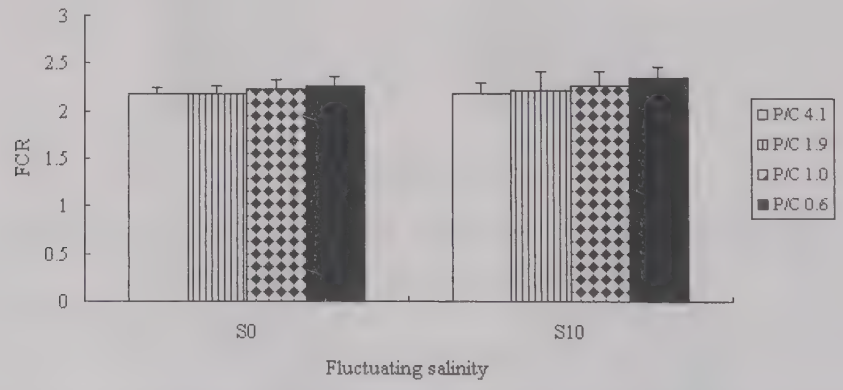

Fig. 6 Effects of fluctuating salinity and different dietary protein/carbohydrate ratio (P/C) on food conversion ratio (FCR) of *Litopenaeus vannamei* juveniles

(values are means of three replications groups for each treatment of *L. vannamei* juveniles; means with different letters are significantly different ($P<0.05$))

3.3 The interaction of salinity fluctuation and dietary protein/carbohydrate ratio on survival and growth of *L. vannamei* juveniles

Nutrient composition in the diet is one of the factors influencing an animal's ability to recover from

osmotic stress, among which the most attention has been paid to carbohydrate [1, 18, 32, 33]. Robertson et al. (1993) found that nutritional requirements of *L. vannamei* varied with culture salinity [34]. Wang et al. (2004) considered that an adequate level of carbohydrate provided in the diets is necessary for the grow-out of *L. vannamei* in the areas where salinity is physically unavoidable [1]. Hence, nutrient requirements and nutritive value of a diet may depend on salinity, and under salinity stressful conditions invoking energy-requiring mechanisms, *L. vannamei* may have greater energetic expenditure for maintenance than it would under more benign conditions; and if this is not provided via the diet, survival and growth can be compromised [1, 6, 14]. Nevertheless, when carbohydrate levels are changed in isoenergetic and isolipidic diets, protein must also be changed. The present study demonstrated a link between the type of stressor and P/C. Since the energetic requirement for osmotic regulation generally increased in response to acute or chronic salinity changes, we speculated that maximizing the carbohydrate content relative to protein in the diet might increase the survival and growth of penaeid shrimp maintained at hyper/hypo-osmoregulatic areas, based on the assumption that diets were formulated to be isoenergetic. In the current experiment, a significant interaction between the effects of fluctuating salinity and P/C was indicted by two-way ANOVA. At 4.1 and 1.9 P/C, food consumption and specific growth rate were higher in the shrimp maintained at S0 as compared with those at S10, while at 1.0 and 0.6 P/C, an inverse trend were observed (Fig. 4 and Fig. 5). These results confirmed that carbohydrate was an important source of energy for *L. vannamei* juveniles and appropriate levels of dietary carbohydrate could meet the long-term extra osmoregulatory energy expenditure and weaken stresses due to effects of fluctuating salinity. If the more effective P/C was maintained, then a reduction in the level of dietary protein by optimizing the quantity of carbohydrate addition without a corresponding reduction in growth might be possible, this would contribute to successful manufacture of a diet on a commercial scale. Similarly, Hari et al. (2006) also reported that the demand for dietary protein level could be significantly reduced in favor of carbohydrate addition to the water column without compromising shrimp production, making farming more economically viable [12].

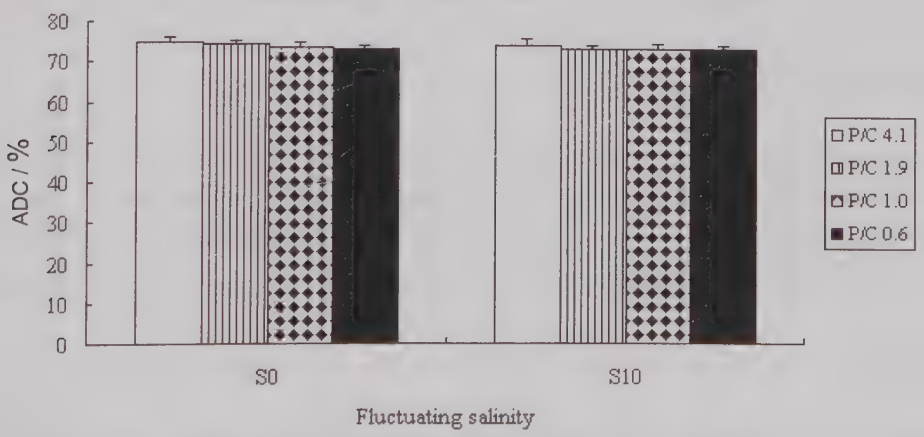

Fig. 7 Effects of fluctuating salinity and different dietary protein/carbohydrate ratio (P/C) on apparent digestibility coefficient (ADC) of *Litopenaeus vannamei* juveniles

(values are means of three replications groups for each treatment of *L. vannamei* juveniles; means with different letters are significantly different (P<0.05))

Moreover, the digestive ability of aquatic animals on a given diet is primarily dependent on the presence of adequate appropriate enzyme activities, and it is generally accepted that the ability of the shrimp to use carbohydrates as a source of energy is closely related to digestive gland enzymatic activity. Wigglesworth and Griffith (1994) reported that laboratory cultured *Penaeus monodon* fed high levels of dietary carbohydrate exhibited high amylotic activity, indicating a possible strategy of the organisms to take full advantage of the capacity of obtaining energy from carbohydrates [35]. Based on the inference that the optimal salinity for growth of *L. vannamei* is not a single point but a range, we speculate that the amylotic activity of *L. vannamei* juveniles probably is higher under natural fluctuating salinity. Consistent with this, at 1.0 and 0.6 P/C, food consumption and specific growth rate were higher in the shrimp maintained at S10 as compared with those at S0 (Fig. 4 and 5), demonstrating that *L. vannamei* juveniles maintained at S10 could use higher level of carbohydrates than the control.

To summarize, the shrimp growth is influenced by a combined effect of salinity changes and different dietary P/C. In our study, the best growth, food consumption and apparent digestibity coefficient were reached in the shrimp group reared at S0 and fed with the diet of 4.1 P/C. It is evident that in the areas where fluctuating salinity condition is physically or economically unavoidable for grow-out of *L. vannamei*, the use of adequate level of carbohydrates provided in the diet may result in higher yields, leading to reduce feed costs and the amount of waste products, and to contribute to sustainable farming. However, because of the complexity and variation of carbohydrate compositions, there are still many problems to overcome for exploiting the potential of carbohydrate for aquaculture. Ideally, each tank should have equal number of replicates for four dietary treatments; nevertheless, the 2×4 factorial design associated with two similar experimental condition tanks did not allow this as three replications for each treatment groups were used (only one of the three replications in one tank, two in another). This is not as serious as pseudo-replication (multiple aquaria submerged in the same tank, sharing the same water, but treated as independent units in analyses), which may affect the experimental results.

Acknowledgements

This study was funded by National Key Project of Scientific and Technical Supporting Programs funded by Ministry of Science & Technology of China (Grant No. 2006BAD09A01, 2006BAD09A06), Jiangsu Provincial Science Foundation for Talent Youths (Grant No. 2006548) and Open Fund of Jiangsu Key Laboratory of Marine Biotechnology (Grant No. 2006HS017).

References

[1] Wang X Q, Ma S, Dong S L, et al. Effects of salinity and dietary carbohydrate levels on growth and energy budget of juvenile *Litopenaeus vannamei* [J]. Journal of Shellfish Research, 2004, 23(1): 231 - 236.

[2] Wei M X, Tong W P, He B M. Effect of typhoon on COD in shrimp pond for industrialized cultivation in the ecological system [J]. Journal of Zhanjiang Ocean University, 2005, 6: 46 - 50.

[3] Rahman M M, Corteel M, Dantas-Lima J J, et al. Impact of daily fluctuations of optimum (27 °C) and high water temperature (33 °C) on *Penaeus vannamei* juveniles infected with white spot syndrome virus (WSSV) [J]. Aquaculture, 2007, 269(1-4): 107 - 113.

[4] Samocha T M, Patnaik S, Speed M, et al. Use of molasses as carbon source in limited discharge nursery and grow-out systems for *Litopenaeus vannamei* [J]. Aquacultural Engineering, 2007, 36(2): 184 - 191.

[5] Mu Y C, Wang F, Dong S L, et al. The effects of salinity fluctuation in different ranges on the intermolt period and growth of juvenile *Fenneropenaeus chinensis* [J]. Acta Oceanologica Sinica, 2005, 27(2): 122 - 126.

[6] Yan B L, Wang X Q, Cao M. Effects of salinity and temperature on survival, growth, and energy budget of juvenile *Litopenaeus vannamei* [J]. Journal of Shellfish Research, 2007, 26(1): 141 - 146.

[7] Roy L A, Davis D A, Saoud I P, et al. Branchial carbonic anhydrase activity and ninhydrin positive substances in the Pacific white shrimp, *Litopenaeus vannamei*, acclimated to low and high salinities [J]. Comparative Biochemistry and Physiology-Part A: Molecular & Integrative Physiology, 2007, 147(2): 404 - 411.

[8] Venero J A, Davis D A, David B R. Variable feed allowance with constant protein input for the pacific white shrimp *Litopenaeus vannamei* reared under semi-intensive conditions in tanks and ponds [J]. Aquaculture, 2007, 269(1-4): 490 - 503.

[9] Wang X Q, Ma S, Dong S L. Effects of temperature and dietary carbohydrate levels on growth and energy budget of juvenile *Litopenaeus vannamei* [J]. Chinese Journal of Oceanology and Limnology, 2006, 24(3): 318 - 324.

[10] Koshio S, Teshima S I, Kanazawa A, et al. The effect of dietary protein content on growth, digestion efficiency and nitrogen excretion of juvenile kuruma prawns, *Penaeus japonicus* [J]. Aquaculture, 1993, 113(1-2): 101 - 114.

[11] Arantakananda P, Lawrence A. Dietary protein and energy requirement of the white-legged shrimp, *Penaeus vannamei* and the optimal protein to energy ratio [M]. From Discovery to Commercalization. European Aquaculture Society, Oostende, Belgium, 1993: 21.

[12] Hari B, Madhusoodana K B, Varghese J T, et al. The effect of carbohydrate addition on water quality and the nitrogen budget in extensive shrimp culture systems [J]. Aquaculture, 2006, 252(2-4): 248 - 263.

[13] Cousin M. Contribution à l'étude de l'utilisation des glucides et du rapport P/E chez *P. vannamei* et *P. stylirostris* [M]. Thèse INA/PG. Paris, 1995: 201.

[14] Rosas C, Cuzon G, Gaxiola G, et al. Metabolism and growth of juveniles of *Litopenaeus vannamei*: effect of salinity and dietary carbohydrate levels [J]. Journal of Experimental Marine Biology and Ecology, 2001, 259(1): 1 - 22.

[15] Dokken Q R. Effects of varying of dietary macronutrient and energy ratios on growth and survival of *Penaeus vannamei* and *Penaeus setiferus* [C]. Dissertation Abstracts International Part B: Sci. Eng., 1987: 48(06): 1 559.

[16] Alava V R, Pascual F P. Carbohydrate requirements of *P. monodon* (Fabricius) juveniles [J]. Aquaculture, 1987, 61: 211 - 217.

[17] Ali S A. Effect of carbohydrate (starch) level in purified diets on the growth of *P. indicus* [J]. Indian J. Fish., 1982, 29: 201 - 208.

[18] Cuzon G, Lawrence A, Gaxiola G, et al. Nutrition of *Litopenaeus vannamei* reared in tanks or in ponds [J]. Aquaculture, 2004, 235(1-4): 513 - 551.

[19] AOAC (Association of Official Analytical Chemists). Official methods of analysis of official analytical chemists international, 16th edn [S]. Association of Official Analytical Chemists, Arlington, VA, 1995.

[20] Liu Y, Wang W N, Wang A L, et al. Effects of dietary vitamin E supplementation on antioxidant enzyme activities in *Litopenaeus vannamei* (Boone, 1931) exposed to acute salinity changes [J]. Aquaculture, 2007, 265(1-4): 351 - 358.

[21] Lucu Čedomil, David W T. Na^+-K^+-ATPase in gills of aquatic crustacea [J]. Comparative Biochemistry and Physiology-Part A: Molecular & Integrative Physiology, 2003, 135(2): 195 - 214.

[22] Taylor H H, Seneviratna D. Ontogeny of salinity tolerance and hyper-osmoregulation by embryos of the intertidal crabs *Hemigrapsus edwardsii* and *Hemigrapsus crenulatus* (Decapoda, Grapsidae): Survival of acute hyposaline exposure [J]. Comparative Biochemistry and Physiology-Part A: Molecular & Integrative Physiology, 2005, 140(4): 495 - 505.

[23] Palacios Elena, Racotta I S. Salinity stress test and its relation to future performance and different physiological responses in shrimp postlarvae [J]. Aquaculture, 2007, 268(1-4): 123 - 135.

[24] Galli L, Stern S. Histological changes in cultured *Penaeus vannamei* induced by low salinity [C]. *In*: W.C. Valenti, S. Zimmermann, C. R. Poli, A.T. Bassanesi Poli, F.R. Moraes, G. Volpato & M. R. Camara, Aquaculture Brazil '98. Sustainable Development, Recife-PE, Brazil, 1998: 2 - 6.

[25] Brito R, Chimal M E, Rosas C. Effect of salinity in survival, growth, and osmotic capacity of early juveniles of *Farfantepenaeus brasiliensis* (decapoda: penaeidae) [J]. Journal of Experimental Marine Biology and Ecology, 2000, 244(2): 253 - 263.

[26] Castille F L J, Lawrence A L. The effect of salinity on the osmotic, sodium and chloride concentrations in the hemolymph of euryhaline shrimp of the genus *Penaeus* [J]. Comp. Biochem. Physiol. A, 1981, 68(1): 75 - 80.

[27] Lin Y C, Chen J C. Acute toxicity of nitrite on *Litopenaeus vannamei* (Boone) juveniles at different salinity levels [J]. Aquaculture, 2003, 224(1-4): 193 - 201.

[28] Huang H J. Factors affecting the successful culture of *Penaeus stylirostris* and *Penaeus vannamei* at an estuarine power plant site: temperature, salinity, inherent growth variability, damselfly nymph predation, population density and distribution and polyculture [D]. PhD. Dissertation, Texas A&M University, 1983: 221.

[29] Wang X Q, Cao M, Ma S, et al. Effects of salinity on survival, growth and energy budget of juvenile *Litopenaeus vannamei* [J]. Marine Fisheries Research, 2006, 27(1): 8 - 13.

[30] Bray W A, Lawrence A L, Leung-Trujillo J R. The effect of salinity on growth and survival of *Penaeus vannamei*, with observations on the interaction of IHHN virus and salinity [J]. Aquaculture, 1994, 122: 133 - 146.

[31] Ponce-Palafox J, Martinez-Palacios C A, Ross L G. The effects of salinity and temperature on the growth and survival rates of juvenile white shrimp, *Penaeus vannamei*, Boone, 1931 [J]. Aquaculture, 1997, 157: 107 - 115.

[32] Fontenot Q, Bonvillain C, Kilgen M. Effects of temperature, salinity, and carbon: nitrogen ratio on sequencing batch reactor treating shrimp aquaculture wastewater [J]. Bioresource Technology, 2007, 98(9): 1 700 - 1 703.

[33] Li E C, Chen L Q, Zeng C. Growth, body composition, respiration and ambient ammonia nitrogen tolerance of the juvenile white shrimp, *Litopenaeus vannamei*, at different salinities [J]. Aquaculture, 2007, 265(1-4): 385 - 390.

[34] Robertson L, Lawrence A L, Castille F L. Interaction of salinity and feed protein level on growth of *Penaeus vannamei* [J]. J. Appl. Acuacult., 1993, 2: 43 - 54.

[35] Wigglesworth J M, Griffith D R W. Carbohydrate digestion in *Penaeus monodon* [J]. Marine Biology, 1994, 120(4): 571 - 578.

盐度波动和蛋白质/碳水化合物比值对凡纳滨对虾存活和生长的影响

王兴强，曹 梅，阎斌伦

（淮海工学院 江苏省海洋生物技术重点建设实验室，江苏 连云港 222005）

摘 要：本实验探讨了盐度波动（S0 和 S10）和蛋白质/碳水化合物比值（P/C: 4.1、1.9、1.0 和 0.6）对凡纳滨对虾存活和生长的影响。实验周期 35 天。结果表明：I）随着饲料中 P/C 比值的降低，对虾特定生长率和吸收效率呈下降趋势，而饲料系数呈上升趋势。在盐度波动 S0 处理中，4.1P/C 比值饲料组对虾的摄食量和特定生长率显著高于 1.0 和 0.6 P/C 比值饲料组；而在盐度波动 S10 处理中，各 P/C 比值饲料处理组差异不显著。II）4.1 和 1.9 P/C 比值饲料处理组中，S0 盐度波动处理组对虾的摄食量和特定生长率高于 S10 盐度波动处理组；而 1.0 和 0.6P/C 比值饲料处理组中，S0 盐度波动处理组对虾的摄食量和特定生长率低于 S10 盐度波动处理组的对虾。对于 4 个 P/C 比值处理组，S0 盐度波动处理组的对虾饲料系数最低。

关键词：凡纳滨对虾；盐度波动；蛋白质/碳水化合物比值；存活；生长

Value evaluation of ecological risk of marine chemical spills

ZHANG Ji-wei [1, 2], YANG Zhi-feng [1], TANG Jun-jian [2], CHEN Chu-han [2]

1. *School of Environment, Beijing Normal University, Beijing* 100875, *China;*

2. *Third Institute of Oceanography, SOA, Xiamen* 361005, *Fujian Province, China*

Abstract: The environmental risk of chemical spills near coastal zones threatens abundant marine ecological resources. By appraising the ecological damage value of the environmental risk of marine chemical spills, we can facilitate decision-making for the development of a coastal zone and establishment of economic policy on coastal zone management. In this study, the ecological effect of the environmental risk of a chemical spill in the Haicang chemical industrial park in Xiamen was identified, after which its impact was forecasted and its ecological damage value was assessed. The information generated in this study will be useful in future studies evaluating marine ecological compensation based on environmental risk analysis.

Keywords: marine; chemical spill; environmental risk; assessment of ecological damage value

1 Introduction

Xiamen is one of the most important coastal cities in China; however, it is dependent on the surrounding marine and coastal ecological environment for its economic development. Recently, industry has been developing rapidly in Xiamen, and this development has included the construction of several large-scale plants that produce dangerous chemicals such as PTA (terephthalic acid) in the coastal zone of the city. The development of such facilities poses a threat to the local marine ecological systems. Currently, the environmental risk management programs designed to assess the threat of chemical spills from such facilities primarily consist of establishing series of emergency responses and measuring the cost of avoiding risk. This results in decreased environmental risk, but does not establish mechanisms for avoiding future risk. Therefore, it is important to develop methods that protect marine ecological safety through rational environmental economic means while accounting for increasing environmental risk.

Marine Protected Areas should benefit from resource distribution that occurs during the course of environmental risk management studies [1]. Such benefits should also resolve the conflict between economic development and environmental protection while enabling the management mode to be converted from the "emergency reaction" to the "innovative prevention" via ecological compensation based on risk analysis. However, the key factor involved in the design and implementation of ecological compensation is how to determine the standard amount of compensation. Indeed, this factor is crucial to ensuring that implementing ecological compensation is effective [2]. As a result, scientific confirmation of the value of ecological damage due to the environmental risk of chemical spills is a key factor for

Received on April 24, 2009

Corresponding author: zjwfruit@126.com

establishing standards of ecological compensation.

Currently, studies being conducted to assess the losses associated with chemical spills generally focus on assessing the expense of remediation, the loss incurred by fisheries, and the loss of personal belongings. However, due to the lack of a method designed to evaluate such losses, we cannot scientifically determine the amount of economic loss incurred by the pollution of marine ecological systems. As a result, victims of chemical spills often do not receive sufficient compensation in China. In China and abroad, the most common methods used to assess the damage caused by marine pollution accidents are the assessment model of economic loss caused by marine disaster[3], the artificial neural networks model[4], the Nature Resource Damage Assessment (NRDA)[5], Habitats Equivalence Analysis (HEA)[6], loss assessment by Chinese fisheries and the method of ecological damage assessment used to evaluate the claim case associated with the oil spill by the *Tasman Sea*[7]. Although studies describing the ecological damage assessment of chemical spills do exist[8], these studies have focused on assessment of the loss caused by chemical spills that already occurred. Currently, there are few studies available to aid in the assessment of marine ecological damage based on environmental risk due to the uncertainty associated with ongoing processes and the complexity of marine ecological resources.

Therefore, this study was conducted to evaluate the ecological effect and calculate the damage value associated with the environmental risk posed by a chemical plant park in Haicang District, Xiamen. The results of this study should serve as a foundation for confirming the standard of marine ecological compensation based on environmental risk analysis.

2 Materials and methods

2.1 General situation of the study area

The Haicang chemical industrial park is located in the south of the Haicang district, which lies on the western portion of Xiamen Island and serves as a chemical industrial base in Fujian province. The leading enterprise in the industrial park, Xianglu Petrochemicals, constructed a PTA production facility in 2002. Currently, Xianglu Petrochemicals produces 2.7 million tons of PTA and 0.8 million tons of polyester annually. To satisfy the enterprise's need to import chemical materials into and to export chemical products from the industrial park, it has designated berth No. 9 to No. 12 in Haicang Harbor, which is located close to the southern portion of the chemical park, as a liquid chemical berth. This berth has a capacity of 30 to 50 thousand tons, a terrestrial area of 0.54 million square meters and total throughput capacity of 11.32 million tons per year, including an oil throughput of 5.96 million tons and a poisonous and deleterious chemical throughput of 5.36 million tons. The chemical berth lies in the Jiulongjiang River firth, which belongs to the Xiamen Precious and Rare Marine Species National Reserve. The core of the reserve, which was created to protect *Sousa chinensis*, is located approximately 1.6 kilometers from Haicang Harbor. The Xiamen Precious and Rare Marine Species National Reserve was built in April 2000 and is operated in an opened management manner. The core of the nature preservation zone includes the entire

western sea area and the firth of the Tong'an Bay in Xiamen, where *Sousa chinensis* are frequently observed. The remaining sea area in Xiamen is considered to be a periphery protection zone for the nature preservation zone.

2.2 Environmental risk simulation of a chemical spill

The author chose PX (p-xylene), which is the material used to produce PTA, as the environmental risk assessment object. PX is very volatile, but does not readily dissolve in water; therefore, it evaporates rapidly after being spilled. According to the comprehensive equation and B.T.M. equation, we calculated the evaporation rapidity, Ef, of PX [9], and then used this information to determine its subsistence time over a given sea area. We also adopted the Lagrange particle track to simulate the excursion of PX. Finally, we employed the substance diffusion transportation equation to simulate the excursion of insoluble PX, and then solved the equation using an Euler- Lagrange model based on the flow field simulation.

2.3 Value evaluation of ecological damage caused by chemical spills

The evaluated object of ecological damage was comprised of four parts: marine ecosystem services, sea water quality, marine biological resources (plankton, benthos, nekton, etc.) and the tidal beach [7]. The author confirmed the marine ecosystem effect caused by environmental risk through evaluation of the damage degree of the four parts caused by a PX spill. This information was then used to construct a value evaluation method and parameter by consulting the evaluation method at home and abroad and then integrating the characteristics specified for this paper. The evaluation method is shown in Tab. 1 below.

Tab. 1 Evaluation method to assess ecological damage caused by a marine PX spill

Damage appraisal object	Evaluation method	Mathematics formula	Parameter meaning
Damage value of marine ecosystem services	ecosystem services method Consulting research results method	$FX_E = \sum_{i=1}^{n} fx_i$ $fx_i = fx_{di} \times fx_{ai} \times s_i \times t_i$	fx_i —the damage of the ith type of marine ecosystem services in 10 thousand Yuan; i —the marine ecosystem type affected by the chemical spill, which primarily consists of tidal wetlands and firth ecosystems in this study; fx_{di} —the commonweal value per unit of the ith type of marine ecosystem services, in 10 thousand Yuan per square kilometer per year. The average commonweal value of the firth ecosystem reported in consult table 12 of the *Technical guideline for ecological damage assessment of marine oil spills*, was 18,295.0*10^4 Yuan per square kilometer per year. The average commonweal value of the tidal wetland ecosystem utilized in this study, which was determined based on the results of a study conducted Chen Peng, was 58,518.2*10^4 Yuan per square kilometer per year. fx_{ai} —the area of the ith type of marine ecosystem services shown inTab. 2 in ha. s_i —the loss of the ith type of marine ecosystem services. This value was determined using the HEA model to evaluate the loss abroad as well as the loss of marine ecosystem services that occurred as a result of changes to the ecological environment. NOAA suggested adopting 3% as the loss of ecosystem services in the HEA model because this percentage is in accordance with the average value of all previous pollution accidents [5]. t_i ——the time required for the marine ecosystem to return to the conditions that were present before the spill occurred, in years. The spilled chemical in the claim case of the oil tanker *Tasman Sea* was crude oil, which is not volatile and persisted in the environment for a long time after the spill. PX is a volatile chemical that leaves the marine ecosystem after approximately 3.6 hours when 100 tons are spilled and after approximately

			11 hours when 1 000 tons are spilled. However, this study assumed that the ecosystem would require 1 year to return to be normal based on the claim case related to the *Tasman Sea* spill.
Damage value of sea water quality	shadow engineering method	$FX_W=W_P+W_C\times S\times H$	W_P—the expense required to build a sewage plant in 10 thousand Yuan. This paper assumed that it would be necessary to build a water treatment plant to dispose of polluted sea water, and that the expense would be 178.38 million Yuan based on the cost of the water treatment plant built to dispose of waste water from the PTA plant. W_C—cost of operation (10 thousand Yuan per year) of the sewage plant based on the cost of treating waste generated by the PTA plant (5 Yuan per ton). S—the sea area affected by the PX spill, as determined using the sea water quality standard of European Union in which the maximum allowable concentration of PX is 300μg/L. H—the average depth of sea water affected by the PX spill, in meters. The depth of the surface layer is 0.5 meters.
Damage value of biology resources	market valuation method	$FX_S=D\times S\times H\times R\times P$	FX_S—the damage value of biology resources in 10 thousand Yuan. D—the density of biology resources in the affected sea area, as determined using data generated by the Third Institute of State Oceanic Administration (SOA). The average density of phytoplankton cells in the study area was determined to be 34.5×10^4 cells/L. The average biomass of phytoplankton in the study area was then determined to be 1799.2 mg/m^3 based on the fresh cell weight of phytoplankton in Kiaochow Bay[15]. The average density of zooplankton was determined to be 241.7mg/m^3. The average density of nekton was 5.46t/km^2; therefore, the percentage of fish was 55.4% and their density was 3.02 t/km^2, while the percent of shellfish was 44.3% and their density was 2.42 t/km^2. The average density of benthos was 77.4 g/m^2. H—the average height of sea water affected by the PX spill in meters. S—the area of polluted biomass in square meters. The concentration of PX that was considered to pose a threat to the marine biological systems was determined based on the results of experiments conducted using typical marine organisms such as *Bacillariophyta, Daphnia magna, Clupea pallasi*, Shellfish and *Mytilus edulis*[16-25]. R—the loss percentage (%). For soluble PX, the biology loss percentage was set at 100%. For insoluble PX, it was necessary to consider the biology avoidance percentage to determine the loss. For this study, the avoidance by fish was chosen as 30%, while the avoidance by shellfish and cephalopods was set at 10%[7][13]. P—the biology price per unit in Yuan. The prices of fish, shellfish and shells were determined based on the current prices at Xiamen market. To determine the cost of species not commonly sold at market, the price was estimated by converting the eco-efficiency of the food chain trophic level. As a reference, the conversion associated with moving one trophic level was 10%[26].
Damage value of the tidal beach	Resumed cost method	$FX_B=X_C+X_D+X_R$	FX_B—damage value of the tidal beach in 10 thousand Yuan. X_C—the cost of reclaiming spilled PX in 10 thousand Yuan. When small areas are polluted (less than 1 km^2), there is little seepage; therefore, manual cleaning is appropriate. The cost of manual cleaning was calculated as follows: 1 employee can clean approximately 100 square kilometers over 2 days, and the average wage was 200 Yuan per day; therefore, the cost was 40 thousand Yuan per square kilometer. For large polluted areas, mechanical cleaning is more appropriate. The cost of mechanical cleaning was calculated as follows: the cost of using a bulldozer is 350 Yuan per hour and five bulldozers are required to clean a large area; the cost of using a lorry is 200 Yuan per hour and 10 lorries are required to clean a large area; the cleaning time is 8 hours; therefore, the cost is 30 thousand Yuan per square kilometer. X_D—disposal PX cost in 10 thousand Yuan. The disposal cost, which was determined based on the cost of operating the Fujian industry solid waste disposal center, was 7 thousand Yuan per ton. X_R—the cost of reconstructing the ecological structure and function and decreasing the PX concentration to a permissive level in 10 thousand Yuan. Commonly used biological techniques were considered to determine this value. The cost included bioremediation cost, as well as the cost of employment, the cost of leasing vehicles and the cost of ongoing environmental monitoring. The bioremediation cost was calculated based on the procedures used to remediate tidal beaches following an oil spill. Specifically, it was assumed that one square meter of polluted area required 0.05kg of bacterial medicament, which costs 5 thousand Yuan per ton. In addition, it was assumed that this method would be used to remediate 30% of the total polluted area according to the range of the sensitive area.

3 Results and discussion

3.1 Environmental risk forecasting of a PX spill

The author simulated the PX spill risk under 16 typical conditions using a wind regime of east wind at 4.5m/s or of south-south-west wind at 3.5 m/s and spilling locations of the loading area in the dock and in the berth. Based on the perennial shipping accidents in Xiamen waters, the amount spilled in the loading area in the dock was assumed to be 100 tons and the amount spilled in the berth was assumed to be 1000 tons. The excursion range after the spill was assumed to be affected by the wind regime, the tide and flow field. The simulated results are shown in Tab. 2 and Tab. 3.

Tab. 2 Polluted area by insoluble PX spilled under different conditions

Spill place	wind regime	Area / km^2	Tide moment			
			high water	Ebb fast tide	low water	flood fast tide
P1: Loading area in the dock	E	Total polluted area	12.22	9.77	11.25	10.98
		Polluted shoal area	0.45	0.39	4.88	6.78
	SSW	Total polluted area	3.29	3.64	2.23	7.80
		Polluted shoal area	0.01	0.04	0	3.60
P2: In the berth	E	Total polluted area	57.44	63.00	66.10	69.72
		Polluted shoal area	0.47	0.56	19.79	10.46
	SSW	Total polluted area	125.24	67.44	34.95	81.28
		Polluted shoal area	0.55	0.64	0.88	4.23

The effects of the insoluble PX were simulated for four typical conditions. When the spill amount was 100 tons, the wind regime was east, and the tide moment was flood fast tide, the spilled PX spreaded to the area between the Jiulongjiang firth and Gulangyu Island, which resulted in a maximum polluted shoal area of approximate 6.78 km^2. When the spilled amount was 100 tons, the wind regime was south-south-west, and the tide moment was flood fast tide, the spilled PX was deposited in the sea area near the dock, which resulted in a maximum polluted shoal area of approximate 3.6 km^2. When the spilled amount was 1 000 tons, the wind regime was east, and the tide moment was low water, the spilled PX flowed to the area between the Jiulongjiang firth and Wuyu Island, and the maximum polluted shoal area was approximate 19.79 km^2. When the spilled amount was 1 000 tons and the wind regime was south-south-west, the spilled PX spread to a larger area. Specifically, the spill areareached the Little Jinmen Island sea area during high tide and Jiulongjiang firth during flood fast tide, which resulted in a maximum polluted shoal area of approximate 4.23 km^2. The courses of the excursion under the conditions described above are shown in Fig. 1.

Tab. 3 Polluted area by soluble PX spilled under different conditions

Spill place	wind regime	tide moment	The polluted area by soluble PX spill / km^2				
			Phytoplankton (*Bacillariophyta*)	Zooplankton (*Daphnia magna*)	Nekton (*Clupea pallasi*)	Nekton (Shellfish)	Benthos (*Mytilus edulis*)
P1: Loading area in the dock	E	high water	1.47	3.18	23.76	0.86	1.84
		Ebb fast tide	1.35	3.55	17.10	0.61	2.20
		low water	1.84	15.19	28.79	2.45	10.53
		flood fast tide	3.43	9.56	29.77	1.47	6.25
	SSW	high water	1.47	2.82	21.44	0.74	1.84
		Ebb fast tide	1.47	3.31	16.29	0.74	2.08
		low water	1.72	12.86	27.44	2.69	9.31
		flood fast tide	3.31	8.70	26.83	1.59	5.76
P2: In the berth	E	high water	18.38	34.91	76.81	12.49	28.79
		Ebb fast tide	18.86	39.08	76.81	12.01	30.01
		low water	24.87	37.73	57.82	15.44	33.44
		flood fast tide	23.15	32.95	49.37	15.93	29.77
	SSW	high water	19.11	37.12	79.87	11.88	30.01
		Ebb fast tide	18.62	38.83	79.38	11.64	29.40
		low water	25.73	37.85	58.43	15.56	33.56
		flood fast tide	23.4	32.95	52.19	16.17	29.52

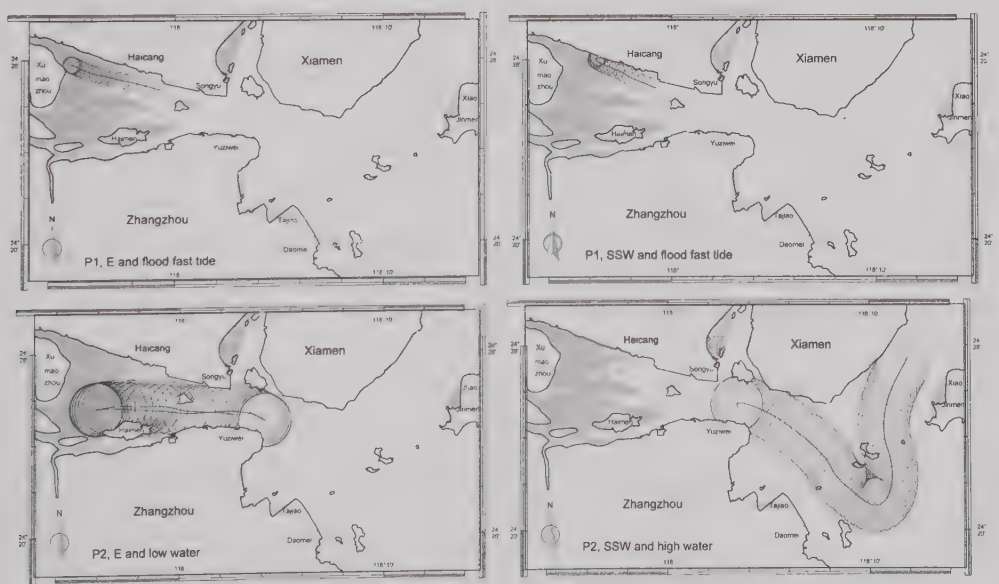

Fig.1 The drift area of insoluble PX under typical conditions

The results for the soluble PX were determined under typical conditions. When the spill amount was 100 tons, the wind regime was east and the tide moment was flood fast tide lead, the maximum effects were on phytoplankton and fish. When the spill amount was 100 tons, the wind regime was east and the tide moment was low, the maximum effects were on zooplankton and benthos. When the spill amount was 100 tons, the wind regime was south-south-west and the tide moment was low, the maximum effect was on shellfish. When the spill amount was 1 000 tons, the wind regime was south-south-west and the tide moment was low water, the maximum effect was on phytoplankton and benthos. When the spill amount was 1 000 tons, the wind regime was east and the tide moment was ebb fast tide, the maximum effect was on zooplankton. When the spill amount was 1 000 tons, the wind regime was south-south-west and the tide moment was flood fast tide, the maximum effect was on shellfish. The polluted area under the above mentioned typical conditions is shown in Fig. 2.

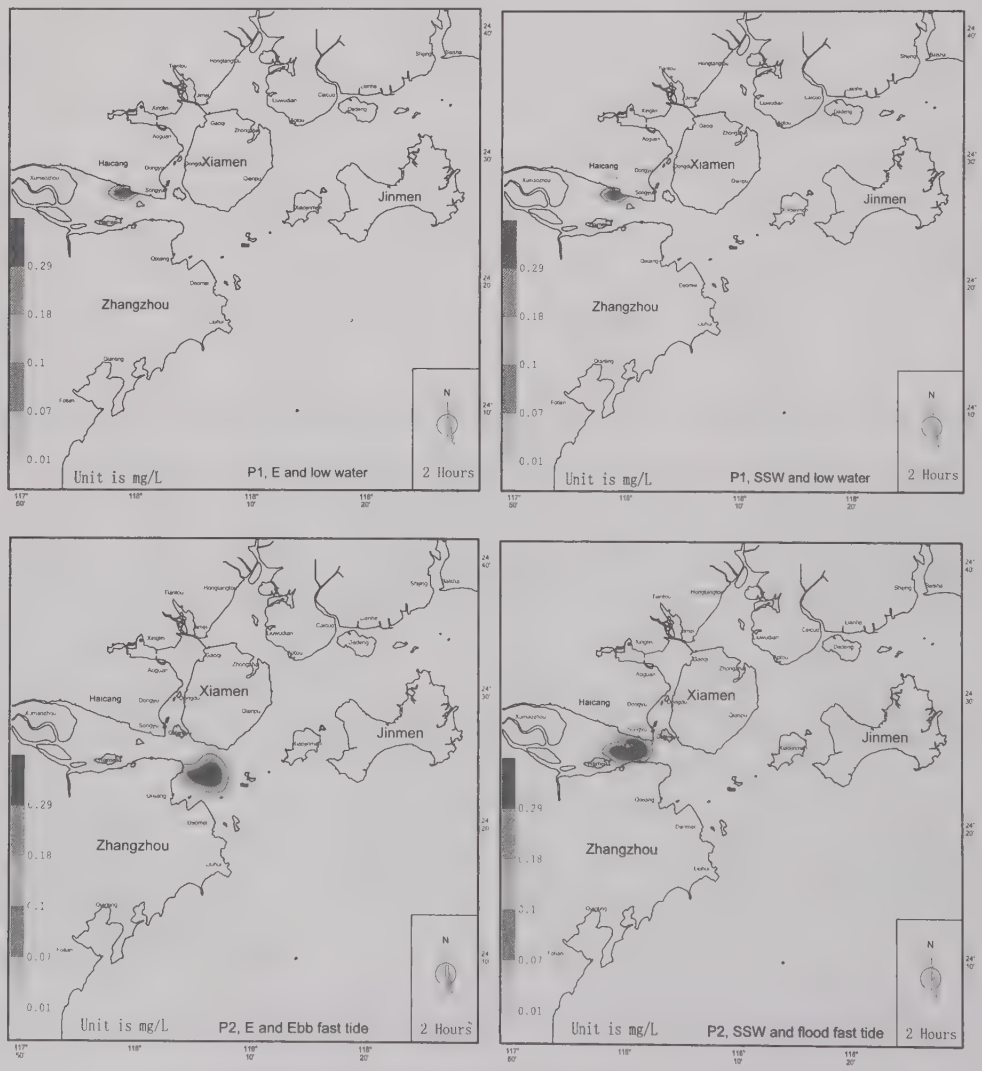

Fig. 2 Increment of soluble PX concentration under typical conditions

3.2 Evaluation of the results of marine ecological damage

The movement track and environmental fate of chemicals after the spill into the sea were affected by the local meteorological and hydrological conditions. The affected area differed greatly under different tide moments and wind regimes. The primary factors responsible for determining the affected area were wind regime, tide moment and spilling amount. As shown in Tab. 4, the loss of marine ecological services and biology resulted in the maximal contribution to the ecological damage value when the model was operated in four damage modes. When the spilled amount was 100 tons and the spill occurred in the chemical berth, the marine ecological loss ranged from 1 012.56 to 3 993.89 ten thousand Yuan and the greatest effect on the marine ecology conditions was the east wind and low water tide. When the spilled amount was 1 000 tons and the spill occurred near the anchorage ground, the marine ecological loss ranged from 13 689.65 to 18 731.929 ten thousand Yuan and the greatest effect on marine ecology occurred when there was a south-south-west wind and high water tide.

Tab. 4 The value of marine ecological damage incurred in response to PX spills under different conditions

Spill place	wind regime	tide moment	Loss of services	Loss of sea water quality	Loss of biology	Loss of tidal beach	Total loss
P1: Loading area in the dock	E	high water	724.996	340.09	711.36	37.34	1813.79
		Ebb fast tide	583.29	241.22	637.20	36.85	1498.56
		low water	1206.32	968.85	1693.22	125.5	3993.89
		flood fast tide	1420.78	581.31	1146.65	148.19	3296.93
	SSW	high water	181.78	292.63	518.21	19.94	1012.56
		Ebb fast tide	204.61	292.63	498.24	20.74	1016.22
		low water	122.39	1063.76	1456.01	0	2642.16
		flood fast tide	862.51	628.77	1061.73	113.98	2666.99
P2: In the berth	E	high water	3209.31	4939.17	5503.32	37.85	13689.65
		Ebb fast tide	3525.33	4749.36	5750.05	41.72	14066.46
		low water	6015.95	6105.75	5667.25	469.08	18258.03
		flood fast tide	5088.79	6299.52	5423.90	258	17070.21
	SSW	high water	6940.17	4697.95	7054.83	38.97	18731.92
		Ebb fast tide	3778.67	4603.04	5790.27	43.54	14215.52
		low water	2024.42	6153.2	5438.77	57.17	13673.56
		flood fast tide	4971.49	6394.43	5792.41	124.69	17283.02

4 Conclusion

The value evaluation of marine ecological damage caused by chemical spills presented here is the precondition and foundation for establishing a marine ecological compensation standard based on environmental risk analysis. This study provides a method of value evaluation of marine ecological damage based on environmental risk and can offer a scientific basis for decision-making, programming and implementing the environmental economic policy for coastal zone development. In addition, the

results of this study indicated that it is technically feasible to gather the required information for such studies; therefore, this value evaluation demonstrates that further studies to refine the method are warranted. Suggested focuses of future studies are provided below:

(1) Based on many types of meteorological and marine hydrological conditions, the method described here utilized 16 typical conditions to simulate environmental changes; however, it can not represent all possible meteorological and hydrological conditions. Therefore, future studies should integrate the simulation model developed here with a marine environmental hydrodynamic database to cover all tidal currents and wind fields.

(2) The environmental fate of the PX spill was estimated based on the course of excursion and diffusion. However, the existing simulation model was designed to predict the course by separating the excursion and diffusion course. Therefore, incorporation of this technique into models used in future studies should enhance the prediction of marine risk.

(3) To determine the value of marine ecological services, this study utilizes existing evaluation results and adopts the average commonwealth value for typical marine ecosystems. This method is useful for large sea areas, but not for small areas; therefore, the results of studies conducted in the local ecosystem should be incorporated to improve the simulations for the study area.

(4) The quantitative studies of marine biology affected by changes in the marine ecosystem require detailed toxicological testing to confirm the safe concentration of chemicals. However, there is a wide variety of marine organisms in the study area and it is not possible to evaluate each of these organisms individually. Furthermore this study was based on the methodology of value evaluation and not on the toxicological tests. Indeed, the only toxicological tests considered in this study were conducted on *Daphnia magna*. The study area lies in the firth of the Jiulongjiang River, which is a freshwater-seawater border-region; therefore, the author chose freshwater species as the reference. However, other species presented in the study should also be considered. To confirm the standard of ecological compensation, toxicological tests must be conducted to guarantee the precision of the simulated results.

Acknowledgements

The project was financially supported by Marine Science Fund of SOA for Young Scholars (No.2008121).

References

[1] Hu Erbang. Practical Technology and Methods for Environmental Risk Assessment [M]. China Environment Science Press, 2000.

[2] Task Force on Eco-Compensation Mechanisms and Policies. CCICED. Eco-Compensation Mechanisms and

Policies in China [M]. Science Press, 2007.

[3] Li Yanan, Zhang Yan, Ma Chengdong. Economics Losses Damage Assessment Model for Marine Disaster [J]. Marine Environmental Science,2000, 19(3): 60 - 63.

[4] Zhu Minghe, Ding Yongsheng, Yin Penhai. Application of BP Neural Network method in Compensation Assessment of Damage Caused by Oil Spill from Ships [J]. Marine Technology, 2005, (1): 65 - 69.

[5] French D, McCay J J, Rowe N W, et a1. Estimation of potential impacts and natural resource damages of oil [J]. Journal of Hazardous Ma. Tefiats, 2004, 107: 11 - 25.

[6] Richard W D, Thomas C G, Desvousges W H. The use of habitat equivalency analysis in natural resource damage assessments [J]. DMogical Economics, 2004, 48: 49 - 70.

[7] Gao Zhen-Hui, Yang Jian-Qiang, Cui Wen-Lin. Evaluation and Application on Environment and Ecological Damage by Oil Spill [M]. Beijing: Ocean Press, 2005.

[8] Ji Dawei, Yang Jianqiang, Gao Zhenhui, et al. Study on Assessment for Eco-environmental Damage Caused by Oil Spill [J] . Journal of Waterway and Harbor, 2006, 27(2): 115 - 119.

[9] Li Youming. Study on Evaluation Pattern of Harmfulness of Chemicals Water Pollution on Bulk-chemical Terminals [J]. Environmental Protection In Transportation, 2002, 23(2):11 - 14.

[10] Deborah P. French M, Nicole W, et al. Spill hazard evaluation for chemicals shipped in bulk using modeling [J]. Environmental Modelling & Software, 2006, (21):156 - 169.

[11] Karin U, Martin D, Frank W, et al. A software tool for designing cost-effective compensation payments for conservation measures [J]. Environmental Modelling & Software, 2007; 23(1): 122 - 123.

[12] Wang Jianhua, Yu Hongbin, Song Yunfa. Numerical Simulation of Oil spill on the Pearl River Estuary [J]. Ocean Technology, 2006, 25 (1): 29 - 32.

[13] HY/T095-2007. Technical guideline for ecological damage assessment of marine oil spill.

[14] Chen Peng. Evaluation on Service Value of Wetland Ecosystem in Xiamen City [J]. Wetland Science,2006, 4 (2): 101 - 107.

[15] Sun Jun, Liu Dongyan, Qian Shuben. Study on phytoplankton biomass [J]. Acta Oceanologica Sinica, 2000, 22 (1): 102 - 109.

[16] Pierre Y C. A spreadsheet program for estimating low toxicit effects [J]. Environmental Toxicity and Chemistry, 1997, 16(4): 802 - 806.

[17] Wang Hong, Shen Yingwa, Lu Ling. Acute Toxicity of Typical Hazard Chemicals Tothree Kinds of Aquatic Organisms [J]. Chinese Journal of Applied and Environmental Biology, 2003, 9(1): 49 - 52.

[18] Gao Hui. Research on Toxicity of Benzmoid Chemicals on Typical Marine Plankton [D]. Dalian: Dalian Maritime University, 2006.

[19] Jiang Yu, Wu Zhihong, Han Xiurong. Toxicity of Polycyclic Aromatic Hydrocarbons(PAHs) to Marine Algae [J]. Marine Sciences, 2002, 26(1): 46 - 50.

[20] Zheng Ronghui, Wang Chonggang. Effects of Polycyclic Aromatic Hydrocarbon Contaminants on Fish's Reproduction Function [J]. Journal of Oceanography In Taiwan Strait, 2004, 23(2): 245 - 252.

[21] Melissa E, Glen J. Van Der Kraak. Stimulatory effects of selcted PAHson testosterone production in goldfish and rainbow trout and possible mechanisms of action [J]. Coparative Biochemistry and physiology, 2001, 130: 249 - 258.

[22] Beatriz P C, Blanca L, Eduardo P, et al. Evaluation of PAH bioaccumulation and DNA damage in mussels (*Mytilus galloprovincialis*) exposed to spilled Prestige crude oil [J]. *Comp. Biochem. Physiol.*, Part C, 2004, (138): 453 - 460.

[23] Stekoll M S, Deysher L. Response of the Dominant Alga *Fucus gardneri* (Silva) (Phaeophyceae) to the Exxon Valdez Oil Spill and Clean-up [J]. Mar. Pollut. Bull., 2000, 40(11): 1 028 - 1 041.

[24] Downs C A, Shigenaka G, Fauth J E, et al. Cellular physiological assessment of bivalves after chronic exposure to spilled Exxon Valdez crude oil using a novel molecular diagnostic biotechnology [J]. Environ. Sci. Technol. 2002, 36: 2 987 - 2 993.

[25] Sean Y S, Johnson L L, Horness B H, et al. Relationship Between Oil Exposure and Reproductive Parameters in Fish Collected Following the Exxon Valdez Oil Spill [J]. Mar. Pollut. Bull., 2000, 40(12):1 139 - 1 147.

[26] Wu Huamei. Ocean Primary Production, Production Elements and Marine Bioresources [J]. Marine Sciences, 1986, 10(6): 62 - 65.

海上化学品泄漏环境风险生态损害价值评估

张继伟[1,2]，杨志峰[1]，汤军健[2]，陈楚汉[2]

（1. 北京师范大学环境学院，北京 100875；2. 国家海洋局第三海洋研究所，福建 厦门 361005）

摘 要：海岸带化工园区化学品泄漏的环境风险问题已经成为威胁我国海洋生态资源的重要因素之一。对海上化学品泄漏的生态环境风险损失进行先期评估，并将价值评估信息纳入到海洋环境管理中，可为海岸带开发以及海岸带管理经济刺激手段的制定提供决策依据。本文选择厦门市海沧化工园区为典型案例区，进行海岸带化工园区化学品泄漏事故的风险生态效应识别与影响预测，评估环境风险的生态损害价值，从而为基于环境风险分析的海洋生态资源生态补偿的研究与实践提供借鉴。

关键词：海洋；化学品泄漏；环境风险；生态损害价值评估

Research of data architecture in digital ocean

ZHANG Feng [1, 2], LI Si-hai [2], SHI Sui-xiang [2]

1. School of the Earth Sciences and Resources, China University of Geosciences, Beijing 100083, China;

2. Key Laboratory of Digital Ocean, National Marine Data and Information Service, Tianjin 300171, China

Abstract: The characters of marine data, such as multi-source, polymorphism, diversity and large amount, determine their differences from other data. How to store and manage marine data rationally and effectively to provide powerful data support for marine management information system and "Digital Ocean" prototype system construction is an urgent problem to solve. Different types of system planning data, such as marine resource, marine environment, marine economy and marine management, and establishing marine data architecture frame with uniform standard are to realize the effective management of all level marine data, such as national marine data, the provincial (municipal) marine data, and meet the need of fundamental information-platform construction.

Keywords: digital ocean, data architecture, data warehouse, data mart, metadata

Introduction

"Digital Ocean" was born along with the developing strategy of "Digital Earth". It got much attention when brought up. "Digital Ocean" means forming integrated system to recover and expect marine on the base of the data collected during marine investigation, marine monitoring, marine surveillance (including satellite, airplane, shipping, buoy, shore station), and social survey, by the technology of database, GIS, network, to construct digital integrated platform and virtual environment. "Digital Ocean" can promote rationally utilizing and efficiently developing the ocean and keep sustainable marine development through describing the modern ocean and simulating the future ocean. In the world today, major maritime powers, such as USA, Russia, UK, France, Germany, Japan and Canada, are pushing forward "Digital Ocean" information system construction. Interaction between modern ocean and digital ocean will be the basic model of developing and utilizing ocean in 21st century.

In order to realize the "Digital Ocean" system, to realize the rational and effective management and store different types of marine data, and to meet the application demand of marine fields, a fairly complete data architecture is needed, which must have seven characteristics:

a) Integrity: Store marine data completely and ensure all desired data can be retrieved.

b) Rationality: Design rational data structures, and consider reasonably the relationships between different parts and data interchange.

c) Independence: Each part of data architecture has its relative independence and performs

Received on June 22, 2010

Corresponding author: zhangfeng@mail.nmdis.gov.cn

corresponding function independently.

d) Security: Guarantee the security of data when stored, accessed and modified.

e) Efficiency: Strike the right balance between saving spaces and increasing the speed of response.

f) Reliability: Ensure the data can be efficiently loaded even the amount of data is large. Guarantee the data be reliable which are delivered to the application system.

g) Consistency: The same data in different parts of system must be consistent.

This paper discusses the structure arrangement of the marine data architecture and the design of application system, and case in the paper proves the applicability of the data architecture.

1 Background

All branches, operation centers and institutes of China State Oceanic Administration saved a large amount of marine science data and related information after years of survey and collection, including marine hydro-meteorology, marine surface meteorology, marine biology, marine chemistry, marine environmental quality, marine geology, marine geophysics, marine basic geography, marine aviation and satellite RS, marine economy, and marine resources. The data covers all oceans of the globe, and the amount of data is more than hundred billion bytes. The key marine data for management and application are to keep these data accessible, maintainable and secure. The service of this system includes information exchange among institutes of China State Oceanic Administration and other departments of marine affairs, data statistics, annual statistics, range statistics, social inquiry and so on.

The characters of marine data such as multi-source, polymorphism, diversity and large amount determine it's different from other data. The multi-source is derived from the different observation techniques, which bring difference of data accuracy and format. Therefore the data structure is complex. The polymorphism means marine data has different format, such as figure, image, text, etc, so the method of processing data is complex. The diversity refers that marine data includes a great variety of subjects, which lead to the complexity of data management.

On the other hand, departments of marine affairs have a large amount of marine data, but thses data, which are not organized and utilized effectively yet, are scattered in different units. A lot of data store still as original form, which makes it difficult to manage, maintain and retrieve. Getting data for specific application analysis accurately is especially difficult, and needs much time and manpower. At present, expertise and traditional statistics are still adopted to the analysis, forecast and decision relating to the ocean, such as meteorology, sea condition, resources, economy and disaster. These non-automatic ways of analysis, forecast and decision greatly affect data utility efficiency. While the technological backward of marine data management affects the accuracy and actual effect of data, and further influences the efficiency of analysis and decision.

To adequately take advantage of the application service of marine data, as the marine administrative department, China State Oceanic Administration provides basic data support for "Digital Ocean".

Upgrading, updating and establishing database of national marine data, developing high quality marine data basic product, and realizing marine data-sharing to the greatest degree are important tasks. Therefore research on architecture of marine data is extremely important.

2 Architecture of marine data

In consideration of bulky architecture of marine data and complex relation among the parts, this study tries to ensure the system structure, application, deployment and maintenance as simple as possible during the process of design and implementation on the premise of meeting need.

Marine data architecture is divided into 5 parts roughly: primary layer, basic layer, integration layer, product layer, subject layer. As shown in Fig. 1.

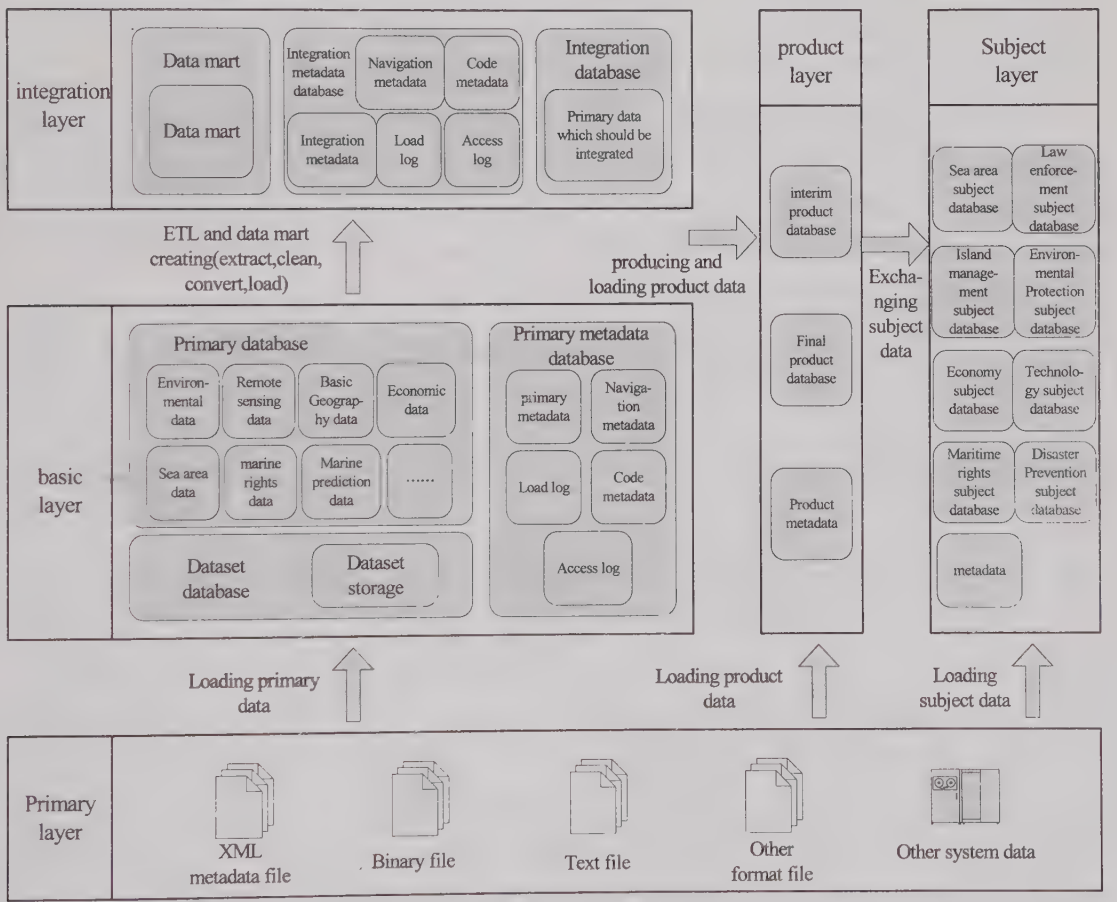

Fig. 1 Marine data architecture

2.1 Primary layer

Primary layer which contains all data source system is composed of original data which is distributed in all servers. This original data includes text file, binary data, XML file for describing metadata (derived

from tool of metadata input), and data file derived from other application system. This data can be divided structurally into structured data, semi-structured data and non-structured data. Maximum data source of marine data architecture comes from standard dataset, which is semi-structured and non-self-describing data. The standard dataset stores different subject data got from marine field survey. After data is preprocessed and pre-calculated based on file, and data file is corrected and calibrated, this data can be loaded into database. This data source is named semi-structured scientific text data source in this study.

Structured relational database is an important data source of marine data architecture as well. At present, all units of China State Oceanic Administration have established lots of relational databases for supporting professional data processing and business system applying. All these databases are important data source of marine data architecture. In addition, non-structured hyper text data sources (Web page), such as the data of marine economy, marine rights and interests (including Marine Laws and Regulations) collected from internet, international public data updated at regular period in website, international exchange data, are the important data sources of marine data architecture as well.

Data source of marine data architecture includes real-time data (for example satellite data), vector graphics data (for example remote sensing data), multimedia data, and other complex format data sources. As shown in Fig. 2. This study considers that data source of marine data architecture is a typical data source with various types, which can be classified as web data source (non-structured), text data source (semi-structured) and relational data source (structured).

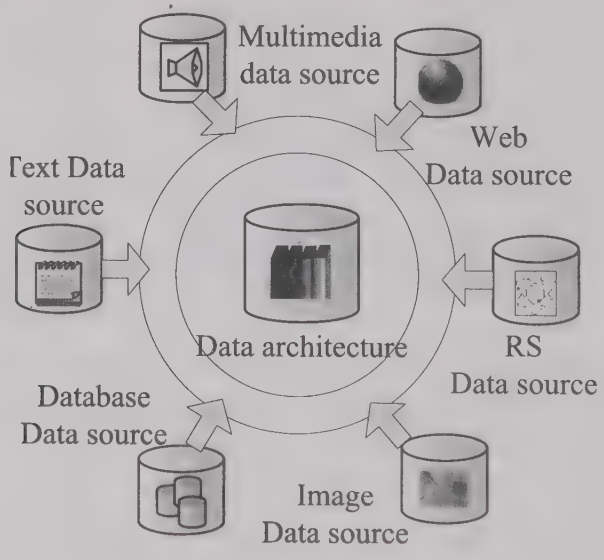

Fig. 2 Data sources of marine data architecture

2.2 Basic layer

Basic layer includes dataset database, basic database and basic metadata database. Dataset database archives data as file unit. Basic database is a relational form of storage of dataset file. Metadata database stores XML metadata, code data, navigation data, loading log, access log and so on.

2.2.1 Dataset database

What dataset database stores is quality tested, standard dataset. Dataset of marine science is generally limited by spatial extension, element type, investigation and gathering batch, which is composed by one or several data file. Standard dataset file realizes the centralized archiving management in the form of dataset database, stores in database in the form of object or file pointer, and logically forms a whole with data in basic database, and makes backup and recover of basic database convenient. At the same time, dataset database can realize quickly retrieving dataset file based on metadata.

2.2.2 Basic database

Basic database is composed of marine data, such as Environmental data, Remote sensing data, Basic Geography data, Economic data, Rights data, Sea Areas data, Marine Environment Forecast data, and other relational metadata. Taking Environment data for example, Marine Environment data are composed of Marine Hydrology data, Marine Meteorology data, Marine Physics data, Marine Chemistry data, Marine Biology data, Marine Geology data, Sea-bed's Topography data, and Marine Geophysics data. The scheme of basic database almost corresponds to format of dataset database, and is the relational storage of dataset file.

2.2.3 Basic metadata database

Basic metadata database includes navigation data, value code metadata, loading log of code metadata, access log and basic metadata. Marine basic metadata is the describing data about the data, which is used to describe basic marine data content, structure, access mode, etc. The use of metadata eliminates the semantic independence and heterogeneity among data resources to a certain degree, and helps realize integration and exchange of data resources. Marine basic metadata is divided into two parts mainly: core metadata and whole metadata.

a) Core metadata: To provide least metadata element set what marine data source needs. Core metadata includes the metadata elements of the following question: what, where, when and who.

b) Whole metadata: To provide obligatory and optional metadata element set what complete marine data source (individual dataset, dataset series, all kinds of marine elements) needs. It can completely define all metadata for identifying, evaluating, excerpting, using and managing marine data.

Data processing professional retrieves data of data layer by core metadata. On the other hand, data processing professional needs check the whole metadata according to data. Some metadata which is relevant to basic layer, such as loading time, information of operator, is common searching criteria and retrieving target employed as well. Not only relational metadata but also XML metadata can be searched by SQL language (the latter must be embed XPath expression in SQL).

Basic metadata include other metadata, for example, logic organizational structure of basic database is stored in navigation data to fast queries; Value code metadata keep record of relationship

between all field value code of basic database and what it represents for transforming when figure showing; Loading log records the information of data loading in basic layer; Access log ensures tracking who has modified data, what, why, when and how for maintaining basic layer data and guaranteeing database security in some degree.

2.3 Integration layer

Processed and cleaned basic data is saved in integration layer for providing data service for data analysis and decision (such as OLAP and data mining) of the upper layer. This layer includes integration database, data mart and relevant metadata.

2.3.1 Integration database

The data which are organized by investigation method in basic database (such as station data, BT data) are reorganized by elements to form integration database. Basic layer data are reload into integration database after data extracted, data cleaned and data converted by ETL. Although integration database is not organized by subjects but elements, this research still follows the way of data warehouse modeling to design integration database, and defines public dimension table, subject dimension table, and private dimension table to satisfy the multi-dimension of marine data.

2.3.2 Data mart

Data mart is the data view which is defined by data analysis professional, incremental maintained automatically, and created against the specific field, and is the subset of integrated large-scale marine data by elements. The amount of data of data mart is much less than integration database, and data mart has much more pertinence. Data analysis, such as data mining, OLAP, can be done faster and better on the base of data mart. Data mart is created by data mart creation tools, and is automatic updated and maintained by system.

2.3.3 Integration metadata database

Basic metadata in basic layer are arranged, and added some background data related to integration database and data mart.

2.4 Product layer

Read-only and customized product data are saved in product layer, which include interim product database, final product database and product metadata. Data product which is produced by the above layer, such as the result of basic data processing, graphic result of OLAP processing, is saved in product layer.

Marine product data may be classified in many ways. It can be classified into interim product and final product by the degree of processing, and also can be classified into normal product and service product from the view of application. These two classification methods play an important guiding role in

the design of product layer.

Interim product is the data product that has been processed to a certain degree, but there is still the room to process and further processing is needed to be final product. For example, standard layer data which are derived from the observed temperature and salinity data are interim products, and the geometrically calibrated data obtained from the remote sensing raw data are interim product as well.

Final product is the data product which can be delivered to user directly. Final data product probably is special marine data view or calculation and statistic result. Such as acquisition time, longitude, latitude, the height and direction of wave of all data acquisition bit in certain range of time, longitude and latitude, the maximum, minimum, average of wave height per month and square area. There are many sources of final product, which may be basic database data or integration database data, results of analysis or mining, and external data. Final product database also includes the result of statistic analysis, OLAP and data mining by external system such as data table, graphic and report.

Normal product is the data product formed by daily processing, which has stable pattern, time of production and quantity. This type of product data will be deeply and widely used. Service product means the single-shot, structure stochastic data product, which is to meet the requirement of marine data user. Generally, normal product is managed by relational database and service product is managed by dataset file.

Overall, product layer includes statistical values data product, graphic and image product, and text product. All these types of product have unified XML metadata. For marine data service department, their duties are to increase product category, ensure quality of product and coverage, and other upper layer application. For example, data in “management information system” and “Prototype System” of “digital ocean”, and subject database come from product data. So product layer is the crucial layer in “digital ocean” system.

2.5 Subject layer

Marine subject information databases which are based on the basic databases and product databases are several practical-application-requirement-oriented subject databases which are established through comprehensive analysis and fusion. Marine subject databases are real subject-oriented database system. These subjects include Sea Area management, Island Management, Environmental Protection, Warning and Disaster Prevention, Marine Economy and Plan, Marine Supervision of Law Enforcement, Maritime Rights, Marine Technology Management, etc. Marine subject databases are very important in “digital ocean” system, which are the main basis of “management information system”.

Subject database can be classified into two categories by the organization of data: one is basic data mainly based on basic data, and the other is application-oriented business data. The first one includes product data and summarizing data which are extracted from basic database by XML data integration system, and are modeled and organized through data warehouse. The second one is derived from the process of system, and is managed by relational database.

3 Planning of application system

Enormous data system needs a good information management system. This study plans the application of data system while designing the data system. The application system has bulky structure and complex relationship. The calling relationship among different parts is shown in Fig. 3. Act up to the principle of light-weight design and realization, except data architecture layer, the upper layers application with the theory of component can be divided into 3 component layers: basic component layer, application component layer and application software layer.

Basic component layer belongs to bottom component layer. All the application of accessing data system must be through basic component. It is composed of three key components which are shared with upper layers: a) Unified authority and access control component can realize the authority and access control of system; b) Access control component monitors all database accesses of data system; c) corporate access control component provides a unified way to access all parts of data system and realizes the connection management and optimization of database.

Application component layer is composed of 16 application-oriented components. These components provide component support to all subsystems of application software layer. Application component is the abstract of general or independent software modules of all subsystems. These components are shared by one or more subsystem.

Application software layer is composed of bulky software systems. According to the practical objective and requirement of marine data system management, this study designs the data directory system, data management system, data service system, data application system, professional application system and user authority management system, and several subsystems. Data system is essentially a distributed system, so how to find the data needed from mass data is a challenge. Data directory system realizes the content management and directory access of all parts of data system, and makes data exchange and information query easy. Data management system realizes day-to-day management function of all database layers, such as metadata loading, metadata management, data backing up, data cleaning, ETL and establishment of subject-oriented data warehouse, etc. Data application system fulfills the tasks of retrieving and inquiring of all database layers, displays and outputs the inquire result. Data service system realizes product generating, value calculating, OLAP and data mining, and provides marine information service. Professional application system realizes some high professional application of Marine Science, which depends on manual intervention, calculation and analysis of marine professional staff, or other tools, to complete. User authority management system realizes the user authority and access control of the above software system.

All the data application systems realize the support of basic components and its application component for application layer. Marine professional can apply system function on the base of these components. These basic components encapsulate data access, user accessing control, authority control

and access control. These technical details are open to marine professional. Application of basic components provides platform and component support for realizing professional application in the future, and enhances the usability and expansibility of application system to a great degree.

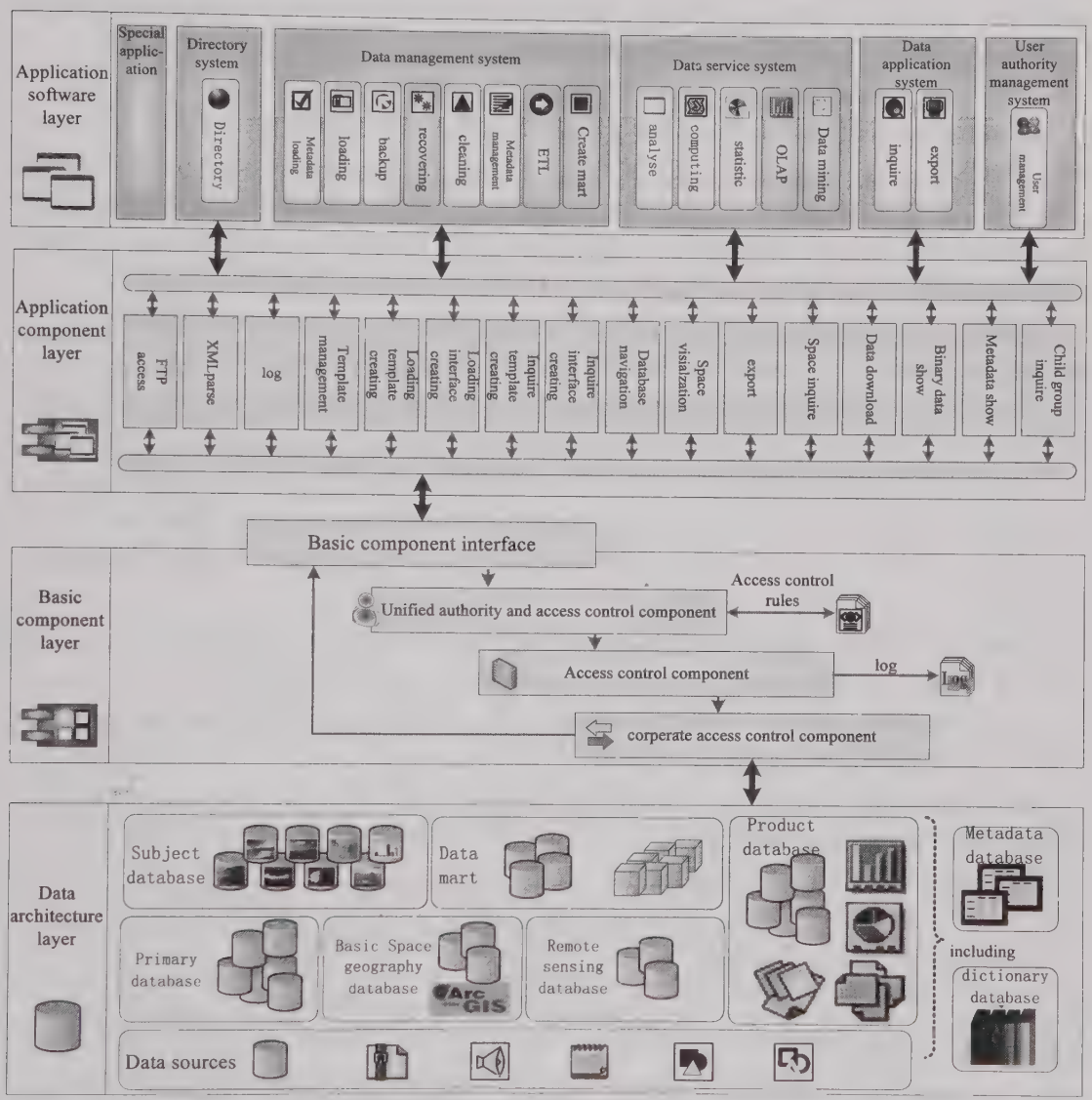

Fig. 3 Relationship of the parts of national marine data architecture

4 Case analysis

Data are the lifeblood of the system. If data do not flow in the system, the system is just a castle in the air. The way of marine data flowing in system is very complex, and bulky data exchange among not only different layers but also inner layer. This study takes the process of gathering marine environment

investigation data of provincial node to national node as example to show how data flow in the system.

Step 1: Gathering data are tested by quality control to satisfy the data quality request of data system.

Step 2: Dataset file is converted to relational data schema, and is loaded into basic layer database. Dataset file itself is filed to basic layer database as well. Metadata extracted from dataset by loading system are automatically loaded to basic metadata database.

Step 3: Data processing staff supplements basic metadata manually.

Step 4: Data processing staff does high data cleaning and duplicate data detecting to further ensure data quality.

Step 5: Data processing staff generates data product on the base of basic database, ensures that this data is loaded into product database of corresponding layer, and fills it with related products metadata at the same time.

Step 6: Basic database data are loaded into integration layer of integration database by ETL software after classified by elements, and are complemented and perfected with metadata.

Step 7: Customize data mart required by customer on the base of integration database, and gather data. Data mart should be stored in product layer as product database if it is data product or in integration layer otherwise. Fill data mart metadata on the base of background such as gathering arithmetic.

Step 8: Provide data service for data mining and OLAP analyzing on the base of data mart.

Step 9: Result of data mining and OLAP analyzing is saved into product layer as product, so is metadata.

Step 10: Subject layer is a type of subject-oriented data. Most marine investigation data in subject database are exchanged to subject layer from product layer by data exchange system.

Step 11: External product, such as dataset file format data and other professional application product data, is loaded into product layer directly.

Step 12: New basic data or amended data generated from subject layer should be saved in product database by data exchange system.

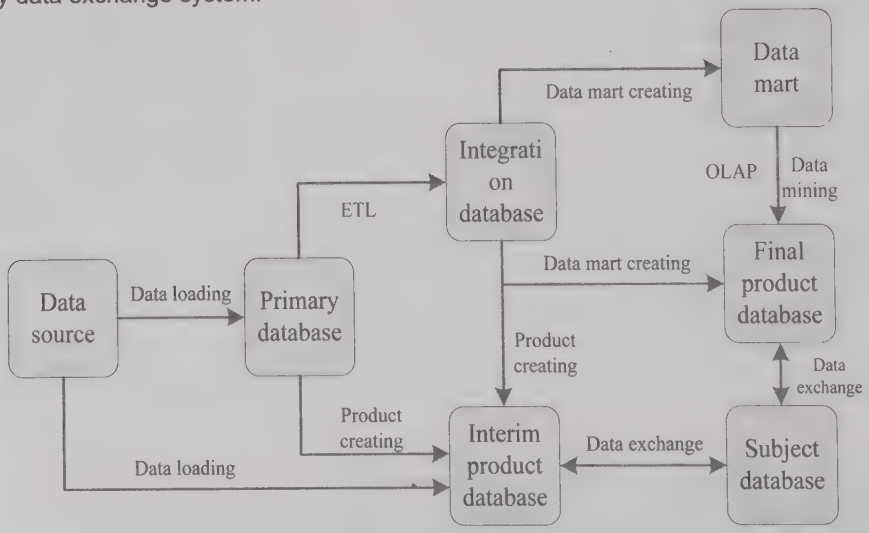

Fig. 4 Data flow diagram

5 Conclusion

Unified planning and layout of marine data architecture is studied from the point of database in this paper. National marine data architecture is complicate in structure, but has some regularity.

a) Data is abstracted from detail from bottom to up, and is integrated step by step.

b) The organization of data is gradually fine, from mean-oriented, element-oriented to subject-oriented, product-oriented and application-oriented.

c) All of the data correspond with its metadata. Unified metadata management is an efficient method to manage complex data.

Data architecture design is to construct unified marine data framework, is the base of effectively managing marine data of all level, and can provide powerful data support for "digital ocean" system construction. In this research, marine data architecture is designed preliminarily at present, and will be revised after deep studying. Internal logical and physical design of all parts will be further discussed.

References

[1] Core A. The Digital Earth: understanding our place in the 21st century [J]. The Australian Surveyor, 1998, 43(2): 89 - 91.

[2] HOU Wenfeng. Tentative Ideas on the Development of Digital Ocean in China [J]. Marine Science Bulletin, 1999, 18(6): 1 - 10.

[3] XIA Dengwen, SHI Suixiang, YU Ge. Study on the Techniques of Marine Data Warehouse and Data Mining [J]. Marine Science Bulletin, 2005, 24(3): 1 - 6.

[4] XUE Huifen, ZHOU Yanxia. A Study on the Application of Warehouse Technology to Ocean Environment Information Management [J]. Marine Science Bulletin, 2005, 24(3): 66 - 71.

[5] KANG Shouling. The Sea Environment Monitoring Data and Quality Management [J]. Meteorological, Hydrological and Marine Instruments, 2003, (3):1 - 6.

[6] Shi Feng, Jie Song, Xuhui Bai, et al. A Web-Based Transformation System for Massive Scientific Data [C]. Proc. of WISE Workshops 2006. 104 - 114.

[7] CHEN Jixiang. Study on XML Application in Marine Data Service [J]. Marine Science Bulletin, 2004, 23(2): 46-50.

[8] TIAn Youqiang, YU Lei, ZHANG Xiaofeng,etc. Design and Implementation of a Marine XML Data Integration System Prototype [J]. Periodical of Ocean University of China, 2005,35(4): 691-696.

[9] JI Peng, ZHANG Chenghui, SUN Rupeng. The System of The Real Time marine Data Transmission Network based on XML [J]. Marine Forecasts, 2006, 23(2): 45 - 50.

[10] LI Zhe, QIN Qiming, WANG Hongqing, et al. Application of COM Technique in Marine Remote Sensing Multidimensional Dynamic Visualization System [J]. Marine Science Bulletin, 2006, 25(1): 70 - 74.

[11] HAN Litao, ZHU Qing, HOU Chengyu. Issues Related to the Construction of the Virtual Environments [J]. Marine Science Bulletin, 2006, 25(4): 1 - 8.

[12] LI Sihai, ZHANG Feng, LIU Zhenmin. A Prototype System of Operational Processing and Application for Marine Environmental Data [J]. Marine Science Bulletin, 2007, 26(3): 81 - 86.

数字海洋数据体系结构研究

张 峰[1,2], 李四海[2], 石绥祥[2]

(1. 中国地质大学（北京）地球科学与资源学院，北京 100083；2. 国家海洋信息中心 数字海洋重点实验室，天津 300171)

摘 要：海洋数据的多源性、多态性和多样性以及数据量庞大等特点决定了其不同于其它数据，如何更加合理有效地存储和管理海洋数据，为海洋综合管理信息系统和“数字海洋”原型系统建设提供有力的数据支撑，是一个紧迫需要解决的问题。本文对各类海洋资源、海洋环境、海洋经济、海洋管理等数据进行统一的体系规划，构建统一标准的海洋数据体系框架，以实现国家、省(市)等各级海洋数据的有效管理，满足“数字海洋”海洋信息基础平台建设需要。

关键词：数字海洋；数据体系结构；数据仓库；数据集市；元数据

海 洋 通 报（英文版）

HAIYANG TONGBAO

2010 年 10 月 第 12 卷 第 2 期

目 次

利用SWAN波浪模式研究北部湾海域台风浪场的波浪方向谱特征 ……周良明 等 (14)

全球变暖对海洋浮游动物的影响 ……张达娟 等 (25)

蓝藻钙信号研究进展 ……卢永忠 (31)

不同时期和生长状态条斑紫菜总可溶性蛋白差异表达初探……孟春晓 等 (37)

夏季南海北部沙壳纤毛虫种类组成及空间分布……刘华雪 等 (46)

用 RAPD 方法对不同色三疣梭子蟹的分析 ……迟大利 等 (54)

华贵栉孔扇贝表型性状相关和路径分析 …… 李俊辉 等 (60)

盐度波动和蛋白蛋/碳水化合物比值对凡纳滨对虾存活和生长的影响 …… 王兴强 等 (73)

海上化学品泄漏环境风险生态损害价值评估 ……张继伟 等 (84)

数字海洋数据体系结构研究 …… 张 峰 等 (96)

Marine Science Bulletin

Marine Science Bulletin publishes papers on marine science and technology including physical oceanography, chemical oceanography, marine biology, marine geology, environmental oceanography, estuarine & coastal sciences, marine technology, digital ocean, coastal zone management, ocean engineering, marine economics, etc., and aims to promote international academic exchange.

Editor-in-Chief: XU Sheng (徐 胜)

Associate Editor-in-Chief: HE Guang-shun (何广顺) LU Ming-sheng (卢明生)

Executive Editor: YANG Rui (杨 瑞) QIU Wen-jing (邱文静) LI Xue (李 雪)
ZHANG Xiao-xian (张潇娴) YUAN Ze-yi (袁泽轶)

English proofed by: WANG Qi (王 琦)

Semi-annually (started in 1999, sum 24)
Publication date: May 15th and Oct. 15th

Marine Science Bulletin **(Vol. 12, No. 2, Oct. 2010)**

Responsible Institution:
State Oceanic Administration of China
Sponsored by:
National Marine Data and Information Service
Edited by:
Office of Marine Science Bulletin (English edition)
Printed by:
Printery of National Marine Date and Information Service

Published by:
Office of Marine Science Bulletin (English edition)
E-mail: msb@mail.nmdis.gov.cn
Tel: (022) 24011287
Address: 93 Liuwei Rd., Hedong District, Tianjin 300171, China

ISSN1000-9620
CN12-1271/N

Price: $ 30.00 / ￥18.00 Per year